

DTIC FILE COPY

①

NUSC Technical Report 7863  
19 December 1986

AD-A227 479

# Channel Modeling and Threshold Signal Processing in Underwater Acoustics: An Analytical Overview

David Middleton  
Office of the Associate Technical  
Director for Technology



DTIC  
ELECTE  
OCT. 15. 1990  
S B D

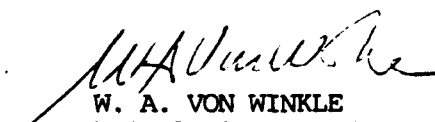
**Naval Underwater Systems Center**  
Newport, Rhode Island / New London, Connecticut

Approved for public release; distribution is unlimited.

# PREFACE

This work was carried out under NUSC Contracts N00140-[84-M-NDB5; 85-M-LD94; 85-M-LB22; and 85-M-MU43] with Dr. David Middleton, Contractor, 127 E. 91st St., New York, New York, 10128, for Code 10, NUSC. The Technical Reviewers were Dr. Roger Dwyer, NUSC, Code 3341 and Dr. W. A. Von Winkle, NUSC, Code 10.

REVIEWED AND APPROVED: 19 DECEMBER 1986

  
W. A. VON WINKLE  
Associate Technical Director for Technology

Unclassified

SECURITY CLASSIFICATION OF THIS PAGE

## REPORT DOCUMENTATION PAGE

1a REPORT SECURITY CLASSIFICATION Unclassified			1b RESTRICTIVE MARKINGS	
2a SECURITY CLASSIFICATION AUTHORITY			3 DISTRIBUTION/AVAILABILITY OF REPORT  Unlimited	
2b DECLASSIFICATION/DOWNGRADING SCHEDULE				
4 PERFORMING ORGANIZATION REPORT NUMBER(S)  TR 7863			5. MONITORING ORGANIZATION REPORT NUMBER(S)	
6a. NAME OF PERFORMING ORGANIZATION  Dr. David Middleton		6b OFFICE SYMBOL (If applicable)  Code 10		7a. NAME OF MONITORING ORGANIZATION
6c. ADDRESS (City, State, and ZIP Code)  127 E. 91 St. New York, NY 10128			7b. ADDRESS (City, State, and ZIP Code)	
8a. NAME OF FUNDING/SPONSORING ORGANIZATION  Naval Underwater Systems Center		8b. OFFICE SYMBOL (If applicable)  Code 10		9. PROCUREMENT INSTRUMENT IDENTIFICATION NUMBER N00140-84-M-NDB5; N00140-85-M-LD94; N00140-85-M-LB22; N00140-85-M-MU43
8c. ADDRESS (City, State, and ZIP Code)  New London, CT 06320			10. SOURCE OF FUNDING NUMBERS	
			PROGRAM ELEMENT NO	PROJECT NC
			TASK NC	WORK UNIT ACCESSION NO
11. TITLE (Include Security Classification) Channel Modeling and Threshold Signal Processing in Underwater Acoustics: An Analytical Overview				
12. PERSONAL AUTHOR(S) David Middleton				
13a. TYPE OF REPORT		13b. TIME COVERED FROM 10/84 TO 8/86		14. DATE OF REPORT (Year, Month, Day) 1986 December 19
15. PAGE COUNT 79 + vii				
16. SUPPLEMENTARY NOTATION				
COSATI CODES			18. SUBJECT TERMS (Continue on reverse if necessary and identify by block number)	
FIELD	GROUP	SUB-GROUP	Underwater acoustic channel modeling; Scattering, generalized channel; Nongaussian signal and noise fields and processes; Threshold signal detection and estimation; (con't. on back)	
19. ABSTRACT (Continue on reverse if necessary and identify by block number)				
<p>An overview of underwater acoustic channel modeling and threshold signal processing is presented which emphasizes the inhomogeneous, random, and nongaussian nature of the generalized channel, combined with appropriate weak-signal detection and estimation. Principal attention is given to the formal structuring of the scattered and ambient acoustic noise fields, as well as that of the desired signal, including both fading and doppler "smear" phenomena. The rôle of general receiving arrays is noted, as well as their impact on spatial as well as temporal signal processing and beam forming, as indicated by various performance measures in detection and estimation. The emphasis here is on limiting optimum threshold systems, with some attention to suboptimum cases.</p> <p>Specific first-order probability density functions (pdf's) for the nongaussian components of typical underwater acoustic noise environments are included along with their field covariances. Several examples incorporating these pdf's are given, to illustrate the (con't. on back)</p>				
20. DISTRIBUTION/AVAILABILITY OF ABSTRACT <input type="checkbox"/> UNCLASSIFIED/UNLIMITED <input type="checkbox"/> SAME AS RPT <input type="checkbox"/> DTIC USERS			21. ABSTRACT SECURITY CLASSIFICATION	
22a. NAME OF RESPONSIBLE INDIVIDUAL David Middleton			22b. TELEPHONE (Include Area Code) 1-203-440-4877	
			22c. OFFICE SYMBOL Code 10	

Unclassified

18. SUBJECT TERMS--Continued

Threshold signal processing; Spatial sampling.

19. ABSTRACT--Continued

applications and general methods involved. The fundamental rôle of the detector structure in determining the associated optimum estimators is noted: the estimators are specific linear or nonlinear functionals of the original optimum detector algorithm, depending on the criterion (i.e., minimization of the chosen error or cost function) selected. Results for both coherent and incoherent modes of reception are presented, reflecting the fact that frequently signal epoch is not known initially at the receiver.

To supplement the general discussion a selected list of references is included, to provide direct access to specific, detailed problems, techniques, and results, for which the present paper is only a guide.

Accession For	
NTIS GRA&I	<input checked="checked" type="checkbox"/>
DTIC TAB	<input type="checkbox"/>
Unannounced	<input type="checkbox"/>
Justification	
By	
Distribution/	
Availability Codes	
Dist	Avail and/or Special
A-1	



## Table of Contents

	<u>Page</u>
List of Figures . . . . .	v
List of Principal Symbols . . . . .	vi
1. Introduction . . . . .	1
1.1 Organization . . . . .	3
2. Formulation . . . . .	5
2.1 The Generalized Channel . . . . .	7
2.2 The Rôle of Scattering Theory . . . . .	8

### Part I. Medium Modeling

3. Inhomogeneous Stochastic Media: Langevin Equations and Solutions . . . . .	10
3.1 Random Media . . . . .	11
3.2 Field Series and Feedback Solutions . . . . .	14
4. Channel Characterization and Statistics . . . . .	16
4.1 Moments of the Received Field . . . . .	16
4.2 Remarks on Arrays . . . . .	17
5. Ocean Volume and Surface Channels: The Received Field X . . .	20
6. Poisson Statistical Models: Non-Gaussian Noise Fields and Received Processes, X . . . . .	25
6.1 Poisson Fields and Statistics . . . . .	25
6.2 Non-Gaussian Process PDF's . . . . .	29
6.3 Summary Remarks (Part I) . . . . .	31

Part II. Acoustic Threshold Signal Processing

7. Threshold Signal Detection . . . . .	32
7.1 Canonical Space-Time Threshold Algorithms . . . . .	34
7.2 LOBD Algorithms . . . . .	35
7.3 Signal Structures for Coherent and Incoherent Reception .	36
7.4 The Bias and Asymptotic Optimality (AO) . . . . .	37
7.5 Suboptimum Algorithms . . . . .	39
8. Threshold Detector Performance . . . . .	39
8.1 Performance Examples . . . . .	40
8.2 Remarks on Suboptimum Performance . . . . .	42
8.3 Discussion: Threshold Detection . . . . .	43
9. Threshold Signal Estimation. . . . .	45
9.1 Canonical Optimum Threshold Estimator Structures:	
AO/LOBE Forms . . . . .	47
A. Equivalent LOBE's for LOBD's . . . . .	47
B. AO Forms of the $g_j^*$ . . . . .	49
C. Suboptimum Estimators . . . . .	51
9.2 An Example: Amplitude Estimation with the SCF:	
Coherent Reception. . . . .	52
9.3 Discussion. . . . .	53
10. Concluding Remarks . . . . .	54

Appendixes:

A.1 Diagram Representations and Solutions [2] . . . . .	A-1
A.2 Canonical Scattering Operator Formalisms: Basic Decomposition	
Principle . . . . .	A-5
A.2-1 Operator Structure and Radiation Event Statistics . . .	A-7
A.2-2 Examples: FOM and Classical Scatter Models . . . . .	A-11
A.3 Bayesian Estimation: A Decision-Theoretic Formulation . . . .	A-15

<u>References</u> . . . . .	R-1
-----------------------------	-----

## List of Figures

	<u>Page</u>
2.1 Operational schematic of a generalized channel: here, a complex, ocean medium and subsequent signal processing ( $I_{R_0}$ )	6
3.1 Schematic scatter channel geometry of source (T), medium (V), and boundaries (S,B), with receiver (R), D = unscattered, or "direct" path, and n is the order of the interactions. Sufficiently high frequencies are assumed to permit illustrative ray paths . . . . .	12
3.2 Feedback Operational Representation (FOR) for the propagation Eq. (3.8), for linear inhomogeneous media . . .	15
4.1 Geometry of array (in $\underline{V}_R$ ), and m <sup>th</sup> - sensor, with beam in direction, $-\hat{i}_{OR}$ . . . . .	19
8.1 Probabilities $P_D^{(*)}$ of detection (8.4) for both coherent and incoherent reception, with processing gain as parameter, for false alarm probability $\alpha_F^{(*)} = 10^{-3}, 10^{-4}, 10^{-5}$ . . . . .	42
A.2-1 Decomposition Principle: $dV = \sum_{k=1}^N v(k)$ ; $dN = \sum_{k=1}^N dN(k)$ : scattering domain resolved into hierarchy of independent, k-coupled scattering elements. . . . .	A-8
A.2-2 Geometry of bistatic surface scatter . . . . .	A-12

# List of Principal Symbols

$A_A$ = overlap index	$J = MN$ = number of space-time field samples
$\alpha, \alpha_I, \alpha_H, \alpha_A$ = fields	
$Q, Q_I, Q_R$ = beam patterns	
$\alpha$ = (in context) a Class B noise parameter, cf. Eq. (6.13)	$K_X, K_\alpha, K_I$ = covariance functions
$a_0$ = input signal-to-noise ratio	$K$ = detector threshold
	$\underline{k}$ = vector wave number
$B_J^*$ = detector bias	$L = \hat{R}\mathcal{L}$ = basic received waveform
	$\hat{L}^{(0)}$ = linear homogeneous medium operator
$c_0$ = mean speed of sound	$\mathcal{L}$ = source field
$\epsilon, \epsilon_0$ = epochs	$\ell_J, \ell$ = log-likelihood ratios
$\hat{\eta}$ = field renormalization operator	$L^{(2)}, L^{(4)}$ = statistical parameters of the noise field
$F_1, F_2, F_n, F_Q$ = characteristic functions	$\hat{M}, \hat{M}_\infty$ = integral homogeneous medium operators
$\underline{F}$ = Fourier transforms	$\mu = p/q$ = ratio of a priori data probabilities
FOM = Faure-01'shevskii-Middleton	
FOR = Feedback operational representation	$N$ = number of time samples; also, number of radiating sources
FOS = Feedback Operational Solution	$dN, dn$ = counting functionals
	$\underline{v}, \underline{v}_0, \underline{v}_{OR}$ = vector spatial frequencies
$G_T$ = source function	
$\hat{G}_T$ = source operator	$\omega = 2\pi f$ = angular frequency
$g_J^*, g_J$ = threshold detector algorithms	$(\hat{\phantom{x}})$ = operator symbol
$\gamma, \gamma_G^*$ = estimators	$p_e^{(\phantom{x})}, p_D^{(\phantom{x})}, p_e^{(\phantom{x})}, p_D$ = error and detection probabilities
$h, h_R, h_F$ = (filter) weighting functions	PTSS = perturbation theoretical series solutions
$\hat{i}_T, \hat{i}_R, \hat{i}_{OT}, \hat{i}_{OR}$ = unit vectors	$\hat{Q}, \hat{Q}^{(0)}, \hat{Q}^{(k)}$ = linear inhomogeneous medium operators



$\hat{R}$  = array operator  
 $\langle \rangle_R$  = radiation event average  
 $\rho$  = process density

$S_{in}$  = input signal  
 $s = i\omega$   
 $\sigma_J^2, (\sigma_J^*)^2$  = detector variances  
 $\sigma$  = pdf or density  
 $\langle \rangle_S$  = average over space and parameters ( $\theta$ )

$T_{AT}, T_{AR}, T_M^{(N)}, T_{R_0}, T_{T_0}$  = transformation operators  
 $\tau_x, \tau_{ox}$  = relaxation times

$\theta$  = signal-to-noise ratio  
 $\Theta$  = error function  
 $\underline{\theta}, \underline{\theta}'$  = sets of parameters

$u, v$  = decisions, messages

$V_T, V_R$  = aperture domains

$w_1$  = first-order pdf

$X(t), x$  = received wave forms

$Z, Z_R, Z_S, Z_\theta$  = domain of integration

# Channel Modeling and Threshold Signal Processing in Underwater Acoustics: An Analytical Overview

## 1. Introduction

The purpose of this paper is twofold: (1) to combine a canonical characterization of random underwater acoustic fields or "channels" with the principle elements of threshold signal processing, in essence, signal detection and extraction; and (2) to provide, in the process, a necessarily concise analytic description of some of the principal formal approaches required to achieve these ends. Accordingly, our presentation is primarily tutorial, in keeping with the space available. This overview seeks to provide one possible albeit rather formal framework for handling the increasingly specialized problems of medium modeling, signal processing, and performance evaluation, which are now encountered in applications. We shall lean heavily on some of the author's recent work on channel characterization [1], [2] and space-time signal processing [3]-[5], as well as on recent related work on the statistical-physical modeling of nongaussian noise and interference fields [6]-[11]. (Tutorial background studies formally relevant to the above are provided in [12], [13] for nongaussian electromagnetic interference (EMI) environments.) In large part we shall be concerned with optimal processing, considered as a limiting form of system structure and performance, to be approximated in practice according to the inevitable economic and operational constraints of the task at hand. [For related, suboptimum systems, we note the parallel telecommunication examples discussed in [4], [14]-[16].]

Thus, our general aim is to provide a framework for integrating the effects of the channel (or medium) and transmission and reception of signals through it, to obtain system optimization and associated performance measures. The complex acoustic channels specifically considered here are the essentially linear underwater media of typical ocean environments, which include volume and interface (surface and bottom) scatter mechanisms, and other inhomogeneities (e.g., gradients, internal waves, etc.). Ambient noise mechanisms must also be considered. These include shipping, biological phenomena, and various geophysical sources, e.g., arctic ice,

seismic activity, etc. For example, see the recent work of Dwyer [17 and refs. therein] on underice ambient noise. For the signal processing following reception we are mainly concerned here with threshold operation, up to the point of signal decoding procedures.

Because the channel exerts such a critical influence on the signals transmitted through it, it is particularly important to include the principal effects whereby these non-ideal, inhomogeneous media degrade and modify the original signal. A canonical characterization [namely, one that is invariant of any particular medium properties (until the medium is specified)] is needed in order to provide the required generality in compact and manageable form, and to allow appropriate approximations in specific cases. Similarly, it is well understood that effective signal processing must incorporate the relevant characteristics of the channel, as well as the desired signal, optimally for limiting, optimal performance and at least adequately, for practical suboptimum systems, which may be more or less close to the ideal, optimum limits.

A critical element of signal processing is spatial sampling, achieved through the array or aperture by which source and receiver are coupled to the medium. In addition to the usual temporal processing, spatial processing becomes important in reducing minimum detectable signal levels whenever the interfering noise fields are nonuniform over the array or aperture, as long as signal wavefront levels are maintained uniform [3]-[5]. This is a further reason for examining the field structure of the acoustic channel (or any channel, for that matter), and for including the specific effects of the coupling arrays in the overall processing program. A second critical feature is the practical fact that the relevant statistics, i.e., the various probability distributions which describe the noise fields and, in part, the desired signal fields as well, are very often highly nongaussian, characteristic of ship, underice, and biological mechanisms, among others [3], [5]. A third important concept is that of threshold signal processing, where it is possible to obtain canonical algorithms, whose forms are independent of the particular noise statistics and signal structures, and which for suitably weak signals are both locally and asymptotically (i.e., as processing gain

is increased) optimum [4], [13], [16]. Applying the specific (non)gaussian distributions indicated by these algorithms then yields the corresponding processing and performance. In practice, of course, optimal structures are limiting forms which are only approximated practically. However, using the theoretical weak-signal optimum with care to avoid destruction of the information-bearing portion of the signal, provides an effective guide to suboptimum algorithms which are "close to" the optimum and which perform effectively at all signal levels: [18], for example.

Because space here limits the detail with which we can accomplish our dual task of channel characterization and threshold signal reception for these underwater acoustic régimes, our treatment is basically a "top-down" approach, proceeding from rather general formulations to more specific examples which allow us to invoke some of the physics of the problems in question. [Extensive references assist the reader in his pursuit of analytical detail and special solutions.] One advantage of the "top-down" approach is that it readily reveals the broad connections between channel physics, effective signal processing procedures, and the general communicational tasks of signal detection and estimation in noisy environments, focused here on underwater acoustic milieux.

### 1.1 Organization

Accordingly, the present paper is organized as follows:

Section 2 gives an introductory review of the general problem, including the channel and the generalized communication processes involved.

Section 3, beginning Part I: Medium Modeling, discusses some typical propagation equations for inhomogeneous deterministic and random media (Langevin equations) and their formal solutions. This includes a number of recent results developed for dealing with (linear) random media, in particular complex scattering channels like the ocean, which combines a variety of interacting scattering mechanisms. [An equivalent diagrammatic formulation is outlined in Appendix A.1.]

Section 4 presents an outline of a second-order statistical representation of these channels, while

Section 5 gives two important illustrative examples for underwater acoustics: I, weak volume scatter, and II, an "exact" ocean surface scatter formalism, with a short discussion of their physical properties and structure.

Section 6 concludes Part I with a summary of poisson field statistics which are needed in the description of both ambient and scattered fields.

Sections 7 and 8, introducing Part II: Acoustic Threshold Signal Processing, summarize some of the main results for threshold signal detection, including space-time sampling, performance results, and examples of optimum and suboptimum detection.

Section 9 then provides a short summary of signal estimation procedures, which are closely related to the detection formalism in the limiting optimum cases. As in detection, these are likewise applied to threshold signal operation, including a specific example of weak signal estimation.

Section 10 completes our analytical overview of signal processing problems associated with the underwater acoustic environment, including supporting references to the technical procedures presented in the accompanying References.

[Supplementing the above, Appendix A.1 outlines elements of diagram methods used here for the solutions of scattering problems, while Appendix A.2 provides a very concise summary of decision-theoretical formalism needed in the signal estimation aspects of reception.] Various new results, appearing in the cited references, are briefly summarized when appropriate. We stress once more the isomorphism between the channel modeling and signal processing structures of the (scalar) forms arising for telecommunications in EMI environments and that reviewed here for underwater acoustic applications. Finally, we emphasize that what is ultimately needed for an effective treatment of the general processing problem is an interdisciplinary approach, ranging from the appropriate physical models to the methods of statistical communication theory (SCT). This will be amply demonstrated in the following sections.

## 2. Formulation

The general situation is embodied in the operational relation [2],  
[19]

$$\{v\} = \underline{T}_{R_0} (\underline{T}_{AR} \underline{T}_M^{(N)} \underline{T}_{AT}) \underline{T}_{T_0} \{u\} , \quad (2.1)$$

where  $\{u\}$  is a set of "messages" to be transmitted and  $\{v\}$  is the ensemble of received messages, or decisions, which are consequent upon the set  $\{u\}$ . The  $\underline{T}_{AT}$ ,  $\underline{T}_M^{(N)}$ ,  $\underline{T}_{AR}$  are general operators which describe respectively the process of coupling to the medium by the transmitting aperture, the effects of the medium itself on the resulting injected space-time signals, and the receiving aperture, by which the received field is converted into a (temporal) wave, for further signal-processing by the receiver itself. The operators  $\underline{T}_{T_0}$ ,  $\underline{T}_{R_0}$  are temporal processes only, representing the overall "encoding" and "decoding" of the original and final "message" sets,  $\{u\}$ ,  $\{v\}$ , in (2.1). This  $\underline{T}_{T_0}$  includes the actual encoding process whereby "messages" are converted to signals, and then are suitably modulated (as narrow-band waves, usually), to drive the transmitting aperture  $\underline{T}_{AR}$ . Conversely,  $\underline{T}_{R_0}$  includes the corresponding decoding process, as well as any appropriate (usually non-linear) signal processing [20], as shown in Fig. 2.1.

In our present study we are concerned essentially with the "signal" portions of (2.1), namely the injected signal,  $S_{in}(t)$ , the received wave,  $X(t)$ , following the receiver aperture  $\underline{T}_{AR}$ , and ultimately here, with the detected wave  $Y = \underline{T}_{Det}\{X\}$  (before any decoding), viz.:

$$Y(t) = \underline{T}_{Det}\{X(t)\} = \underline{T}_{Det}\{\underline{T}_{AR} \underline{T}_M^{(N)} \underline{T}_{AT}\{S_{in}\}\} = \underline{T}_{Det} \underline{T}_{AR} \alpha , \quad (2.2)$$

where  $S_{in}$  is an injected (possibly encoded) signal and where

$$\alpha(\underline{R}, t) = \underline{T}_M^{(N)} \underline{T}_{AT}\{S_{in}\} = \underline{T}_M^{(N)}\{-G_T\} \quad (2.3)$$

is the field at some point  $(\underline{R}, t)$  in the medium in question, and  $G_T$  is a source function. Here  $G_T$  and  $X(t)$  are explicitly given by

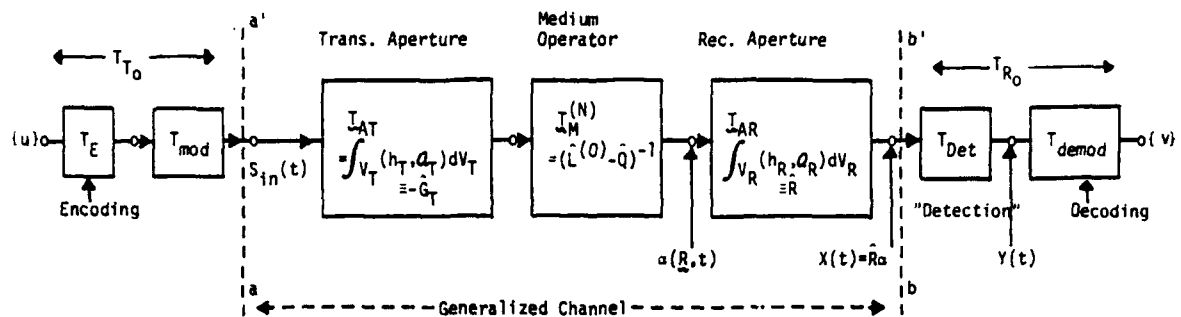


Figure 2.1 Operational schematic of a generalized channel: here, a complex, ocean medium and subsequent signal processing ( $T_{R0}$ ).

$$G_T = \hat{G}_T S_{in} = G_T(\underline{\xi}, t | S_{in}) = \int_{-\infty}^{\infty} h_T(t-\tau, t | \underline{\xi}) S_{in}(\tau, \underline{\xi}) d\tau \quad (\equiv h_T * S_{in}), \quad (2.4a)$$

and

$$X(t) = \hat{R}\alpha = \int_R dV_R(R) \int_{-\infty}^{\infty} h_R(t-\tau, t | R \in V_R) \alpha(R, \tau) d\tau = \int_R h_R * \alpha dV_R, \quad (2.4b)$$

where the source and array operators,  $\hat{G}_T$ ,  $\hat{R}$  are respectively†

$$\hat{G}_T \equiv \hat{G}_T(t, \underline{\xi} | \tau) \equiv \int_{-\infty}^{\infty} h_T(\tau, t | \underline{\xi}) ( )_{R, t-\tau} d\tau; \quad (2.5)$$

$$\hat{R} \equiv \hat{R}(t | R, \tau) = \int_R dV_R \int_{-\infty}^{\infty} h_R(\tau, t | R \in V_R) ( )_{R, t-\tau} d\tau \quad (= I_{AR}). \quad (2.6)$$

We remark that  $h_{T,R}$  are respectively the filter weighting functions, now four-dimensional (i.e., spatio-temporal) quantities, of the transmitting and receiving apertures, which may be time-varying as well as frequency selective. Their space-time fourier transforms are the (complex) beam patterns

$$a_{T,R}(\underline{v}, f | t) \equiv \mathfrak{F}_{\underline{\xi}, t}^{-1} \mathfrak{F}_{\tau} \{h_{T,R}\} = \int_{R, V_T} d\underline{\xi} e^{2\pi i \underline{v} \cdot \underline{\xi}} \int_{-\infty}^{\infty} h_{T,R} e^{-i\omega \tau} d\tau, \quad \omega = 2\pi f, \quad (2.7)$$

with  $\underline{v}$  a vector spatial frequency (which may itself be a complex function of frequency,  $f$ ), when the medium is absorptive.

†Throughout, we denote operators by ( $\hat{\cdot}$ ).

## 2.1 The Generalized Channel

For the linear media assumed throughout, the field  $\alpha$  obeys a partial integro-differential equation of the form [2]

$$\boxed{(\hat{L}^{(0)} - \hat{Q})\alpha = -G_T + [\text{b.c.'s} + \text{i.c.'s}]}, \quad (2.8)$$

where  $\hat{L}^{(0)}$  is a linear (scalar) partial differential operator with  $\hat{L}^{(0)}$  associated with the homogeneous portion of the medium. Here  $Q$  is, in general, a (scalar, linear) integro-differential scattering operator, which describes the interaction of the incident (homogeneous) field with the (differential, or local) scattering (i.e., re-radiating elements) of the inhomogeneous portion of the medium. Boundary (b.c.) and initial conditions (i.c.) are, of course, a necessary part of (2.8), as indicated.

Since we are dealing generally with random media, inasmuch as  $\hat{Q}$  contains random as well as deterministic components, we are concerned with the appropriate ensembles,  $\{\alpha\}$ ,  $\{X\}$ , etc. The ensemble of equations (2.8) governing propagation of the field is now the Langevin equation ([2]; [20], chapter 10). Since, formally,

$$\{\alpha = (\hat{L}^{(0)} - \hat{Q})^{-1} (-G_T)\}, \quad (2.9)$$

comparison with (2.3) shows that

$$\{T_M^{(N)} = (\hat{L}^{(0)} - \hat{Q})^{-1}\}. \quad (2.10)$$

This, and Eqs. (2.2), (2.3), are shown schematically in Fig. 2.1.

For the purely deterministic special cases we seek solutions of (2.8) directly. However, for the general situation of random media, the "solutions" of the corresponding Langevin equation (2.9) are the various statistics of the field  $\{\alpha\}$ , e.g., the various moments  $\langle\alpha\rangle$ ,  $\langle\alpha_1\alpha_2\rangle$ , etc., and the moments of the (linear functionals) of the field,  $\{X(t)\}$ , cf. (2.4b), e.g.,  $\langle X\rangle$ ,  $\langle X_1X_2\rangle$ , etc., and more comprehensively, the various probability densities (and distributions) of  $\alpha$  and  $X$ . Thus we are interested here primarily in the means  $\langle\alpha\rangle$ ,  $\langle X\rangle$ , the intensities  $\langle\alpha^2\rangle$ ,  $\langle X^2\rangle$ , and the covariances ( $-\langle\alpha_1\alpha_2\rangle$ ,  $-\langle X_1X_2\rangle$ ). [Appendix A.1 provides a short introduction to various methods of evaluating  $\langle\alpha\rangle$ ,  $\langle\alpha_1\alpha_2\rangle$ , etc.] Accordingly,



for the purposes of this paper, we shall define the generalized channel here as the sequence of operations indicated by (2.2), viz.  $X(t)$ , or in a less restricted sense, by the resultant field  $\alpha$ , (2.3), cf. Fig. 2.1. Consequently, the desired statistical description of the generalized channel is just that of  $X = \hat{R}\alpha$ , or of  $\alpha$ , namely, the various above-mentioned moments.

When  $X$  is a gaussian process, these first- and second-order moments are sufficient for subsequent signal processing ( $T_{R_0}$  in Fig. 2.1), to yield  $\{v\}$ . But, as is often the case,  $X$  here is not gaussian, so that at least first-order distributions of  $X$  must be developed for effective processing. This is discussed further in Section 6.2 below.

## 2.2 The Rôle of Scattering Theory

The stochastic character of the medium or channel (as above), arises, of course, from the random spatio-temporal inhomogeneities within and bounding the medium. Our quantitative description of the medium now as a generalized communication channel accordingly must be made in terms of an appropriate scattering theory, particularly one which is capable of including both the geometrical and statistical features of real-world situations in manageable fashion. We include formally as a special case of scattering models that of ambient noise, where now the secondary radiating or scattering sources are replaced by primary sources, cf. Sec. 6.1.

Some recent new approaches [1] provide additional technical and insightful methods for "solving" the Langevin equations (2.9) of this general underwater acoustic channel. These include:

- I. The concept of Feedback Operational Solutions (FOS), cf. Sec. 3.2 ff., to represent the canonical Langevin equation (2.9);
- II. The ability to handle possibly interacting scattering modes (the so-called "M-form") (Sec. 2.5 of [1]); and
- III. The observation that boundaries, wave surface and ocean bottoms for example, can be treated as distributed inhomogeneities in an otherwise infinite medium (Sec. 2.2, [1]).

The first item (I) relates the analytic solutions and diagram methods to a generalized, i.e., four-dimensional, feedback theory and formalism; the second (II) offers a simple taxonomy for accounting for any significant

scattering interaction, e.g., surface with volume scatter, etc.; and the third (III) greatly simplifies the analysis, at least in the usual far-field (or "radiation-field") cases, by effectively converting distributed (or integral) boundary conditions into local, or differential boundary conditions, i.e., plane-wave, at-a-point b.c.'s.

Finally, we must note that scattering theory, particularly with respect to acoustic and electromagnetic propagation, is a venerable field of study, with a correspondingly vast literature. A full citation of the principal publications to date is well beyond our capabilities here. However, a useful and extensive summary of modern "classical" methods and results, chiefly in the electromagnetic cases, has recently been given by Ishimaru [22], along with extensive references. An earlier and more mathematical discussion of scattering problems has been provided in the interesting review paper by Frisch [23]. For acoustical scattering, particularly in the ocean and at its interfaces, the somewhat later review articles by Fortuin [25] and Horton [26] regarding surface scatter are especially noted. In the latter connection, see also [11], [43]-[56]; in particular, Bass and Fuks [48] and [43]-[45], [47], [49], and [50], for wave-surface scattering. Other important recent studies, devoted principally to volume scatter, are described by Flatté et al. [46]. Tatarskii's significant work [24] is also well known and is also especially appropriate to the treatment of both acoustic and electromagnetic scattering in the atmosphere, and contains, as well, many useful references.

An important departure from "classical continuum theory" [25], [26] is the so-called FOM theory (after Faure [28], Ol'shevskii [29], and Middleton [31]). This latter is based on first-order, i.e., independent poisson point-scatter models. Various elements of the author's more recent approaches [2], which include both the "classical" and FOM theories as particular components of the general multiple-scatter régime, cf. Appendixes A.1, A.2 have already been presented in different stages of evolution and development since 1973, [32], [40]. The essentially mature form is described in [2].

## Part I. Medium Modeling

### 3. Inhomogeneous Stochastic Media: Langevin Equations and Solutions

Starting with the appropriate equations of state, mass, and momentum conservation, one can obtain by suitable approximations ([2], [21]) of the resulting nonlinear propagation equations, linearized "wave equations," which are special variants of (2.8). It is more convenient, however, to proceed with the canonical form (2.8) directly. Here  $\hat{L}^{(0)}$  is a linear differential operator, with coefficients independent of  $(\underline{R}, t)$ , while  $\hat{Q}$ , also linear, may be an integro-differential (or global) operator and is dependent on position  $(\underline{R}, t)$ . (This character of  $\hat{Q}$  arises from scattering element doppler, cf. [36].) For the moment we regard  $\hat{Q}$ , and hence (2.8), as deterministic.

An important example for acoustic propagation in underwater media is the case of inhomogeneous, absorptive media [2], for which (2.8) is specifically [33], [24]

$$\left\{ (1 + \tau_x(\underline{R}, t) \frac{\partial}{\partial t}) \nabla^2 - \frac{1}{c_0^2} [1 + \varepsilon(\underline{R}, t)] \frac{\partial^2}{\partial t^2} \right\} \alpha = -G_T, \quad (3.1)$$

where

$$\therefore \hat{L}^{(0)} \equiv (1 + \tau_{ox} \frac{\partial}{\partial t}) \nabla^2 - \frac{1}{c_0^2} \frac{\partial^2}{\partial t^2}; \quad \hat{Q} \equiv \frac{\varepsilon}{c_0^2} \frac{\partial^2}{\partial t^2} - \tau_{ox} \gamma_x \frac{\partial}{\partial t} \nabla^2, \quad (3.1a)$$

with  $\tau_x \equiv \tau_{ox} \cdot (1 + \gamma_x[\underline{R}, t])$  generally. When  $\tau_{ox} = 0$ , (3.1) reduces to the more familiar "extended" Helmholtz equation

$$\left\{ \nabla^2 - \frac{1}{c_0^2} [1 + \varepsilon(\underline{R}, t)] \frac{\partial^2}{\partial t^2} \right\} \alpha = -G_T, \quad (3.2),$$

with

$$\hat{Q} = \frac{\varepsilon}{c_0^2} \frac{\partial^2}{\partial t^2}; \quad \hat{L}^{(0)} \equiv \nabla^2 - \frac{1}{c_0^2} \frac{\partial^2}{\partial t^2}. \quad (3.2a)$$

Here

$$\underline{R} = \underline{\hat{x}}_x x + \underline{\hat{x}}_y y + \underline{\hat{x}}_z z \quad (3.3)$$

and rectangular cöordinates are assumed throughout, so that  $\underline{\nabla} \cdot \underline{\nabla} = \nabla^2$ , etc. Specifically,  $c_0$  = (constant) wave-front speed,  $\varepsilon$  embodies the effects of velocity gradients, internal wave phenomena, and/or (weak) local turbulence; while  $\tau_x$  represents the effects of relaxation absorption (due to  $Mg_2SO_4$  and other salts).

With inhomogeneous (but still deterministic) media conventional techniques of solution fail, largely because the medium is not reciprocal, and there is no general way of applying and evaluating the initial conditions over the various volume integrals which appear in the development of the generalized Huygen's principle (GHP) when  $\hat{Q} \neq 0$  ([2]). Moreover, since these media are space-time variable in their inhomogeneities, e.g.,  $\hat{Q} = \hat{Q}(\underline{R}, t | \dots)$ , either locally, or because of local doppler [36], such media do not support space- and time-harmonic solutions [2], nor are the standard perturbational and variational techniques of the "classical" approaches [35] generally applicable, particularly when  $\hat{Q} = \hat{Q}(\underline{R}, t | \dots)$  and is a random operator, as will be the case here. Finally, in addition to all these difficulties is the usually insurperable one of bounded media when the boundaries themselves are random and moving.

### 3.1 Random Media

Accordingly, entirely new approaches are required, for manageable solutions of (2.8) generally (and (3.1) in particular), which embody the physical realities of the application in question ([2], [21]), and which, in particular, include both the random character of  $\hat{Q}$ , i.e.,  $\varepsilon(\underline{R}, t)$  in (3.1) etc., and the random doppler effects [36], as well. These involve incorporating the effects of boundaries into the now random inhomogeneity operator  $\hat{Q}$ , as well as different types of scatter mechanisms, e.g.,  $\hat{Q} = \hat{Q}_S + \hat{Q}_{vol} + \hat{Q}_{Bottom}$ , etc., with  $\hat{Q}_{vol} = \hat{Q}_{Inh} + \hat{Q}_{Disc}$ , where  $\hat{Q}_{Inh}$  represents the continuously (random) variations in medium properties, while  $\hat{Q}_{Disc}$  embodies the effects of localized, or discrete particles, bubbles, etc. A typical geometry is sketched in Fig. 3.1, showing the usual variety of interactions.

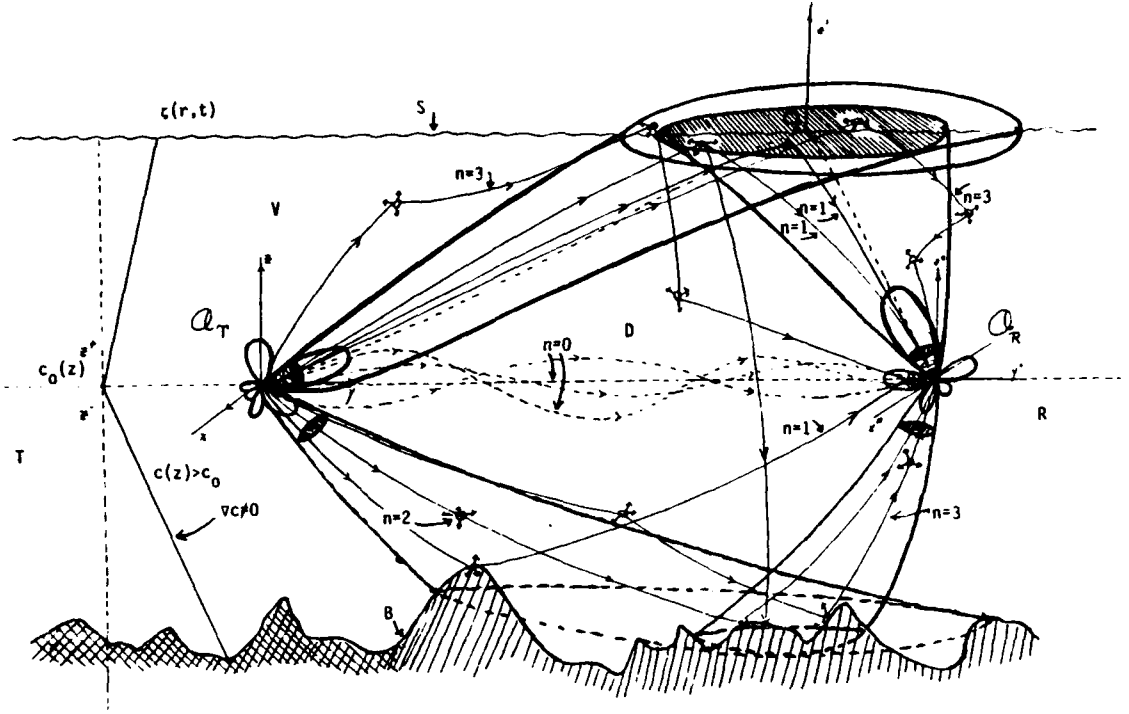


Figure 3.1: Schematic scatter channel geometry of source (T), medium (V), and boundaries (S,B), with receiver (R), D = unscattered, or "direct" path, and  $n$  is the order of the interactions. Sufficiently high frequencies are assumed to permit illustrative ray paths.

For these linear media, with  $\hat{L}^{(0)-1} = \hat{M}$  (which also includes boundary and initial conditions), it is easily seen that, in operator form, (2.8) becomes, for each member of the ensemble of propagation equations:

$$(\hat{I} - \hat{M}\hat{Q})\alpha = \hat{M}(-G_T) ; \quad \alpha = \alpha_H + \alpha_I ; \quad \alpha_H \equiv \hat{M}(-G_T) , \quad (3.4)$$

where  $\hat{I}\alpha = \alpha$ , etc. We note that  $\alpha_H$ , (3.4), is the unscattered field, or field of the purely deterministic, i.e., homogeneous portion of the medium here. Moreover, because any boundaries are included in  $\hat{Q}$ ,  $\hat{M}$  is replaced by  $\hat{M}_\infty$ , so that now

$$\alpha_H = \hat{M}_\infty(-G_T) , \quad (3.4a)$$

where the infinite domain operator for the homogeneous component of the medium becomes

$$\hat{M}_{\infty} = \hat{M}_{\infty}(\underline{R}, t | \underline{R}', t') = - \int_{-\infty}^{\infty} dt' \int_{(\infty)} d\underline{R}' q(\underline{R}, t | \underline{R}', t')_{\infty}(\underline{R}', t') \quad (3.5a)$$

$$= -\underline{\mathfrak{F}}_s^{-1}(\hat{Y}_{0,\infty}) = -\underline{\mathfrak{F}}_k^{-1}\underline{\mathfrak{F}}_s^{-1}\{\hat{y}_{0,\infty}\}. \quad (3.5b)$$

Here

$$\hat{y}_{0,\infty} = \hat{y}_0(\underline{k}, s) \int dt' \int_{(\infty)} e^{-i\underline{k} \cdot \underline{R}' - st'}(\underline{R}', t') d\underline{R}', \quad (3.5c)$$

$$\hat{Y}_{0,\infty} = \hat{Y}_{0,\infty}(s | \rho) \int dt' e^{-st'}(\underline{R}', t')$$

and

$$\underline{k} = \hat{i}_x k_x + \hat{i}_y k_y + \hat{i}_z k_z = 2\pi \underline{v} \quad (3.5d)$$

is a vector wave number, with  $\underline{v}$  a vector spatial frequency, cf. (2.7).

Here  $g_{\infty}$  is the green's function of the corresponding infinite, homogeneous medium ( $\hat{Q} = 0$ ). For the ocean medium supporting propagation according to (3.1a), we have specifically the (homogeneous) operator (kernels)

$$Y_{0,\infty} = \frac{e^{-\rho \frac{s}{c_0} (1 + \tau_{0x} s)^{-1/2} - st'}}{4\pi \rho (1 + \tau_{0x} s)^{1/2}}; \quad (3.6a)$$

$$y_{0,\infty} = [k^2 (1 + \tau_{0x} s) + s^2 / c_0^2]^{-1}; \quad \rho \equiv |\underline{R} - \underline{R}'|; \quad k^2 = \underline{k} \cdot \underline{k}. \quad (3.6b)$$

For the extended Helmholtz equation (3.2), (3.2a), Eqs. (3.6) for the homogeneous part reduce to the simpler relations

$$Y_{0,\infty} = \frac{e^{-\rho s / c_0 - st'}}{4\pi \rho}; \quad y_{0,\infty} = (k^2 + \frac{s^2}{c_0^2})^{-1}; \quad (3.7)$$

$$\therefore M(\underline{R}, t | \underline{R}', t')_{\infty} = \frac{\delta(t - t' - \rho / c_0)}{4\pi \rho}.$$

### 3.2 Field Series and Feedback Solutions

The ensemble solution of (3.4) is now given formally by [2], [21]):

$$\alpha = \left( \frac{\hat{1}}{\hat{1} - \hat{M}_\infty \hat{Q}} \right) \alpha_H = (\hat{1} - \hat{\eta}_\infty)^{-1} \alpha_H ; \quad \hat{\eta} \equiv \hat{M}_\infty \hat{Q} , \quad (3.8)$$

where  $\hat{\eta}$  is now the random field renormalization operator (FRO), when considered over all member equations of the Langevin equation. As long as  $\|\hat{\eta}\| < \infty$  (for each member equation), (3.8) supports a series expansion:

$$\alpha = \alpha_H + \left( \frac{\hat{\eta}}{\hat{1} - \hat{\eta}} \right) \alpha_H = \alpha_H + \sum_{n=1}^{\infty} \hat{\eta}_\infty^{(n)} \alpha_H : \quad \|\hat{\eta}\| < 1; \quad (3.9)$$

$$(\text{or } \alpha = - \sum_{n=0}^{\infty} (\hat{\eta}^{-1})^{(n+1)} \alpha_H, \quad 1 < \|\hat{\eta}\| < \infty). \quad (3.9a)$$

(Usually it can be shown that  $\|\hat{\eta}\| < 1$ , [2]; we remark, also, that  $\hat{M}_\infty$  and  $\hat{Q}$  do not usually commute, but commutation can always be achieved in the proper transform space, usually  $(\underline{k}, s)$ -space [2].) The expansion (3.9), or (3.9a), is called a Perturbation Theoretical Series Solution (PTSS), with the convergence condition as indicated formally above.

Equations (3.8), (3.9) are exact (ensemble) solutions. Eq. (3.8), moreover, is called the Feedback Operational Solution (FOS), since  $\hat{M}_\infty$  may be interpreted as a "feedforward" and  $\hat{Q}$ , a "feedback" operator, cf. [2], [11], in the manner of Fig. 3.2. In fact, the PTSS in (3.9), expressed as a series of loop iterations formally, indicates computationally how exact numerical solutions may be approached. The evaluation of the PTSS may then be viewed as both a problem in modern control and computational theory, extended now to four dimensions and governed by partial (rather than ordinary) differential equations and influenced by a radiation condition (on  $\hat{M}_\infty$ ), as well as boundary conditions applied locally to  $\hat{Q}$ .

However, the formal solutions (3.8), (3.9) are not very useful in their present form since  $\hat{\eta}$  is still a random operator. To achieve useful results the Langevin equations must be converted into various

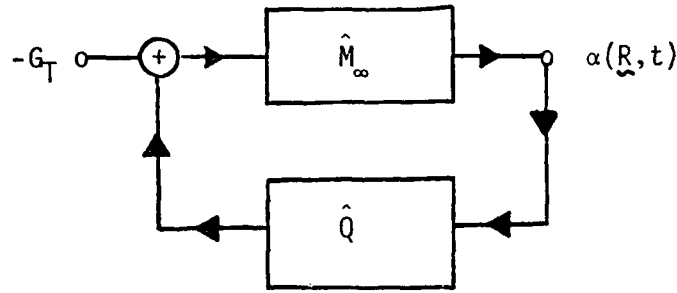


Figure 3.2 Feedback Operational Representation (FOR) for the propagation Eq. (3.8), for linear inhomogeneous media.

deterministic forms, which represent the various moments of the scattered field, as we have noted above in Sec. 2.1. This is done in the manner described in Appendix A.1 and leads to suitable replacement of the random  $\hat{Q}$  by an appropriate deterministic operator  $\hat{Q}_1^{(d)}$ ,  $\hat{Q}_{12}^{(d)}$ , etc. for the first-, second-, and higher-order moments of the field  $\alpha$ , cf. Secs. A.1-1. Thus, we get a Dyson equation for  $\langle \alpha \rangle$ , a form of the Bethe-Salpeter equation for  $\langle \alpha_1 \alpha_2 \rangle$ , etc. For example, the FOR of Fig. 3.2 applies now, with  $\alpha$  replaced by  $\langle \alpha \rangle$  and  $\hat{Q}$  by  $\hat{Q}_1^{(d)}$ . Then, by approximating  $\hat{Q}_1^{(d)}$ , etc., the various terms of the PTSS can be evaluated, although this is not an easy matter.

Finally, we observe that the ensemble solutions (3.8), (3.9) may also be insightfully described by equivalent diagram representations, which are also particularly useful in suggesting appropriate, simplifying approximations. A concise summary of this approach is provided in Appendix A.1, some results of which we use below in the text, cf. Sec. 5 ff. Related methods, involving path integrals and various models of distributed ocean inhomogeneities, with particular attention to long distance sound transmission in the ocean, are treated in the recent important studies of Flatté et al. [46]. These offer a variety of techniques for realizing the inhomogeneity operator  $\hat{Q}$  and its associated statistics (see, for example, Chapter 10 of [40].)



#### 4. Channel Characterization and Statistics

The (random) channel operator  $\underline{I}_M^{(N)} (= (\hat{I} - \hat{\eta})^{-1} \hat{M})$ , cf. (3.8), is next conveniently written

$$\underline{I}_M^{(N)} = \left\{ \hat{I} + \frac{\hat{\eta}}{\hat{I} - \hat{\eta}} \right\} \hat{M} \equiv \hat{M} + \hat{I} \equiv \hat{\eta} ; \quad \therefore \hat{I} = \frac{\hat{\eta}}{\hat{I} - \hat{\eta}} \hat{M}, \quad (4.1)$$

where we separate the homogeneous ( $\hat{M} = \hat{M}_\infty$  here) from the scatter operator,  $\hat{I}$ , cf. (3.4) et seq. We note that for ambient fields, in addition to the desired signal source ( $S_{in}$ ), we replace the source function  $-G_T$ , in the Langevin equations (2.8), (3.4), by  $-G_T - G_A$ , where now  $G_A$  is a localized, or a distributed, ambient "noise" source with an associated field,  $\alpha_A = \hat{M}_\infty(-G_A)$ . In any case, it is at once evident that the medium operators  $\hat{M}, \hat{I}$  ( $\therefore \hat{\eta}$ ) are unchanged.

##### 4.1 Moments of the Received Field

Mostly for reasons of analytical complexity, channel characterization is usually formulated in terms of the lower moments, e.g., the mean and covariance operators associated with  $\hat{I}$ . The pertinent moment operators here are, directly from (4.1),

$$\begin{aligned} \hat{\eta} &= \hat{M} + \langle \hat{I} \rangle, \quad \hat{K}_I \equiv \langle \hat{I}_1 \hat{I}_2 \rangle - \langle \hat{I}_1 \rangle \langle \hat{I}_2 \rangle ; \\ \langle \hat{\eta}_1 \hat{\eta}_2 \rangle &= \hat{M}_1 \hat{M}_2 + \hat{M}_1 \langle \hat{I}_2 \rangle + \hat{M}_2 \langle \hat{I}_1 \rangle + \langle \hat{I}_1 \hat{I}_2 \rangle, \end{aligned} \quad (4.2)$$

and with higher moments similarly determined. These moment operators are, of course, deterministic, as a result of averaging. (Note that  $\hat{I}_{1,2} = \hat{I}(\underline{R}_{1,2}, t_{1,2} | \underline{R}', t')$ , etc.,  $(\underline{R}_1, t_1), (\underline{R}_2, t_2)$  being (generally) different points in the field.)

Expressions for the corresponding moments of the received wave  $X(t)$  are found from

$$X(t) = \hat{R}_t = \hat{R}(\hat{M} + \hat{I})(-G_T - G_A) = \hat{R} \left[ \hat{I} + \frac{\hat{\eta}}{\hat{I} - \hat{\eta}} \right] (\hat{H}^+ \hat{A}). \quad (4.3)$$

Thus, the mean received waveform and various second moments are respectively

$$\langle X \rangle = \hat{R} \langle \alpha \rangle = \hat{R}(\hat{M}_\infty + \langle \hat{I} \rangle)(-G_T - G_A) \quad (4.4)$$

$$\langle X_1 X_2 \rangle = \hat{R}_1 \hat{R}_2 \langle \alpha_1 \alpha_2 \rangle = \hat{R}_1 \hat{R}_2 \hat{\eta}_1 \hat{\eta}_2 G_1 G_2, \quad G = G_T + G_A, \quad (4.5)$$

with

$$\begin{aligned} K_X(t_1 t_2) &\equiv \langle X_1 X_2 \rangle - \langle X_1 \rangle \langle X_2 \rangle = \hat{R}_1 \hat{R}_2 (\langle \alpha_1 \alpha_2 \rangle - \langle \alpha_1 \rangle \langle \alpha_2 \rangle) \\ &= \hat{R}_1 \hat{R}_2 \hat{K}_I(G_1 G_2), \end{aligned} \quad (4.6)$$

where from (3.8) and (3.9), and (4.1), we see that all orders of moments of the inhomogeneity operator  $\hat{Q}$  appear in the above.

Equivalent diagram representations for the scatter operator  $\hat{I}$  and field covariance operator  $\hat{K}_I$ , (4.2), are given in Appendix A.1.

#### 4.2 Remarks on Arrays

The array operators (2.4b) and (2.6), which appear in (4.3) et seq. for the received wave, can be rewritten alternatively as

$$\hat{R} \equiv \int_{-\infty}^{\infty} d\tau \int_{V_R} ( ) h(\underline{\eta}, t-\tau) \underline{R} d\underline{\eta}, \quad dV_R \rightarrow d\underline{\eta}. \quad (4.7)$$

Here  $V_R$  once more is the region occupied by the physical array itself (in the field  $\alpha$ ) and  $\underline{\eta}$  locates the array element  $d\underline{\eta}$  with respect to  $0_R$ , the coördinate origin of (here) the receiving array, cf. Fig. 4.1. The array is a space-time linear filter.

In practice, most physical arrays consist of an assemblage of  $m = 1, 2, \dots, M$  discrete, but distributed elements, each of which samples the radiation field,  $\alpha$ . Thus, the array operator (4.7) may be expressed in more detail formally as a vector operator

$$\underline{\hat{R}} = \int_{-\infty}^{\infty} d\tau \int_{R_m} ( ) h_m(\underline{\eta}, t-\tau) \underline{R} d\underline{\eta} = \{ \hat{R}_m \}, \quad \underline{\eta} \in \{ R_m \}, \quad (4.8)$$

which defines each "component,"  $\hat{R}_m$ . The relation (4.8) may be simplified further to the idealized but still very useful situation of "point" sensors, e.g.,  $L_{\max}^{(m)} \ll \lambda_0$ : maximum sensor dimension (each  $m$ ) is always much less than the acoustic wavelength. Thus, (4.8) becomes

$$\hat{R}_{\text{"point"}} = \{ \delta(\underline{r} - \underline{r}_m) \int_{-\infty}^{\infty} d\tau h_m(t - \tau)_R \}, = h_{mn-R} \delta(\underline{r} - \underline{r}_m), \quad (4.9)$$

all  $m$ ; where

$$h_{mn-R} \equiv \int_{-\infty}^{\infty} ( ) h_m(\underline{r}_m, t_n - \tau)_R d\tau \quad (4.9a)$$

for temporal sampling  $t_n = n\Delta t$ ;  $n = 1, \dots, N$ , as well. It is convenient to use  $j = m, n = 1, \dots, J = MN$  as a single index for space-time sampling, so that now

$$\hat{\underline{R}} = \{ \hat{R}_{j=m,n} \} = \{ \hat{R}_j \} \quad (4.10)$$

is a  $J$ -component vector. Consequently, the sampled, received field  $\underline{x}$  in (4.3) becomes explicitly

$$\underline{x} = \{ X_j \} = \hat{\underline{R}} \underline{\alpha} = \left\{ \int_{-\infty}^{\infty} h(\underline{r}_m, t_n - \tau)_R \alpha(\underline{r}_m, \tau) d\tau \right\}; \quad \underline{r}_m = \underline{r}_0 + \underline{r}_m. \quad (4.11)$$

Thus,  $\underline{x} = \{ X_{j=m,n} \}$  is the received data vector, after linear space-time filtering and sampling. Equation (4.11) is the basic relation, given the field  $\alpha$ , which constitutes the received, sampled waveform. This, in turn, is the fundamental input to the "signal-processing" systems noted in Fig. 2.1, which are the principal topic of Part II following.

For narrow-band signals in the medium we can provide a more detailed structure to  $h_m( )_R$  above. In fact, by combining, i.e., summing, the  $m (=1, \dots, M)$  outputs of each receiving sensor with appropriate delays  $\Delta\tau_m$ , we can form a beam (in the far field of the incoming signal), e.g.,

$$\underline{x} = \{ X_n \} = \{ \sum_m X_{j=m,n} \} = \left\{ \sum_m A_R^{(m)}(\underline{v}_0 - \underline{v}_{0R}; f_0) e_m(t_n - \Delta\tau_m) \right\}, \quad (4.12)$$

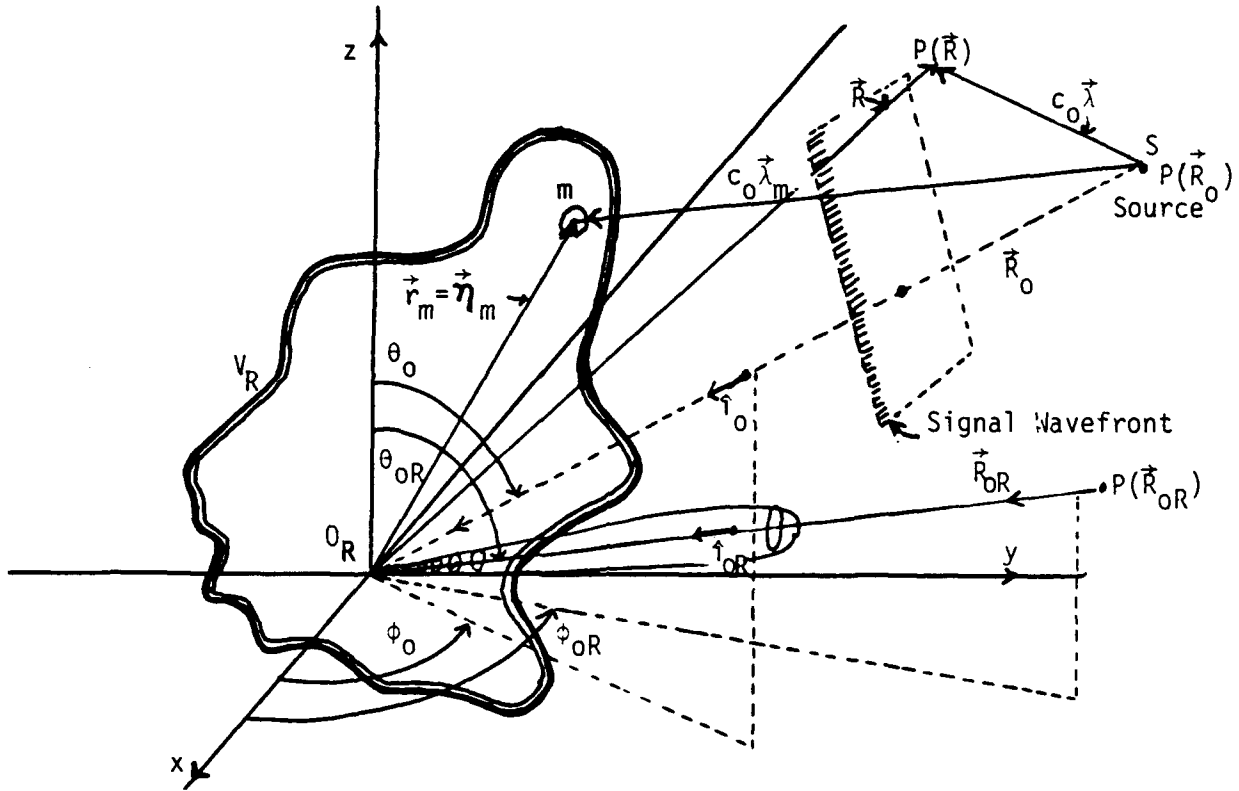


Figure 4.1 Geometry of array (in  $V_R$ ), and  $m^{\text{th}}$ -sensor, with beam in direction  $-\hat{i}_{OR}$ .

where

$$\left. \begin{aligned} A_R^{(m)} &= |A_R^{(m)}(f_0)| e^{2\pi i (\omega_0 - \omega_{OR}) \cdot \vec{r}_m - i\phi_R^{(m)}(f_0)}; \\ \Delta\tau_m &\equiv \tau_m - \hat{\tau}_m = (\hat{i}_0 - \hat{i}_{OR}) \cdot \vec{r}_m / c_0, \end{aligned} \right\} \quad (4.12a)$$

in which  $\omega_{OR} = \hat{i}_{OR} f_0 / c_0$ ,  $\omega_0 = \hat{i}_0 f_0 / c_0$  are wave numbers, respectively associated with the beam direction  $\hat{i}_{OR} (\equiv \vec{R}_{OR} / |\vec{R}_{OR}|)$  and the direction of the field's wave-front,  $\hat{i}_0 = \vec{R}_0 / |\vec{R}_0|$ . The geometry of the  $m^{\text{th}}$ -sensor, the beam, and signal wavefront are shown in Fig. 4.1, where specifically the unit vectors  $\hat{i}_0$ ,  $\hat{i}_{OR}$  are given by

$$\hat{i}_0(R) = \hat{i}_x \cos\phi_0(R) \cos\theta_0(R) + \hat{i}_y \sin\phi_0(R) \cos\theta_0(R) + \hat{i}_z \sin\theta_0(R). \quad (4.13)$$

In (4.12),  $|A_R^{(m)}|$  and  $\phi_R^{(m)}$  are the amplitude and phase of the  $m^{\text{th}}$ -sensor's response, at the center frequency ( $f_0$ ) of the received signal, here the field  $\alpha$ . For a vertical array of  $2M_0+1=M$  sensors, for example, we have

$$\begin{aligned} \underline{r}_m &= \underline{\hat{i}}_z m \Delta \ell, & (-M_0, \dots, m, \dots, M_0) \\ \therefore \Delta \tau_m &= \frac{m \Delta \ell}{c_0} (\sin \theta_0 - \sin \theta_{0R}), \end{aligned} \quad (4.14a)$$

in which  $\Delta \ell$  is the sensor spacing. For a similar, but horizontal array,

$$\underline{r}_m = \underline{\hat{i}}_x m \Delta \ell \text{ and } \therefore \Delta \tau_m = \frac{m \Delta \ell}{c_0} [\cos \phi_0 \cos \theta_0 - \cos \phi_{0R} \cos \theta_{0R}]. \quad (4.14b)$$

For a narrow-band signal field  $\underline{\hat{i}}_0$  is usually known, or findable. Thus, the "beam" can be steered, that is, pointed in the direction of the desired signal, by choosing  $\underline{\hat{i}}_{0R} = \underline{\hat{i}}_0$ , or setting the path delays  $\tau_m$  in Fig. 4.1 such that  $\Delta \tau_m = 0$ , cf. (4.12a). However, for an ambient or scattered noise field, each of which is the superposition of a number of possible (undesired) signal fields randomly phased with respect to one another,  $\underline{\hat{i}}_0$  is randomly distributed in space. There is consequently no distinct noise field wavefront or wavefront direction, and  $\underline{\hat{i}}_0$  must be averaged over in suitable fashion. [See Secs. 8.2 and Sec. 9 of [4], for example; also, (6.10b) and Sec. 7.3 ff.]. This randomness of  $\underline{\hat{i}}_0$  in the case of noise fields usually leads to spatial non-uniformity of the interfering field, which can often be exploited to increase the processing gain in signal reception, by effectively increasing the number of independent spatial noise samples vis-à-vis the (nearly) uniform desired signal field, cf. Sec. 10 of [4].

## 5. Ocean Volume and Surface Channels:

### The Received Field X

Both the important cases of weak volume scatter in the ocean and ocean surface scatter are well approximated by at most the scattering element interacting with the homogeneous field,  $\alpha_H$ , the former because multiple scatter effects are usually quite ignorable, the latter from the physical geometry of the wave surface, which likewise discourages

multiple scatter except within a typical wave crest-to-crest domain, cf. Fig. 3.1, ( $n=1$ ). (Similar considerations usually apply for ocean bottoms, as well, cf. Fig. 3.1. We shall, however, consider only the modes  $M=S,V$ , here), observing also that  $O(30-40 \text{ db})$  they are effectively independent ([21], thesis): there is negligible coupling in the ocean between surface (bottom) and volume scatter.)

Accordingly, a 1st-Born approximation suffices (as indicated by the dotted lines in (A.1d), (A.2a), and we write for the received field,  $X$ , from (A.1d):

$$X = \hat{R}_\alpha = \hat{R} \left( \begin{array}{c} \xrightarrow{\hat{M}} \textcircled{T} \\ \text{M} \end{array} + \begin{array}{c} \xrightarrow{\hat{Q}_M} \textcircled{T} \\ \text{S or V} \end{array} \right) = \hat{R}(\alpha_H + \hat{M}\hat{Q}_M\alpha_H) \quad (5.1)$$

$\xrightarrow{\hat{M}} \textcircled{T} \xleftarrow{\hat{Q}_M} \textcircled{T} \quad M = S, V.$   
 $\textcircled{T} = -G_T$

The mean wave,  $\langle X \rangle$ , is, with  $\langle \hat{Q}_M \rangle = \bullet$ , cf. (A.2a):

$$\therefore \langle X \rangle = \hat{R}\langle \alpha \rangle \doteq \hat{R} \left( \begin{array}{c} \xrightarrow{\alpha_H} \textcircled{T} + \bullet \xrightarrow{\alpha_I} \textcircled{T} \\ \alpha_H \quad \alpha_I \end{array} \right) = \left\{ \begin{array}{l} \hat{R}\alpha_H + \hat{R}\hat{M}\langle \hat{Q}_M \rangle\alpha_H \\ X_H + X_I \end{array} \right\} \quad (5.2)$$

The second-moment of  $X$ , (5.1) in (4.5), is found to be, on averaging over the phases ( $\phi$ ) of the input signal.

$$\langle\langle X_1 X_2 \rangle\rangle_\phi = \langle \hat{R}_1 \hat{R}_2 \langle \alpha_1 \alpha_2 \rangle \rangle_\phi \doteq \langle \hat{R}_1 \hat{R}_2 [\hat{1} + \hat{M}_1 \hat{M}_2 \cdot \left\{ \langle \hat{Q}_1^{(0)} \hat{Q}_2^{(0)} \rangle_S + \langle q_1^{(1)} q_2^{(1)} \rangle + \sum_{k=2}^{\infty} \langle q_1^{(k)} q_2^{(k)} \rangle \right\} \alpha_{H1} \alpha_{H2}] \rangle_\phi \quad (5.3a)$$

$$\begin{aligned} \langle\langle X_1 X_2 \rangle\rangle_\phi &= \langle \hat{R}_1 \hat{R}_2 \left( \begin{array}{c} \uparrow \\ \text{"homog."} \end{array} \right) + \begin{array}{c} \xrightarrow{k=0} \textcircled{O}_{11} \textcircled{O}_{22} \\ \text{"classical": coherent} \end{array} + \begin{array}{c} \xrightarrow{k=1} \textcircled{\bullet}_{11} \textcircled{\bullet}_{22} \\ \text{+ incoherent} \end{array} + \begin{array}{c} \xrightarrow{(k \geq 2)} \textcircled{\bullet}_{11} \textcircled{\bullet}_{22} \\ \text{multiple-scatter: incoher.} \end{array} \rangle_\phi \\ &= \text{unscat.} \left\{ \begin{array}{l} \text{FOM:} \quad \text{coh.} \quad + \quad \text{incoherent} \quad (0) \end{array} \right. \quad (5.3b) \end{aligned}$$

where

$$O \equiv \hat{q} = \hat{Q} - \langle \hat{Q} \rangle_R \leftarrow O-O = \chi\{v^{(0)} = \sum_{k=1} (\langle v^{(k)} \rangle_{R+\Delta v^{(k)}})\};$$

$$\hat{Q}(0) \equiv \langle \hat{Q} \rangle_R = 0, \therefore \langle \hat{Q}(0) \rangle_S = \langle \hat{Q} \rangle = \bullet = \langle O \rangle_R.$$

$$\text{---}\overset{\frown}{\text{---}}\equiv \langle \rangle_{\text{S:space av.}\times \underline{\theta}} \ ; \ \bullet_1 \overset{\frown}{\text{---}} \bullet_2 = \langle \hat{q}_1 \hat{q}_2 \rangle \text{ etc. } \overset{\frown}{\text{---}} = \langle \rangle = \langle \rangle_{R,S} \ , \quad (5.4)$$

via (A.2-6). Note that the (total) average,  $\langle \rangle$ , as in Appendix A.1 et seq., involves both an average over radiation events and an average over random spatial (S) and parameter values ( $\theta$ ), embodied in  $\langle \rangle_S$ , cf. (5.4) and, particularly, Appendix A.2.

It is the Decomposition Principle, embodied in  $\hat{Q}_M$ , ( $M = S, V, B$ ), Eq. (A.2-5) et seq., which allows us to resolve the inhomogeneity operator into sets of distinct and (statistically) independent entities as specifically exhibited in Eqs. (5.3). Moreover, and most important, the entities ( $k=0$ ,  $k=1$ ,  $k \geq 2$ ) in (5.3) above (and in (5.1), with the help of (5.4)) have an explicit physical interpretation: Thus, the terms  $k=0$  contain both the coherent and incoherent radiation contributions, from all orders ( $k \geq 1$ ) of radiation interactions, e.g., single- and multiple scattering ( $k \geq 2$ ), for example. Consequently, if  $v^{(k)}$  represents the density of (illuminated)  $k$ -coupled scattering elements ( $k \geq 1$ ), then  $\langle v^{(k)} \rangle_R$  is the coherent radiative contribution, where  $\langle \rangle_R$  is the average over the radiation events associated with the ensemble of potential (re-)radiating sources. In a similar way

$$\Delta v^{(k)} \equiv v^{(k)} - \langle v^{(k)} \rangle_R \quad (5.5a)$$

is the fluctuation in the density of k-coupled radiating elements, and is always associated with incoherent radiation. Accordingly, we have

$$v(0) = \sum_{k=1}^{\infty} (\langle v(k) \rangle_{R+\Delta v(k)}) = \sum_{k=1}^{\infty} v(k) \equiv v, \quad (5.5b)$$

showing the basically coherent and incoherent elements of the scattering or source region containing these various  $k \geq 1$  types of elements. The (average) density of coherent radiators is  $\langle v^{(0)} \rangle_R = \sum \langle v^{(k)} \rangle_R$ , since  $\langle \Delta v^{(k)} \rangle_R = 0$ . The number of "radiation events" occurring in a small region  $d\Lambda$  of the illuminated or emitting domain  $\Lambda$  is  $dN$ , so that  $v = dN/d\Lambda = v^{(0)}$ . A taxonomy and interpretation for the  $dN$ , similar to (5.5a,b), can be constructed: One has now

$$dN^{(0)} \equiv \sum_{k=1}^{\infty} (\langle dN^{(k)} \rangle_R + dn^{(k)}) = \sum_{k=1}^{\infty} dN^{(k)}. \quad (5.5c)$$

The relations (5.6) et seq. obviously apply if one replaces  $v$  etc. by  $dN$ ; see also Sec. 6.1 following.

Since the medium in question is linear, the scattering or inhomogeneity operator,  $\hat{Q}$ , is a linear functional of the  $v^{(k)}$ , i.e., of  $v^{(0)}$ , e.g.,  $\hat{Q} = \mathcal{L}(v^{(0)})$ , thus containing all types of radiation interaction effects. Moments of  $v^{(0)}$ , or more generally, of  $\hat{Q}_M$ , which appear in (5.2), (5.3) above, are readily indicated: we have

$$\langle \hat{Q} \rangle = \mathcal{L}\{\langle v^{(0)} \rangle\}, \text{ where } \langle v^{(0)} \rangle = \langle \langle v^{(0)} \rangle_R \rangle_S. \quad (5.6)$$

This is different from zero, in scattering, if specular reflection geometry (both on a surface and in a volume) is available. The second-order moments are instructive:

$$\langle \hat{Q}_1 \hat{Q}_2 \rangle = \mathcal{L}\{\langle v_1^{(0)} v_2^{(0)} \rangle\}, \quad (5.7a)$$

where now

$$\langle v_1^{(0)} v_2^{(0)} \rangle = \langle \langle \Delta v_1^{(0)} \Delta v_2^{(0)} \rangle_R \rangle_S + \langle \langle v_1^{(0)} \rangle_R \langle v_2^{(0)} \rangle_R \rangle_S. \quad (5.7b)$$

Equation (5.7b) contains both incoherent ( $\sim \Delta v^{(0)}$ ) and coherent terms ( $\sim \langle \Delta v^{(0)} \rangle_R$ ), of all orders ( $k \geq 1$ ) of coupled scattering or radiating elements. The associated covariance of  $\hat{Q}$  is



$$K_{\hat{Q}} = \mathcal{L}\{\langle v_1^{(0)} v_2^{(0)} \rangle - \langle v_1^{(0)} \rangle \langle v_2^{(0)} \rangle\}, \quad (5.7c)$$

which embodies wholly incoherent radiation.

We now distinguish two principal classes of radiation models from which scattered and ambient acoustic (and electromagnetic) noise fields can be constructed. These are (1): the "classical" cases, where the number of "radiation events" (e.g., reradiations or ambient emissions) are the same for each member of the ensemble, so that  $\langle v^{(k)} \rangle_R = v^{(k)}$ , and  $\therefore \Delta v^{(k)} = 0$ , all  $k \geq 0$ . And (2): the quantized cases, where  $\langle v^{(k)} \rangle_R$ , and  $\therefore \Delta v^{(k)}$ , can be nonvanishing, reflecting the fact that the number of radiation events is variable over the ensemble. The latter is typical of the so-called poisson radiation models [11], developed recently for both scattering [28]-[32], [40] and ambient noise [3]-[6], [52].

For the poisson scattering cases there is the so-called FOM (Faure [28], Ol'shevskii [29], Middleton [31]) model, based on an independent poisson point-process, where

$$(\text{FOM}): \quad v^{(0)} = v^{(1)}; \quad v^{(k)} = 0; \quad k \geq 2, \quad (5.8)$$

namely, all multiple scatter is neglected. For this model the coherent and incoherent contributions are found to be linear functionals of

$$\langle v^{(0)} \rangle_R = \langle v^{(1)} \rangle_R, \quad \text{or} \quad \langle v^{(0)} \rangle = \langle v^{(1)} \rangle \equiv \sigma^{(1)}; \quad (5.9a)$$

$$\begin{aligned} (\text{FOM}): \quad K_{\Delta v}(0) &= \langle v_1^{(0)} v_2^{(0)} \rangle - \langle v_1^{(0)} \rangle \langle v_2^{(0)} \rangle \\ &= \langle \sigma^{(1)} \delta(\underline{z}_2 - \underline{z}_1) \rangle_S + \langle \langle v_1^{(1)} \rangle_R \langle v_2^{(1)} \rangle_R \rangle_S - \langle v_1^{(1)} \rangle \langle v_2^{(1)} \rangle, \end{aligned} \quad (5.9b)$$

where  $\underline{z}_1, \underline{z}_2$  embody spatial, temporal and parametric coördinates and  $\sigma^{(1)}(\underline{z})$  is the average density of scattering in the illuminated region  $\Lambda$ . The FOM model is quasi-phenomenological and avoids dealing explicitly with the boundary conditions, which are now contained in a (linear) ad hoc response function  $\gamma_0 h(t-t_2)$ , with "cross-section"  $\gamma_0$ , developed and

empirically adjusted for the problem at hand [43]-[45].

On the other hand, in the classical approach, the density fluctuations of radiation events are always zero, as noted above, so that (5.7b),  $\langle v_1^{(0)} v_1^{(0)} \rangle = \langle v_1^{(0)} v_2^{(0)} \rangle$ , is an identity, and (5.7c) describes the covariance of  $v^{(0)}$ , or  $\hat{Q}$ . Again, in the usual applications, multiple scatter is neglected ( $v^{(k)} = 0$ ,  $k \geq 2$ ). One has, here for surface scatter cases, specifically

$$\gamma_0 \langle v^{(0)} \rangle_R = \gamma_0 v^{(0)} \doteq \gamma_0 v^{(1)} \doteq RS \frac{\omega}{c} \hat{n}_g (\hat{i}_T - \hat{i}_R) \quad (5.10)$$

under a Kirchoff approximation, [27], [28], where  $R, S$  are respectively the (average) plane-wave reflection coefficient and shadowing function,  $\omega (=2\pi f)$  is the angular frequency of the incident radiation,  $c_0$  = phase speed of sound in water,  $\hat{n}_g = (\hat{i}_x \zeta_x + \hat{i}_y \zeta_y - \hat{i}_z) / \sqrt{1 + \zeta_x^2 + \zeta_y^2}$  is the normal to the wave surface  $\zeta(\underline{r}, t)$ , with  $\zeta_x = \partial \zeta / \partial x$ , etc., and  $\hat{i}_T, \hat{i}_R$  are unit vectors from source and receiver to the scattering element on  $\zeta$ . See [25]-[27], [37]-[39] as well as [47]-[51], for detailed development of the classical theory. See Sec. 6 following and Appendix A.2 for further discussion of these poisson field models.

## 6. Poisson Statistical Models: Non-Gaussian Noise Fields and Received Processes, X

Because of the effectively discrete nature of the inhomogeneity models and the analogous structure of the ambient field sources, the fundamental statistics of both the fields  $\alpha(\underline{R}, t)$  generated in the medium and the received waves,  $X(t)$ , are poissonian. This is directly the case for the ambient noise and weakly scattered field components, which constitute much of the interference in practical operation. In many cases, i.e., where there may be a few relatively strong sources or scatterers outstanding from the majority, the resultant field and received process  $X$  are highly nongaussian, while the weaker background is, as expected, well described by a limiting gaussian process. We note some of the important results below.

### 6.1 Poisson Fields and Statistics

A (scalar) poisson field  $\alpha(\underline{R}, t)$ , here an underwater acoustic field generated by potentially many independent sources, may be represented by

$$\alpha(\underline{R}, t) = \int_{\underline{Z}(\underline{Z}_R \times \underline{Z}_S \times \underline{\theta})} \mathcal{L}(\underline{R}, t | \underline{z}) dN(\underline{Z}(\underline{z})), \quad (6.1)$$

where  $\underline{z} = \underline{z}_R \times \underline{z}_S \times \underline{\theta}$ , in which  $\underline{z}_R$  represent radiation epochs,  $\underline{z}_S$  are spatial variables, and  $\underline{\theta}$  are structural or waveform parameters;  $\underline{Z} = \underline{Z}_R \times \underline{Z}_S \times \underline{Z}_\theta$  is the associated composite space of these quantities;  $\mathcal{L}$  is the wave field for a single emitting source. Here  $dN$  is a counting functional, and in general,  $d\Lambda$ ,  $\underline{z}_R$ ,  $\underline{z}_S$ ,  $\underline{\theta}$  are random (process and) variables. This counting functional is represented by

$$dN(\underline{Z}) = \sum_{p=1}^P \delta(\underline{\lambda} - \underline{\lambda}_p) \delta(\underline{\theta} - \underline{\theta}_p) \delta(t - t_p), \quad (6.2)$$

for  $P$  discrete sources potentially emitting, or reradiating, at times  $t_p$  in region  $\Lambda$ , where

$$dN(\underline{Z}) = dN(\Lambda = p; t_p; \underline{\theta}) = (d\underline{Z})^p e^{-d\underline{Z}} / p!, \quad p \geq 0 \quad (6.2a)$$

with  $d\underline{Z} = \sigma_S d\Lambda d\underline{\theta}' dt' w_1(\underline{\theta}') w_1(t')$ , etc., in which  $t'$  is a random emission time or epoch. For poisson fields,  $dN$  is a poisson process obeying (6.2a) such that for  $dn = dN - \langle dN \rangle$ ,

$$\langle dn_1 \dots dn_Q \rangle = \rho(\underline{z}_1) d\underline{z}_1 \prod_{j=1}^{Q-1} \delta(\underline{z}_{j+1} - \underline{z}_j) d\underline{z}_{j+1}; \quad \langle dn_1 \rangle = 0; \quad (6.3)$$

e.g.,

$$\langle dn_1 dn_2 \rangle = \rho(\underline{z}_1) \delta(\underline{z}_2 - \underline{z}_1) d\underline{z}_1 d\underline{z}_2, \quad (6.3a)$$

where  $\rho(\geq 0)$  is the "process density," cf. (A.2-12). Thus, for the mean field  $\langle \alpha \rangle$  and field covariance  $K_\alpha$  we have, on applying (6.3) to (6.1), the familiar relations

$$\langle \alpha(\underline{R}, t) \rangle = \int_{\underline{Z}} \mathcal{L}(\underline{R}, t | \underline{z}) \rho(\underline{z}) d\underline{z}; \quad (6.4a)$$

$$K_\alpha(\underline{R}_1, t_1; \underline{R}_2, t_2) = \int_{\underline{Z}} \mathcal{L}(\underline{R}_1, t_1 | \underline{z}) \mathcal{L}(\underline{R}_2, t_2 | \underline{z}) \rho(\underline{z}) d\underline{z}, \quad (6.4b)$$

with analogous results for the higher moments. Since  $X = \hat{R}\alpha$ , cf. (2.4b), (5.1), the corresponding results for the received process  $X$  are

$$\left. \begin{aligned} \langle X(t) \rangle &= \int_{\underline{z}} L(t|\underline{z}) \rho(\underline{z}) d\underline{z}, \quad L = \hat{R}\mathcal{L} \end{aligned} \right\} \quad (6.5a)$$

$$\left. \begin{aligned} K_X(t_1, t_2) &= \int_{\underline{z}} L(t_1|\underline{z}) L(t_2|\underline{z}) \rho(\underline{z}) d\underline{z}. \end{aligned} \right\} \quad (6.5b)$$

The  $Q^{\text{th}}$ -order characteristic function (c.f.) is readily found to be ([10], [31], Part I)

$$\log F_Q(i\xi_1, \dots, i\xi_Q | \alpha_1, \dots, \alpha_n \text{ or } X_1, \dots, X_Q) =$$

$$\langle \int \rho(\underline{z}', z) [\exp\{i \sum_{\ell=1}^Q \xi_{\ell} (\mathcal{L}_{\ell} \text{ or } L_{\ell})\} - 1] dz \rangle_{\underline{z}'}, \quad (6.6)$$

where  $\underline{z} = (\underline{z}', z)$  and  $z = t/\bar{T}_S$  is a normalized time, with  $\mathcal{L}_1 = \mathcal{L}(R_1, t_1 | \underline{z})$ ,  $L_1 = L(t_1 | \underline{z})$ , etc. [The limiting gaussian cases follow formally from (6.6) by expanding the exponent through  $O(\xi_k \xi_{\ell})$  and dropping higher-order terms.] The associated  $Q^{\text{th}}$ -order probability density function (pdf) is formally, with  $y = \mathcal{L}$  or  $L$ :

$$w_Q(y_1, \dots, y_Q) = \int_{-\infty}^{\infty} \exp\{i \sum_{\ell} \xi_{\ell} y_{\ell}\} F_n(i\underline{\xi} | \underline{y}) \frac{d\underline{\xi}}{(2\pi)^Q}; \quad d\underline{\xi} = d\xi_1 \dots d\xi_Q, \text{ etc.} \quad (6.7)$$

Evaluating (6.7) based on (6.6) is generally nontrivial. Only the cases  $n = 1, 2$  appear analytically manageable, but fortunately  $w_1(y)$  is sufficient to give us useful results in signal processing applications, as we shall observe in Part II following. [The case  $Q = 2$ , e.g.,  $w_2(y_1, y_2)$  allows us to extend the "classical" theory of signals and noise through (zero-memory) nonlinear devices to include specific nongaussian noise processes and fields, as recent work has shown [10].] We remark that our ability to construct the field covariance (6.4b) allows us to estimate the degree of spatial processing gain ( $1 \leq M' \leq M$ ) attainable when the

field is nonuniform in space. Here  $M'$  is the estimated number (not necessarily integral) of effectively independent sensors, out of a total  $M$ , cf. comments in Sec. 1 above, and Refs. [3]-[5]; also Sec. 8.3 ff.

As a specific example, for the many "far-field" situations where it is meaningful to talk of beams and beam patterns, cf. Sec. 4.2, the basic (complex) field  $\mathcal{L}$  can usually be described (in the far-zone) by an expression of the form

$$\hat{\mathcal{L}} = \frac{\hat{S}_{OT}}{\lambda^\gamma} \int_{-\infty}^{\infty} \hat{S}_T(f|z_0) Q_T(\lambda|f) e^{i\omega \mu_d (t - \varepsilon - |R_0 - R|/c_0)} df, \quad (6.8)$$

where now  $\mathcal{L}$  in (6.1), (6.4), (6.6) is  $\mathcal{L} = \text{Re } \hat{\mathcal{L}}$ . Here the typical source is treated as essentially a point source, with a non-uniform beam pattern  $Q_T$ , Fig. 4.1, and  $\lambda = |R_0 - R|/c_0$ , with  $\lambda_m = |R_0 - r_m|/c_0$  the distance of the  $m^{\text{th}}$ -array element from the typical source, and  $\gamma > 0$ . Here, also,

$$\hat{S}_T(f|z) \equiv \left( \int_{-\infty}^{\infty} \int_{-\infty}^{\infty} a(t-\tau) s_T^*(\tau) e^{i\phi_a(t-\tau)} d\tau \right) e^{-i\omega t} dt, \quad \omega = 2\pi f, \quad (6.9)$$

represents the source waveform  $s_T^*$  with a fading mechanism,  $ae^{i\phi_a}$ ;  $\mu_d (\equiv 1 + \varepsilon_d) = \text{doppler coefficient in (6.8)}$ , while  $z (= \bar{T}_S t)$  is a (normalized) time, cf. (6.6).

From the above we can show, for instance, that the covariance of the interference output of the receiving array, i.e.,  $X(t) = \hat{R}\alpha$ , (4.12), becomes, for these sources narrow-band about frequency  $f_0$

$$K_1(\tau)_R = \frac{1}{2} B^2 A_{(A \text{ or } B)} \left\langle \frac{1}{R^{2\gamma}} \text{Re}[M_a(\tau) D_1(\omega_0)] \hat{K}_0(\tau) \langle |Q_R(\omega_0 - \omega_{OR}, f_0)|^2 \rangle_{\hat{f}_0} \right\rangle, \quad (6.10)$$

where  $M_a(\tau) = \text{complex covariance of the fading, } ae^{i\phi_a}$ ;  $D_1(\omega_0 \tau) = \langle e^{i\omega_0 \mu \tau} \rangle_{\varepsilon_d}$  is the doppler "smear" factor, and

$$\langle |Q_R|^2 \rangle_{\hat{f}_0} = \sum_{m, m'} \frac{A_m A_{m'}^*}{A^2} \langle e^{(2\pi i/\lambda_0)(\hat{f}_0 - \hat{f}_{OR}) \cdot (r_m - r_{m'})} \rangle_{\omega_0, \phi_0 \equiv \hat{f}_0} \quad (6.10a)$$

\*  $\hat{K}_0$  is the typical interfering source covariance (of  $s_T^*$ )

represents the averaged beam pattern, over all the different angles  $(\theta_0, \phi_0)$  of arrival of the various interfering source wavefronts;  $A_m$  = (complex) element weighting,  $A$  = normalization factor. For example, for an equally weighted vertical array (4.14a) when  $w_1(\theta_0, \phi_0) = 1/\pi^2$ ,  $-\pi/2 < \theta_0 \leq \pi/2$ ;  $0 \leq \phi_0 \leq \pi$ , i.e.,  $(\theta_0, \phi_0)$  are each uniformly distributed, for the  $mm'$  element in (6.10a) we get

$$\langle Q_R^{(m)} Q_R^{(m')*} \rangle_{\hat{\omega}_0} = e^{2\pi i \Delta_{mm'} \sin \theta_0 R} J_0(2\pi \Delta_{mm'}); \quad \Delta_{mm'} = (m-m')\Delta\ell/\lambda_0, \quad (6.10b)$$

where  $\Delta\ell$  is the interelement spacing and  $\lambda_0 (= 2\pi c_0/\omega_0)$ . Generally, the random angles of arrival "smear" the beams. Moreover, Eq. (6.10b) in (6.10a), (6.10) shows at once the (statistical) nonuniformity of these interference fields, as seen over a typical array, when the array is large enough, e.g.,  $2M\Delta\ell/\lambda_0 = L/\lambda_0 = O(1 \text{ or more})$  here, cf.  $J_0(2\pi\Delta_{mm'}/\lambda_0)$  in (6.10c), etc.: the field covariance as sampled by the array elements is clearly quite nonuniform. [We shall return to this point in Sec. 7.3 ff.]

## 6.2 Non-Gaussian Process PDF's

As we have emphasized in previous work [4], [6]-[8], [10], [13], [15], [16], [52], involving EMI interference, and analogously here for underwater acoustic applications, most noise environments can be characterized in three main classes of nongaussian process or field: \* Class A, or "coherent" noise, producing negligible transients in a typical receiver; Class B, "impulsive," i.e., broadband vis-à-vis the receiver, generating transients; and Class C = Class A + Class B, in various combinations. Typically, Class A--for example, reverberation, ship noise, etc.--or Class B (biologic (shrimp), ambient ice, microseisms, impulsive ship noise, etc.), predominate in most instances.

-----  
\*An important exception is the case of one (or a small number) of interfering signal sources of known emission behavior, whose deleterious effects can often be removed by selective temporal ( $\equiv$  frequency) or spatial deletion.

For our subsequent detection and estimation algorithms (Part II ff.), we shall need a more sophisticated statistic than just the process or field covariance functions, although these are always useful. Specifically, we shall need the (first-order) probability density of the (total) interference,  $X(t)$ ,  $w_1(x|H_0)$ , as obtained from (6.7), since we are going to sample in such a way as to produce independent noise samples, cf. Sec. 7 ff. For this we set  $Q=1$  in (6.6) and carry out the resulting evaluations, along the lines described in [6], [8]. The result, finally, for Class A interference is found to be, typically, at the  $m^{\text{th}}$ -array element now

$$F_1(i\xi|X^{(m)})_{A+G} = e^{-\sigma_G^{(m)2} \xi^2/2-A_A} e^{A_A e^{-\xi^2 \Omega_{2A}^{(m)}/2}} [1 + \psi_1^{(m)}(\xi^2)_A], \quad (6.11)$$

where  $\sigma_G^{(m)2}$  = mean intensity of the gaussian component,  $\Omega_{2A}^{(m)}$  = mean intensity of the (usually much stronger) nongaussian interference, both at the  $m^{\text{th}}$ -array element. Here because of the assumed (local) homogeneity of the noise field,  $\sigma_G^{(m)} = \sigma_G$ ,  $\Omega_{2A}^{(m)} = \Omega_{2A}$ ;  $A_A$  = overlap index or "usage" parameter [7], which is typically  $O(0.1-1)$  for nongaussian underwater acoustic interference. The quantity  $\psi_1^{(m)}$  is a correcting factor, which can noticeably modify the "tails" of the associated pdf, cf. (6.11), (6.12), when the potentially interfering sources are widely distributed in space ("Quasi-canonical" cases, [8]).

When these sources are not so widely distributed,  $\psi_1 \doteq 0$ , and we have the more familiar "canonical" and approximately canonical Class A cases. For these latter the pdf associated with (6.11) is

$$w_1(x_{m,n}|H_0)_{A+G} = e^{-A_A} \sum_{p=0}^{\infty} \frac{A_A^p}{p! \sqrt{4\pi\sigma_{pA}^2}} e^{-x_{mn}^2/4\sigma_{pA}^2}, \quad (6.12)$$

where  $\Gamma_A' = \sigma_G^2/\Omega_{2A}$ ;  $2\sigma_{pA}^2 = (p/A_A + \Gamma_A')/(1+\Gamma_A')$ , and  $x_{m,n} = x_{m,n}/\sqrt{\Omega_{2A}(1+\Gamma_A')}$  is the normalized input data sample, at array element  $m$  and at time  $t_n$ .

(For the "anatomy" of the noise parameters  $\Gamma'_A$ ,  $\Omega_{2A}$ , see [7], [8].)

Class B interference is similarly developed: we find that [6]

$$w_1(x_{m,n}|H_0)_{B+G} = \frac{e^{-x_{\min}^2/\Omega}}{\pi\sqrt{\Omega}} \sum_{p=0}^{\infty} \frac{(-1)^p}{p!} A_{\alpha}^p \Gamma\left(\frac{p\alpha+1}{2}\right) {}_1F_1\left(-\frac{p\alpha}{2}; \frac{1}{2}; \frac{x_{m,n}^2}{\Omega}\right).$$

(6.13)

Here  $\alpha = \frac{2-\mu}{\gamma}$  is a parameter based on source distribution ( $\sim \lambda^{-\mu}$ ) and propagation law ( $\sim \lambda^{-\gamma}$ ), while  $\Omega$  is a normalization factor [chosen to cut off the tails of (6.13) at some very small residual probability and insure that  $\int w_1 dx = 1$ : (6.13) does not support a finite intensity, e.g.,  $\overline{x^2} \rightarrow \infty$ , unless the pdf is suitably truncated.]

Finally, we emphasize again the canonical nature of these nongaussian models: the forms of the pdf's are independent of the particular noise mechanisms involved. Of course, for specific applications, we must estimate the relevant parameter values and insert them appropriately in the chosen algorithm. Thus, we may say that signal processors based on these noise models are parametrically adaptive, based on the above statistical-physical models of the acoustic noise or interference environment.

### 6.3 Summary Remarks (Part I)

In the preceding sections (Part I) we have outlined a formal apparatus, illustrated by some simple examples and specific results. This apparatus provides a general approach for obtaining the needed noise, signal fields, and received process models, which constitute the inputs to our subsequent signal processors, namely, signal detectors and estimators. Key features of these inputs which must be taken into account are (i) the generally nongaussian character of the accompanying noise, or additional acoustic interference from localized sources; (ii) the spatial, as well as temporal character of the noise and signals; (iii) the salient features of propagation in a typically inhomogeneous medium which includes discrete, continuous, and distributed inhomogeneities; and (iv) the spatial coupling to the medium itself. The controlling factors, as always, are ultimately physical. These, in turn, may be expected to impact strongly upon the



design and operation of the subsequent signal processing, as we shall see in Part II following. Finally, but not least, we stress again the direct analogy between the underwater acoustic field and process models outlined here and corresponding EMI models developed for telecommunication applications: the formal structures, and ambient noise models (neglecting multiple scatter) are the same, as are the basic processing concepts, so that results from the latter discipline can be translated to the former, with appropriate attention to the governing physics. In any case, our approach emphasizes the concept of the generalized channel, in the manner of Fig. 2.1 above, where in addition to propagation questions, we include the necessarily coupled signal processing ones, centered on the critical limiting threshold cases.

## Part II. Acoustic Threshold Signal Processing

### 7. Threshold Signal Detection

We are now ready to outline the aforementioned canonical approaches to signal processing, when the desired signal is weak compared to the noise background. Here, of course, the desired signal (and undesired noise) are the received, scattered and/or ambient acoustic fields, now sampled by our distributed arrays (cf. Sec. 4.2). Our principal tasks are to detect a desired signal, and then, having determined its existence in the accompanying noise, to extract some one or more desired attributes of the signal, namely, to perform so-called "signal estimation."

As before [7], [15], [16], we focus our attention primarily on the "on-off" threshold, or weak-signal detection situation, involving now nonuniform interference fields ( $I$ ), where the decision process is the hypothesis test:  $H_1: S \oplus I$  vs.  $H_0: I$  alone. A canonically optimum theory is again possible: canonical in the sense that the formal results for detector structures and performance are independent of any detailed physical mechanism, as well as of specific signal waveforms and noise statistics [16]. Although the results are no longer optimum for stronger signals, they are generally absolutely better than for weak signals, which in turn is normally satisfactory for applications. Moreover, an optimal

theory suggests reasonable suboptimum procedures which can have the advantage of structural and operational simplicity, as well as performance close to optimum [15], [16].

Three modes of detection are noted: (i) coherent, when signal epoch is known precisely at the receiver; (ii) incoherent, when signal epoch is unknown; and (iii) composite, in which a sum of modes (i) and (ii) is employed, to take advantage of any signal epoch information available [16]. Since weak signals are postulated, large processing gains (here space-time-bandwidth products  $J$ ) are needed to achieve acceptably small probabilities of decision error. This ensures that the detection algorithm in question will be asymptotically optimum (AO) (as  $J \rightarrow \infty$ , or  $J \gg 1$  practically), and normally distributed under  $H_0$ ,  $H_1$  provided a suitable bias term  $B_j^*$  (independent of the data and determined a priori) is employed. (The importance of the proper bias, generally, is stressed in [16].) These results enable us to calculate performance directly in canonical form.

For specific applications we must, of course, "calibrate" our canonical algorithms to the particular interference environment. This requires establishing: (1) the Class (A, B, or C) of interference, and (2) estimating the relevant parameters of the associated probability densities  $w_1(x)_A$ ,  $w_1(x)_B$ , etc., [15], [54]. This can be done if we can construct the EMI scenario, for example [4], [8], or directly by empirical observation [6], [7]. Thus, these (detection) systems are adaptive and include adaptive beam-forming here. Their often considerable improvement over conventional (i.e., "matched-filter" or correlation) detectors stems from this essential feature, [7], [16].

In this necessarily concise overview we confine our effort to an outline of some of the principal results of the extensions of our earlier work to include spatial processing [3], [4]. The present section is organized as follows: Sections 7.1-7.4 provide examples of general and specific space-time processing algorithms, the latter for independent sampling; [Section 6 earlier presents some results for nongaussian field models]. Section 8 ff. treats performance, in both optimum and suboptimum cases. Section 8.3 completes our detection treatment here, with a brief discussion of the principal assumptions and conditions.

### 7.1 Canonical Space-Time Threshold Algorithms

To obtain the desired optimum (binary) decision algorithms  $\mathfrak{L}_J^*$  we form first, as usual [20], [54], the generalized likelihood ratio, now extended to include spatial as well as temporal sampling, e.g.,

$$\mathfrak{L}_J^* \equiv \log \Lambda_T(\underline{x}|\theta) = g_J^*(\underline{x}|\theta) + t_J^*(\underline{x}|\theta), \quad (7.1)$$

where  $J = MN$ , with  $N$  = number of temporal samples of the received data  $\underline{x} = (x_1 \dots x_{j=mn} \dots x_J)$ , at each of the  $M$  sensors, e.g.,  $\underline{x}_m = (x_{m1}, \dots, x_{mn=j}, \dots, x_{mN})$ , with  $j = 1, \dots, mn, \dots, J=MN$ , alternatively, over all sensors. Here  $\theta$  denotes an input signal-to-noise ratio;  $g_J^*$ ,  $t_J^*$  are respectively the desired algorithm and a remainder series, which vanishes prob. 1 under  $H_0$ ,  $H_1$  if certain conditions are satisfied [cf. Sec. 7.4 ff.].

For these threshold cases  $\log \Lambda_J$  is expanded about  $\theta = 0$ , with one or two terms in the data  $(\underline{x})$  retained, depending on the mode of reception. The required bias term,  $B_J^*(\theta)$ , is obtained from the average over  $\{\underline{x}\}$  with respect to the null hypothesis  $H_0$  of the next nonvanishing term in the  $g_J^*$ -expansion. Thus, we write formally

$$\mathfrak{L}_J^* = g_J^* = \theta F_1(\underline{x})_J + \frac{\theta^2}{2!} F_2(\underline{x})_J + O(\theta^3, \theta^4), \quad (7.2)$$

where for the coherent and incoherent detection modes we have

$$g_J^*(\underline{x})_{\text{coh}} = \theta F_1(\underline{x})_J + B_J^*(\theta^2)_{\text{coh}}; \quad B_{J-\text{coh}}^* = \frac{\theta^2}{2!} \langle F_2(\underline{x})_J \rangle_{H_0} + \log \mu; \quad (7.3a)$$

$$g_J^*(\underline{x})_{\text{inc}} = \frac{\theta^2}{2!} F_2(\underline{x})_J + B_J^*(\theta^4)_{\text{inc}}; \quad B_{J-\text{inc}}^* = \langle O(\theta^4; \underline{x}) \rangle_{H_0} + \log \mu. \quad (7.3b)$$

The specific structure of  $F_1$ ,  $F_2$  depends, data-wise, on the basic pdf  $w_J(\underline{x}|\theta=0)$  of the interference alone, and on the desired signal waveform structure. Here  $\mu = p/q$ ,  $p+q=1$ , ( $p, q > 0$ ), where  $p, q$  are respectively the a priori probabilities that the data sample  $\underline{x}$  contains (or does not contain) a signal. The decision process  $(\delta)$  is

$$\underline{\text{decide } H_1 \text{ if } g_J^* \geq \log K} \quad \text{or} \quad \underline{\text{decide } H_0 \text{ if } g_J^* < \log K} \quad (7.3c)$$

where  $K$  is a threshold in the usual way.

Both because of much needed technical simplicity, and the fact that it can be shown [4] that comparatively little further improvement in performance is obtained by fully correlated sampling vis-à-vis (non-sparse) independent (space and time) sampling, we focus henceforth on this latter case. Moreover, although the theory has been developed for the general case of nonstationary and inhomogeneous fields [4], we shall describe results here only for the (often) applicable local stationary, homogeneous régimes.

## 7.2 LOBD Algorithms

Locally optimum Bayes detector (LOBD) algorithms for coherent and incoherent detection are found under the above detection modes (7.3a), (7.3b) to be explicitly [4]:

### A. Coherent Detection

$$g_J^*(x)_{\text{coh}} = B_{J\text{-coh}}^* - \sum_{m=1}^M \sum_{n=1}^N \ell(x_{m,n}) \langle \theta_{m,n} \rangle, \quad J = MN \quad (7.4)$$

with

$$\langle \theta_{m,n} \rangle = \langle a_{on} s_n^{(m)} \rangle; \quad \ell(x_{m,n}) \equiv \left. \frac{d}{dx} \log w_1(x|H_0) \right|_{x=x_{m,n}} \quad (\equiv \ell_{m,n}). \quad (7.4a)$$

### B. Incoherent Detection

$$g_J^*(x)_{\text{inc}} = B_{J\text{-inc}}^* + \frac{1}{2!} \sum_{m,m'}^M \sum_{n,n'}^N \{ \ell_{m,n} \ell_{m',n'} + \ell'_{m,n} \delta_{mm'} \delta_{nn'} \} \langle \theta_{m,n} \theta_{m',n'} \rangle, \quad (7.5)$$

where now

$$\langle \theta_{m,n} \theta_{m',n'} \rangle = \overline{a_0^2} \hat{m}_{|n-n'|}^{(mm')} \quad (7.5a)$$

with

$$\hat{m}_{|n-n'|} \equiv \overline{a_{on} a_{on'}} / a_0^2 ; \quad \rho_{|n-n'|}^{(m-m')} \equiv \langle s_n^{(m)} s_{n'}^{(m')} \rangle , \quad (7.5b)$$

and

$$\ell'_{m,n} = \left. \frac{d\ell}{dx} \right|_{x=x_{m,n}} , \quad \text{cf. (7.4a).}$$

In the above,  $s_n^{(m)} = s^{(m)}(t_n)$  is the normalized signal waveform at time  $t_n$  at the  $m^{\text{th}}$ -sensor, with  $\langle s_n^{(m)2} \rangle = 1$ ;  $a_{on}^{(m)} = a_{on} = a_o(t_n)$  here (signal field uniform over the array), with  $a_{on} = A_o(t_n)/\sqrt{2\psi}$ , in which  $\psi = I(I' + N)$  is the sum of the intensities (at the receiving aperture) of the nongaussian interference  $I'$  and gaussian noise  $N$ . (Here  $\psi_n^{(m)} \rightarrow \psi$ , because of the postulated homogeneity and stationarity, cf. above.) The normalized data samples are  $x = x_{j=m,n}/\sqrt{\psi}$ , with the desired signal vector  $\underline{s} = \{\underline{s}^{(m)}\} = \{a_{on}^{(m)} s_n^{(m)} / \sqrt{\psi}\}$ . Here  $w_1$  is the first-order pdf of the total interference: because of independent sampling  $w_j = \prod_{m,n} w_1(x_{m,n})$ .

### 7.3 Signal Structures for Coherent and Incoherent Reception

Specifically, we note also that in realistic situations involving fading and doppler uncertainties the desired signal structure is

$$s_n^{(m)} = \sqrt{2} \cos\{(\omega_0 + \omega_d)(t_n - \epsilon_0) - \omega_0 \Delta\tau_m - \phi_n\} , \quad t_n = n\Delta t \quad (7.6)$$

where  $\omega_d$  = random doppler shift,  $\epsilon = \epsilon_0$  = signal epoch which is a priori known in coherent detection;  $\phi$  = possible phase modulation, for the typical narrow-band signals used in most acoustic environments. The net path delay,  $\Delta\tau_m$ , from the  $m^{\text{th}}$ -element to some selected reference point associated with the array, is given by

$$\Delta\tau_m \equiv (\hat{\underline{r}}_0 - \hat{\underline{r}}_{0R}) \cdot \underline{r}_m / c_0 = (\underline{v}_0 - \underline{v}_{0R}) \cdot \underline{r}_m / f_0 , \quad (\underline{v} \equiv \hat{\underline{r}}/\lambda_0 ; c_0 = \lambda_0 f_0) \quad (7.7)$$

where  $\hat{\underline{r}}_0, \hat{\underline{r}}_{0R}$  are respectively the unit vectors in the direction of the (incoming) signal wavefront, and the main axis of the beam formed by

the equivalent spatial alignment of the  $M$  elements;  $\underline{r}_m$  is the (vector) distance from the  $m^{\text{th}}$ -element in the array to the reference point. Thus, when the beam is steered to the signal direction,  $\hat{\underline{i}}_{OR} = \hat{\underline{i}}_0$ , cf. Fig. 4.1, and  $\Delta\tau_m = 0$ , so that  $s_n^{(m)} = s_n$ : the sampled signal component is now independent of  $m$  in (7.4), (7.4a) above, for coherent detection.

For the incoherent cases (7.5), (7.5a,b), (where  $\epsilon_0$  is now random), we have, for a fixed signal wavefront direction,

$$\rho_{|n-n'|}^{(mm')} = e^{-[\Delta\omega_d(n-n')\Delta t]^2/2} \cos[\omega_0(n-n')\Delta t + k_0(\hat{\underline{i}}_0 - \hat{\underline{i}}_{OR}) \cdot \underline{\Delta r}_{mm'}],$$

$$k_0 = 2\pi/\lambda_0 = \omega_0/c_0 \quad (7.8)$$

with  $\underline{\Delta r}_{mm'} \equiv \underline{r}_m - \underline{r}_{m'}$ , and there is no degradation of the beam pattern. This signal correlation function,  $\rho_{|n-n'|}^{(mm')}$ , is clearly maximized (when summed over  $m, m'$ , in (7.5), for example) when the receiving beam is pointed at the normal ( $\hat{\underline{i}}_0$ ) to the incoming signal wavefront, e.g.,  $\hat{\underline{i}}_0 = \hat{\underline{i}}_{OR}$ . Thus,  $\rho_{|n-n'|}^{(mm')} = \rho_{|n-n'|}$ , also. Alternatively, when the desired signal wavefront is perturbed, arriving from various different directions, beam structure is destroyed and  $\rho_{|n-n'|}^{(mm')}$  is much reduced, with a consequent serious degradation of performance [cf. (6.10b) and Sec. 8 ff.]. Doppler smearing ( $\Delta\omega_d \geq \epsilon \neq 0$ ), of course, always reduces the wavefront (and waveform) coherence of the desired signal [cf. (7.6), (7.8)], similarly degrading performance, as one would expect [cf. Sec. 6.1 above].

Finally, we note that because of the postulate of independent sampling, space and time processing are interchangeable operations, cf. (7.4), (7.5): we can process over the array ( $m=1, \dots, M$ ) at any given instant ( $t_n$ ), or equivalently, at each array element ( $m$ ), over time ( $n=1, \dots, N$ ). The choice is a matter of technical convenience. In addition, we observe that for coherent detection, (7.4), (7.6), (7.7), single beams are formed ( $\sim s_n^{(m)}$ ), while in incoherent detection product beams are generated ( $m, m'$ ) in (7.5).

#### 7.4 The Bias and Asymptotic Optimality (AO)

As explained above, cf. (7.3a,b), the bias terms for  $g_j^*$  are found here to be

$$\hat{B}_{J\text{-coh}}^* = -\frac{L^{(2)}}{2} \sum_{m=1}^M \sum_{n=1}^N \langle a_{on}^{(m)} \rangle^2 \langle s_n^{(m)} \rangle^2 \quad (7.9)$$

generally. With fading and doppler smear (7.9) becomes

$$B_{J\text{-coh}}^* = \log \mu \equiv \hat{B}_{J\text{-coh}}^* = -a_0^2 (1-\eta) M N L^{(2)} H_1(N \Delta t \Delta \omega_d), \quad (7.9a)$$

where  $0 \leq 1-\eta \leq a_0^2 / \langle a_0^2 \rangle < 1$  is a fading parameter (no fading:  $\eta = 0$ ; deep fading:  $\eta = 1$ ), and

$$H_1(x) \equiv \sqrt{\pi} \Theta(x) / 2x, \text{ with } \Theta(x) = (2/\sqrt{\pi}) \int_0^x e^{-t^2} dt = \text{erf } x, \quad (7.9b)$$

represents the effects of doppler smear.

Similarly, for the incoherent cases one gets

$$B_{J\text{-inc}}^* = -\frac{1}{8} \sum_{m,m'}^M \sum_{n,n'}^N \{ (L^{(4)} - 2L^{(2)^2}) \delta_{mm'} \delta_{nn'} + 2L^{(2)^2} \} \rho_{|n-n'|}^{(mm')} \hat{m}_{|n-n'|}^{(m,m')} \cdot \langle a_0^{(m)} a_0^{(m')} \rangle \langle s_n^{(m)} s_n^{(m')} \rangle \quad (7.10)$$

which reduces for rapid (one-sided) fading and negligible doppler to

$$B_{J\text{-inc}}^* = \log \mu \equiv \hat{B}_{J\text{-inc}}^* = -a_0^2 \left\{ \frac{M N (1-\eta) L^{(2)}}{2} \right\}^2. \quad (7.10a)$$

(For no or slow fading one sets  $\eta = 0$  in (7.10a).) The result (7.10a) assumes  $N \gg 1$  ( $M \geq 1$ ) and the usual nongaussian noise situation  $L^{(4)} \approx 2L^{(2)^2}$ , where specifically [4], [16]

$$L^{(2)} \equiv \langle x^2 \rangle_{H_0}, \text{ all } m, n, = \int_{-\infty}^{\infty} (w_1'/w_1)^2 w_1 dx, > 0, \text{ cf. (7.4a);} \quad (7.11a)$$

$$L^{(4)} \equiv \int_{-\infty}^{\infty} (w_1''/w_1)^2 w_1 dx (> 0). \quad (7.11b)$$

Thus,  $L^{(2)}$ ,  $L^{(4)}$  are statistics of the (total) interference,  $I$ , including the gaussian noise component.

For asymptotic optimality, ("A0" as  $J \rightarrow \infty$ , or  $J \gg 1$ ) a sufficient condition--always fulfilled for small ( $> 0$ ) input signals, e.g.,  $1 \gg \overline{a_0^2} > 0$ --is that

$$\text{var}_{H_0} g_J^* \equiv \langle (g_J^*)^2 \rangle_0 - \langle g_J^* \rangle_0^2 \equiv (\sigma_{0J}^*)^2 = -2\hat{B}_J^* \quad (\doteq \text{var}_{H_1} g_J^*). \quad (7.12)$$

As noted above, this permits us to terminate the expansion (7.1) in the form (7.2), for large  $J(=MN)$ , and still ensure the desired small probabilities of decision error in the decision process (7.3c). [An equivalent (sufficient) condition for A0 is that  $g_J^*$ , as  $J \rightarrow \infty$ , is gaussian, with variance  $(\sigma_{0J}^*)^2$  and means  $\log \mu \mp (\sigma_{0J}^*)^2/2$  under  $H_0, H_1$  respectively, cf. Sec. 2B of [16].] (In most earlier work the proper bias was omitted, cf. Secs. IIb, IV, VA of [16], so that the resulting detection algorithms are neither locally optimum nor A0.)

### 7.5 Suboptimum Algorithms

Suboptimum algorithms are handled in the same general fashion. Instead of the quite complex characteristics  $(\sim \ell_{m,n})$  in  $g_J^*$ , (7.4), (7.5) one can use much simpler forms: for the simple correlator one sets  $\ell_{m,n} \rightarrow x_{m,n}$ , and for the hard-limiter correlator,  $\ell_{m,n} \rightarrow \text{sgn } x_{m,n}$  (with the  $\ell'_{m,n}$  term omitted in (7.5)). The former is well-known to be (threshold) optimum generally in gauss noise,  $w_1(x) = e^{-x^2/2}/\sqrt{2\pi}$ , while the latter is threshold optimum in Laplace noise,  $w_1(x) = (\sqrt{2})^{-1} \exp(-\sqrt{2}|x|)$ ,  $\langle x^2 \rangle = 1$ ;  $\langle x \rangle = 0$ , cf. Sec. III of [11].

## 8. Threshold Detector Performance

Because of the large samples involved ( $J = MN \gg 1$ ) and their independence, the test statistic  $g_J^*$  is asymptotically normally distributed, under both  $H_0$  and  $H_1$  with  $\text{var}_{H_0} g_J^*$ , provided the input signal is suitably small [cf. (7.12) and II,B of [16], etc.]. This permits a direct calculation of performance. For the important detection cases here, we have the familiar Neyman-Pearson (N.P.) form [15] of the probability of correctly detecting the presence of a desired signal:



$$P_D^{(*)} \approx \frac{p}{2} \{ 1 + \Theta \left[ \frac{\sigma_{0J}^{(*)}}{\sqrt{2}} - \Theta^{-1}(1 - 2\alpha_F^{(*)}) \right] \} , \quad (8.1)$$

where  $\alpha_F^{(*)}$  is the (conditional) false alarm probability of incorrectly deciding the signal is present when only noise occurs, again  $\Theta(x) = \text{erf } x$ , cf. (7.9a), and

$$\sigma_{0J}^{(*)} = \sqrt{\text{var}_{H_0} g_J^{(*)}} . \quad (8.2)$$

For suboptimum detectors we drop the superscript \*. Explicitly,  $\alpha_F^{(*)}$  is given by

$$\alpha_F^{(*)} \approx \frac{1}{2} \left\{ 1 - \Theta \left[ \frac{\sigma_{0J}^{(*)}}{2\sqrt{2}} + \frac{\log(K/\mu)}{\sqrt{2} \sigma_{0J}^{(*)}} \right] \right\} ; \quad (8.3)$$

for  $\mu$ , cf. Eq. (7.3) et seq. In the usual applications,  $\mu = 1$ , i.e.,  $p = q = \frac{1}{2}$ . (In communication applications, when the decision criterion in the so-called Ideal Observer [15], [16],  $\mu = 1$  also, i.e.,  $p = q = \frac{1}{2}$  and one has a symmetric "on-off" channel for which the error probability (per decision or per baud, symbol, etc.) is now

$$P_e^{(*)} = pp_e^{(*)} \approx \frac{1}{2} \left\{ 1 - \Theta \left[ \frac{\sigma_{0J}^{(*)}}{2\sqrt{2}} \right] \right\} [\mu = 1; K = 1]. \quad (8.4)$$

### 8.1 Performance Examples

The key element in measuring performance is clearly  $\sigma_{0J}^{(*)}$ , cf. (8.1)-(8.4). We list below a variety of specific forms for  $\sigma_{0J}^{(*)}$ :

A. Coherent Detection:  $(\sigma_{0J}^{*})_{\text{coh}}^2 = 2\bar{a}_0^2(1-\eta)\text{MNL}^{(2)}_{H_1}(N\Delta t\Delta\omega_d) \equiv 2\bar{a}_0^2 \Pi_{\text{coh}}^{*}$ , (8.5)

cf. [4], [15], [16].

B. Incoherent Detection [4]:  $(\sigma_{0J}^{*})_{\text{inc}}^2 = 2\bar{a}_0^2 \left[ \frac{\text{MNL}}{8} L^{(4)}_{+2L} \right]^{(2)}_{(11Q_N-1!)} \equiv 2\bar{a}_0^2 \Pi_{\text{inc}}^{*}$ , (8.6)

where  $Q_N$  is the signal structure factor, which in these stationary, homogeneous cases becomes explicitly

$$Q_N \equiv 1 + \frac{1}{N} \sum_{n,n'}^N \hat{m}_{|n-n'|}^2 \rho_{|n-n'|}^2; \quad \hat{m}_0 = \hat{m}_{0R}, \quad \text{cf. (7.8) et seq.,} \quad (8.6a)$$

which is maximized when the beam formed is directed at the desired signal source.

Here  $\Pi^*$  is the space-time-bandwidth product, and the  $\overline{a_0^2}$  factor is defined as the minimum detectable signal,  $\langle a_0^2 \rangle_{\min}^*$ .

Evaluation of  $Q_N$  for various conditions of doppler "smear" and fading gives results like [4]:

$$(\sigma_{0J}^*)_{\text{inc}}^2 \left| \begin{array}{l} \text{2-sided, slow-fading;} \\ \text{coherent signal } (\Delta\omega_d \neq 0) \end{array} \right. \doteq \overline{a_0^2}^2 (MNL^{(2)}/2)^2 \doteq (\sigma_{0J}^*)_{\text{inc}}^2 \left| \begin{array}{l} \text{1-sided, no,} \\ \text{slow; coh. sig.} \end{array} \right. \quad (8.7a)$$

$$(\sigma_{0J}^*)_{\text{inc}}^2 \left| \begin{array}{l} \text{1-sided, very rapid;} \\ \text{coh. sig.} \end{array} \right. \doteq \overline{a_0^2}^2 \{MN(1-n)L^{(2)}/2\}^2. \quad (8.7b)$$

In all cases here we note that  $\sigma_{0J}^* \sim \sqrt{J}$ : increasing the "space-time-bandwidth product" by increasing the number of both the independent spatial and temporal samples (M,N) clearly improves performance, from (8.1), (8.4).

It is usually convenient to relate the probability controls, here  $p_D^{(*)}$ , to the processing gain,  $\Pi^{(*)}$ , and minimum detectable signal,  $\langle a_0^2 \rangle_{\min}^*$ , by means of the following relations, obtained from (8.5), (8.6) in (8.7), (8.4), viz.:

$$\langle a_0^2 \rangle_{\min\text{-coh}}^{(*)} = (C_{N.P.}^{(*)})^2 / \Pi^{(*)}; \quad \langle a_0^2 \rangle_{\min\text{-inc}}^{(*)} = C_{N.P.}^{(*)} / \sqrt{\Pi^{(*)}}, \quad (8.8)$$

where  $\frac{(*)}{N.P.} \equiv 0^{-1}(2p_D^{(*)}-1) + 0^{-1}(1-2p^{(*)}) = \sigma_{0J}^{(*)}/\sqrt{2}$  specifically. From (8.8) vs. (8.5), (8.6) we find  $\Pi^*$  at once.

For nongaussian noise fields  $L^{(2)}$ ,  $L^{(4)}$  can be quite large  $O(10^4, 10^8)$ , typically, for, say, Class A noise with  $A_A = 0.3$ ,  $\Gamma_A = 10^{-5}$ . Similar orders of magnitude are noted for typical Class B cases; ([9]; see Figs. 4-7 of [16]). However, for gaussian noise  $L^{(2)} = 1$ ,  $L^{(4)} = 2$ .

Figure 8.1 shows the probability of detection,  $p_D^{(*)}$ , versus the minimum detectable signal,  $\langle a_0^2 \rangle_{\min}^{(*)}$ , with processing gain  $\Pi^{(*)}$  as parameter,

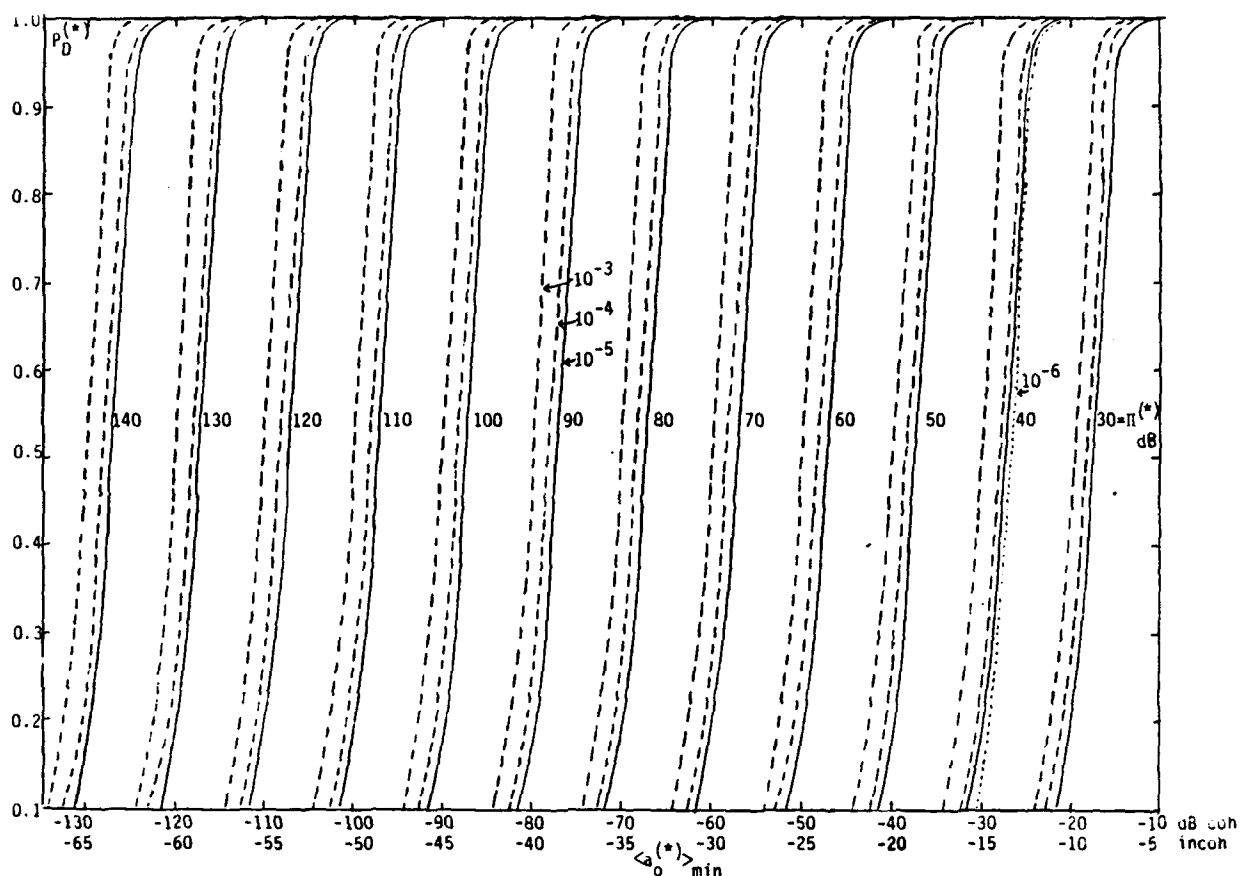


Figure 8.1 Probabilities  $P_D^{(*)}$  of detection (8.1) for both coherent and incoherent reception, with processing gain as parameter, for false alarm probability  $\alpha_F^{(*)} = 10^{-3}, 10^{-4}, 10^{-5}$ .

for various levels of false alarm probability:  $\alpha_F^{(*)} = 10^{-3}, 10^{-4}, 10^{-5}$ . Clearly, coherent detection is better, by a factor 2 in dB, than incoherent detection with the same processing gain, cf. (8.5) vs. (8.6). For example, with a processing gain of 80 dB,  $\alpha_F^{(*)} = 10^{-3}$ , and a required  $p_D^{(*)} = 0.80$ , we see that  $\langle a_0^2 \rangle_{\min\text{-coh}}^{(*)} = -33$  dB, while  $\langle a_0^2 \rangle_{\min\text{-inc}}^{(*)} = -66$  dB.

## 8.2 Remarks on Suboptimum Performance

The performance of suboptimum systems is readily obtained canonically (in the threshold régime) if we define a degradation factor  $\phi_d$  by the ratio

$$\phi_d \equiv \pi/\pi^* \quad , \quad (8.9)$$

Here  $\Pi$  is the processing gain for a suboptimum detector, employed against the same (not necessarily gaussian) noise. This factor,  $\phi_d$ , measures by how much the minimum detectable signal for the suboptimum system must be raised vis-à-vis that of the optimum to achieve the same performance,  $P_D = P_D^*$  (or  $p_D = p_D^*$ ), viz.  $\sigma_{oJ} = \sigma_{oJ}^*$  in (8.1), so that

$$\langle a_o^2 \rangle_{\text{min-coh}}^* = \langle a_o^2 \rangle_{\text{min-coh}} \phi_{d\text{-coh}}; \quad \langle a_o^2 \rangle_{\text{min-inc}}^* = \langle a_o^2 \rangle_{\text{min-inc}} \sqrt{\phi_{d\text{-inc}}}. \quad (8.10)$$

For example, for a coherent detector optimized against gauss noise,  $L^{(2)} = 1$  in (8.5), so that  $\phi_d = (L^{(2)})^{-1} \ll 1$  measures the degradation when such a detector is used in strongly nongauss noise instead of one properly "matched" to this noise. Thus, if  $\Gamma_A' = 10^{-5}$ ,  $A_A = 0.3$ , we have  $L_A^{(2)} = 50$  dB, Fig. 4, [16], so that the optimum detector can detect a minimum detectable signal 50 dB less than the correlation detector in this noise. In a similar way, two suboptimum detectors can be compared:  $\phi^{(1 \text{ vs. } 2)} \equiv \Pi^{(1)}/\Pi^{(2)} = \phi_d^{(1)}/\phi_d^{(2)}$ . The quantity  $\sqrt{\phi_d}$  is also seen to be equal to the Asymptotic Relative Efficiency (ARE,  $\theta > 0$ ). [See Section IV,B of [16].]

### 8.3 Discussion: Threshold Detection

In the preceding sections we have sketched some of the main results for the development of optimum threshold detection in nongaussian and nonuniform EMI fields. This extends earlier work, [55]-[57], for example, to include in addition to the nongaussian field, the often important situation where the fields received by an antenna (array) are not uniform over the array elements, basically because of the size of the antenna vis-à-vis the wavelengths of the received fields. In addition, we have outlined briefly various elements in the construction of statistical physical models of the acoustic field, including the needed pdf's.

Our analysis has postulated independent (noise) samples in space and time. The latter are practically achievable without much difficulty by slightly increasing the sampling period ( $O(50\%)$ ). Independent spatial sampling, however, is not generally possible with non-sparse arrays, because of the non-uniformity of the noise-field and unequal

spacing of the zeros of the correlation functions of this field, cf. (6.10), (6.10a,b). In practice, this means that effectively one may have  $1 \leq M' < (<)M$  equivalent "independent" spatial samples: some spatial processing improvement over a single element (or single beam,  $M=1$ ) is obtainable, but not the full  $M$ -factor theoretically achievable if independent spatial sampling is truly obtained. Nevertheless, for such noise fields as (6.10) (in addition to improving beam resolution), it can be worthwhile to use relatively large arrays (vs.  $\lambda_0$ ), as  $M' > 1$ , and  $\therefore \sigma_{0J}^* \sim \sqrt{M'N'}$ , cf. (8.5), (8.6), is larger than  $\sigma_{0N}^* = \sqrt{N}$ ,  $M=1$ .

Of course, algorithms like (7.4), (7.5) are not optimum when the sampling is not independent, but they are comparatively close: preliminary estimates for typical Class A interference indicate that only  $O(2-3 \text{ dB})$  improvement is theoretically obtainable if all correlations were taken into account, i.e., if one uses the  $J$ -joint pdf  $w_J(\underline{x})_N$  rather than  $\prod_{j=1}^J w_1(x_j)$  for the basic pdf used in the general expansions (7.2)-(7.3b) above. This is one compelling argument for developing "independent-sample" algorithms; another is that there are no tractable, or known  $J^{\text{th}}$ -order models ( $J > 1,2$ ) for the underlying pdf,  $w_J$ .

It is instructive to observe that beam-forming is automatically achieved on setting the relative path delays  $\Delta\tau_m$ , (7.7), equal to zero, regardless of the particular geometrical locations of the array elements. Thus, we can have arbitrary distributions of elements, but still reconstruct the desired signal wavefront by proper delays (i.e., maximize  $\rho^{(mm')}$ , cf. (7.8)). Beams formed here in this manner are adaptive, weighted beams. The important trade-offs are coherent space-time signal wavefronts vs. incoherent (uncorrelated) noise field samples, thus increasing the effective statistical sample under  $H_1$  vs.  $H_0$ , i.e., lowering the (here) joint probabilities of Type I and II errors, e.g.,  $\min_{\delta} (q\alpha + p\beta^*)$ ,  $\delta =$  decision rule, viz. (7.3c).

In a broad sense these optimum algorithms seek first, thus, to "match" the receiver to the noise, via  $\ell_{m,n}$ , cf. (7.4), (7.5), and then to "match" the desired signal to these processed input data,  $\ell(x_{m,n})$ . It is the "tails" of the noise pdf which are significant vis-à-vis gaussian noise: the nongaussian interference falls off much more slowly, so that the transfer characteristic,  $\ell$ , between  $x$ -input and  $\ell$ -output includes a

limiting or clipping feature, as well. For this reason, limiters can be good approximations to the actual characteristic, giving performances not many dB worse than the theoretical optimum. Of course, actual differences will depend on the particular EMI field to which the receiver is adapted, i.e., for which the field parameters ( $\Omega_2$ ,  $A$ ,  $\Gamma'$ ,  $\alpha$ , etc.) have been estimated. Finally, it is emphasized that threshold detectors of the above types are useful and give noticeable improvement over conventional systems when the space-time-bandwidth product,  $\Pi_j^{(*)}$ , is large, so that the required small probabilities of error  $P_e^{(*)}$  can be obtained. (For a discussion of asymptotic optimality,  $A_0$ , bounds on  $\langle a_0^2 \rangle_{\min}^{(*)}$ , etc., as well as some numerical examples, see again [15], [16].)

### 9. Threshold Signal Estimation

As is well-known, in the Bayes theory [20], [58] estimation is the "twin" of detection: the former aims to determine the particular characteristics of a desired signal, e.g., amplitude, waveform, phase, frequency, etc., once the signal has been detected, while the latter is concerned with the basic question of the desired signal's presence or absence. In a very broad sense "estimation" can be regarded as an extension of detection: both subsume appropriate cost functions for the derivation of optimal algorithms and for the measures and comparisons of performance. In fact, in a more general Bayesian sense detection and estimation are the two, coupled component elements of the composite process of signal extraction: detection and estimation joined together by a suitable cost function, reflecting the frequent situation where it is not completely certain, for the estimation process, that the desired signal is present, which, in turn, results in biased estimators [59].

Here, however, we shall assume that the desired signal is known a priori to be present, and that certain waveform and parameter features of the signal are to be estimated, when the accompanying acoustic interference is highly nongaussian (the "classical" situation of gaussian noise is a special case of our general model). How the estimators are unbiased. In any case, we may expect the estimation process, particularly optimum estimation (in the Bayes theory [58], [20]), to be closely related

to the detection process, since both are derived from approximate likelihood functions [60], [61]. This will be seen explicitly in the canonical threshold theory outlined below (cf. Sec. 9.1).

From the practical underwater acoustic viewpoint, signal estimation is a common communication requirement: signal amplitude (or level), waveform, frequency, epoch, modulation are each important elements of the reception process, whether it be telecommunications, radar, television (and their analogues in acoustical and optical régimes). Designing receivers for effective threshold performance usually ensures better (but not necessarily optimum) performance at strong-signal levels. As in the detection cases [16], an optimal theory provides limiting estimation algorithms and performance, which are models to be approximated in practice. Also, as in detection, a canonical theory is possible in the weak-signal cases (as long as reasonably large time-bandwidth products are permitted, of course: the desired signal must be "extractable" under the observational constraints). Such a canonical theory also provides standards against which practical, suboptimum (i.e., approximate) algorithms can be evaluated and compared [15], [16].

As in threshold detection theory [16] a fundamental problem now in developing effective threshold estimation algorithms is to obtain expressions of limited complexity, which retain their optimum nature when sample size ( $J$ ) becomes increasingly large. The latter is the case, of course, when the signal is weak, since large effective data samples are required for small expected errors in the resulting estimates--analogous to small probabilities of decision error in optimum (threshold) detection. However, just as in detection [16], without a suitable "bias" term in the extraction algorithm this algorithm demands progressively more terms in its approximative form. This rapidly defeats the key requirement of processing feasibility, particularly for signals and interference of practical use, and destroys analytic tractability as well.

Accordingly, we parallel our preceding summary review of (binary) space-time threshold detection theory (Secs. 7, 8), and present now a concise summary of optimum and suboptimum threshold signal estimation, for the three generic modes of reception noted earlier for detection: (1) coherent

estimation, (2) incoherent estimation, and (3) composite estimation, where a linear combination of the coherent and incoherent algorithms is employed. [Because of spatial limitations we shall confine our explicit illustrations to the simplest situation of amplitude (or scale) estimation, where signal waveform is otherwise known at the receiver. However, the effects of fading, doppler, and other propagation conditions can be included, as in the detection examples above, Secs. 7, 8. The general formalism outlined here, nevertheless, is quite capable of providing explicit algorithms in the more complex situations involving waveform, frequency, phase estimation, etc.] As before, the interference is additive, generally nongaussian, and is either Class A or Class B interference (i.e., respectively coherently or incoherently received in the (linear) front-end stages of a typical narrow band receiver, accompanied by (additive) external and internal gaussian noise [7], [15], [16], [18]. These interference models account for most of the practical cases.

#### 9.1 Canonical Optimum Threshold Estimator Structures; AO/LOBE Forms

A canonical optimum estimator is represented by  $\gamma^* = \gamma_0^*(\underline{\theta}|\underline{X})$ , where  $\underline{\theta} = (\theta_1, \dots, \theta_M)$  is the parameter set to be estimated on the basis of  $\underline{X}$ ; the received data,  $\sigma$  refers to the pdf of  $\underline{\theta}$  (see Appendix A.3). As noted at the beginning of Sec. 9, the critical problem in developing explicit locally optimum threshold estimators (LOBE's) from the general (all signal level) forms (A.3-6), (A.3-8) is to terminate the desired series approximation properly, i.e., without an excessive number of terms and in such a way that these estimators are asymptotically optimum (AO), as well. This situation precisely parallels that for optimum threshold detection, already treated by the author in [15], [20]. In fact, the approach here is to convert the various likelihood functions  $\sigma F_n$ ,  $\sigma W_n$  above, from which the LOBE's are determined, cf. (A.3-4), (A.3-8), into likelihood ratios, equivalent now to a suitable statistical test among two distinguishable hypothesis ( $H_1$ ,  $H_2$ ), etc. Then LeCam's results [60] as applied by Levin [61] are used to obtain at least a sufficient condition of AO for the "LOBD" form from which the resultant AO LOBE is then constructed, according to the error function (QCF, SCF, etc.) chosen.

#### A. Equivalent LOBE's for LOBD's

We consider first the SCF case, cf. (A.3-7), with the optimizing rule (A.3-8) for generating the UMLE's,  $\underline{\gamma}^*$ . Since the (linear) operation of



differentiation in (A.3-8) is unaffected if we subtract  $\log F_J(\underline{x}|0)$ , we see that (A.3-8) becomes

$$\frac{\partial}{\partial \theta_{\hat{m}}} \{ \log \sigma(\theta_{\hat{m}}) + \lambda_J^{(10)}(\underline{x}|\theta_{\hat{m}})_{SCF} \} \Big|_{\theta_{\hat{m}} = \gamma_{\hat{m}}^*} = 0, \quad \hat{m} = 1, \dots, \hat{M} \quad (9.1)$$

where  $\theta = (\theta_{\hat{m}}, \theta')$ , in which  $\theta_{\hat{m}}$  is the particular parameter to be estimated, with

$$\lambda_{J-SCF}^{(10)} \equiv \log \{ \langle F_J(\underline{x}|\underline{s}(\theta_{\hat{m}}, \theta')) \rangle_{\theta'} / F_J(\underline{x}|0) \} \quad (9.1a)$$

now the (logarithms of the) generalized likelihood ratio representing the test states  $H_1(S \oplus N)$  vs.  $H_0(N)$ , which is the familiar "on-off" or "signal and noise" vs. "noise alone" situation in detection theory.

In a similar way we see that the rule (A.3-6) for obtaining the Bayes estimators for the QCF (A.3-5) can be equivalently expressed in terms of another likelihood ratio by

$$\{\gamma_{\hat{m}}^*\}_{QCF} = \{ \int_{\Omega_{\theta_{\hat{m}}}} \theta_{\hat{m}} \sigma(\theta_{\hat{m}}) e^{\lambda_J^{(21)}(\underline{x}|\theta_{\hat{m}})}_{QCF} d\theta_{\hat{m}} \}, \quad (9.2)$$

where now

$$\lambda_{J-QCF}^{(21)} \equiv \log \langle F_J(\underline{x}|\underline{s}(\theta_{\hat{m}}, \theta')) \rangle_{\theta'} / \langle F_J(\underline{x}|\underline{s}) \rangle_{\theta} . \quad (9.2a)$$

This likelihood ratio,  $\lambda_{J-QCF}^{(21)}$ , represents the binary-signal detection situation where we test  $H_2(S \oplus N)$  vs.  $(H_1(S \oplus N), \text{i.e., } S^{(2)} \equiv \underline{s}_{\hat{m}})$ , that portion of  $\underline{s}$  containing  $\theta_{\hat{m}}$  only, and  $\underline{s}^{(1)} = \underline{s}$ , cf. (9.2a). Thus we note that  $\gamma_{\hat{m}-SCF}^*$  is a linear functional of  $\lambda_J^{(10)}$ , cf. (9.1), whereas the  $\{\gamma_{\hat{m}-QCF}^*\}$  are (monotonic) nonlinear functionals of  $\lambda_J^{(21)}$ , cf. (9.2).

Having cast these estimators in likelihood ratio form, we can now proceed directly as in the previously developed optimum threshold detection theory ([13], [16], Appendix A.3; [15], Appendix) to obtain the needed approximate forms for  $\lambda_J = g_J^*(\underline{x}, \theta_{\hat{m}}) + t_J(\underline{x}, \theta_{\hat{m}}) \doteq g_J^*$ , where it is shown that as  $J \rightarrow \infty$ ,  $t_J \rightarrow 0$  prob. 1 on  $H_1$  vs.  $H_0$  (or  $H_2$  vs.  $H_1$ ), i.e.,  $\lambda_J \doteq g_J^*$  is AO as  $J \rightarrow \infty$ , cf. (7.12) et seq. Because of the functional relations (9.1), (9.2),  $\gamma_{\hat{m}}^*$  is likewise then AO, as well as LOBE, i.e., is AOB (asymptotically Bayes estimator). Now specifically (9.1), (9.2) become

$$\text{SCF:UMLE} \left[ \frac{\partial \log \sigma_1(\theta_{\hat{m}})}{\partial \theta_{\hat{m}}} + \frac{\partial g_{J\text{-SCF}}^*}{\partial \theta_{\hat{m}}} \right]_{\theta_{\hat{m}} = \gamma_{\hat{m}}^*} = 0; \quad (9.3)$$

$$\text{QCF:LMSE} \{ \gamma_{\hat{m}}^* \} = \left\{ \int_{\Omega_{\theta_{\hat{m}}}} \theta_{\hat{m}} \sigma_1(\theta_{\hat{m}}) e^{g_{J\text{-QCF}}^*} d\theta_{\hat{m}} \right\}, \quad (9.4)$$

where the  $g_j^*$  are given explicitly in the next section. A sufficient condition that  $g_j^*$  is AO is that  $g_j^*$  be asymptotically normal, with means  $\mp[\text{var}_0 g_{J\text{-SCF}}^*, \text{var}_1 g_{J\text{-QCF}}^*]$ ,  $\mp = H_0, H_1$ ; or  $H_1, H_2$ , and variances  $\text{var}_0 g_{J\text{-SCF}}^*$ ,  $\text{var}_1 g_{J\text{-QCF}}^*$ , respectively. [Note, also, that because we have assumed the desired signal is a priori known to be [55] present,  $\log u = \log(p/q)$  of the detection forms, cf. (2.4) of [20], are omitted here in the formation of  $\ell_j^{(10)}$ ,  $\ell_j^{(21)}$  above.]

#### B. AO Forms of the $g_j^*$

From Sec. 3.2 of [15], and from [20] suitably adapted, we have specifically the needed structures of  $g_j^*$  required in (9.3), (9.4) for determining the associated AO LOBE's. Specializing to the practically useful cases of independent data (i.e., noise) samples and locally stationary noise processes, which we shall henceforth assume in the remainder of our treatment, we have once more, cf. Sec. 7.2

##### (1) Coherent Reception (SCF)

$$g_{J\text{-coh}}^* = -\frac{1}{2} \sigma_{0J\text{-coh}}^{*2} - \sum_j^J \langle a_{0j} s_j \rangle_{\underline{\theta}}, \quad \ell_j \quad (9.5)$$

##### (2) Incoherent Reception (SCF)

$$g_{J\text{-inc}}^* = -\frac{1}{2} \sigma_{0J\text{-inc}}^{*2} + \frac{1}{2!} \sum_{ij}^{J(=MN)} (\ell_i \ell_j + \ell_i^! \ell_j^!) \langle a_{0i} a_{0j} s_i s_j \rangle_{\underline{\theta}}, \quad (9.6)$$

### (3) Composite Reception (SCF)

$$g_{J\text{-comp}}^* = g_{J\text{-coh}}^* + g_{J\text{-inc}}^* , \quad (9.7)$$

where, as in Sec. 7 et seq.,  $a_{oi} = a_o(t_i)$ , etc. is a (normalized) signal amplitude,  $s_i = s(t_i, \theta, \underline{\theta}')$  is a normalized signal waveform, such that  $\langle s^2 \rangle = 1$ , and  $\ell_i = d \log w_i(x_i)/dx_i$ ,  $\ell_i' = d\ell_i/dx_i$ , where  $w_1(x_i)$  = first order pdf of the interference (nongauss + gauss) above, in the usual way. Specifically, here and henceforth in Sec. 9,  $a_{oj} = a_{on}^{(m)}$ ,  $s_j = s_n^{(m)}$ , since  $j = m, n$ , cf. Sec. 7.2 et seq. In this way we include the spatial, as well as temporal description of the sampled waves. Thus  $i = (m, n)$ ;  $j = (m', n')$ , when used in the incoherent cases.

The proper bias terms are given by  $\hat{B}_J^* = -\sigma_{oJ}^{(*)2}/2$ , cf. (7.12), or (7.9), (7.10), with (7.11), etc. [We must be careful here and henceforth to distinguish between the various averaged signal parameters ( $\underline{\theta}'$ ) and the unaveraged ones  $\{\theta_m\}$ , which are to be estimated.]

Similarly, for the QCF the associated  $g_J^*$  needed in (9.4) are

#### (1) Coherent Reception (QCF)

$$g_{J\text{-coh}}^{(21)*} = B_{J\text{-coh}}^{(21)*} - \sum_j \ell_j [\langle a_{oj} s_j \rangle_{\underline{\theta}'} - \langle a_{oj} s_j \rangle_{\underline{\theta}}] . \quad (9.9)$$

#### (2) Incoherent Reception (QCF)

$$g_{J\text{-inc}}^{(21)*} = B_{J\text{-inc}}^{(21)*} + \frac{1}{2!} \sum_{ij} (\Delta\rho)_{ij} (\ell_i \ell_j + \ell_i' \delta_{ij}) , \quad (9.10)$$

and (3)

$$g_{J\text{-comp}}^{(21)*} \Big|_{\text{QCF}} = (g_{J\text{-coh}}^{(21)*} + g_{J\text{-inc}}^{(21)*})_{\text{QCF}} ,$$

cf. (9.7). Here  $(\Delta\rho)_{ij} \equiv \langle a_{oi} a_{oj} s_i s_j \rangle_{\underline{\theta}'} - \langle a_{oi} a_{oj} s_i s_j \rangle_{\underline{\theta}}$ , and the proper biases for AO behavior are

$$B_{J\text{-coh}}^{(21)*} = - \frac{\sigma_{J\text{-coh}}^{(21)*}}{2} = - \frac{L(2)}{2} \sum_j^J [\langle a_{oj} s_j \rangle_{\underline{\theta}}^2 - \langle a_{oj} s_j \rangle_{\underline{\theta}}^2] \quad (9.11)$$

$$B_{J\text{-inc}}^{(21)*} = - \frac{\sigma_{J\text{-inc}}^{(21)*}}{2} = - \frac{1}{8} \sum_{ij}^J \{ (L^{(4)} - 2L^{(2)^2}) \delta_{ij} + 2L^{(2)^2} \} \Delta R_{ij}, \quad (9.12)$$

where  $\Delta R_{ij} \equiv \langle a_{oi} a_{oj} s_i s_j \rangle_{\underline{\theta}}^2 - \langle a_{oi} a_{oj} s_i s_j \rangle_{\underline{\theta}}^2 (\neq (\Delta \rho)_{ij})$ .

### C. Suboptimum Estimators

We parallel the treatment in [15], [20], where  $g_j^*$  is replaced by the suboptimum  $g_j$ , now appropriately adapted to the estimation structures (i.e., hypothesis test) required by the SCF, QCF, etc. We illustrate the procedure with the case of SCF and the use of simple (cross- and auto-) correlation receivers, well-known to be threshold optimum in gauss interference. Now (9.5)-(9.7) reduce to this case directly on setting  $\ell_i = -x_i$  ( $\therefore \ell_i^1 = -1$ ), and  $\therefore L_{\text{gauss}}^{(2)} = 1$ ,  $L_{\text{gauss}}^{(4)} = 2$ . Similarly, for the QCF cases (9.8), (9.9), we make the same substitutions, in both the bias and data portions of  $g_{\text{QCF}}^*$ .

In the important cases of clipper-correlators, which are optimum in Laplace noise and which are well known to be effective against non-gaussian noise, cf. [15], we replace  $\ell_i$  by  $\text{sgn } x_i$  (and omit  $\ell_i^1$ ), with appropriate modifications of the bias terms, cf. Sec. 3.3 of [15] for details. The basic pdf's for which these various correlation detector-forms (and hence estimator forms via (9.1), (9.3)) are optimum, are respectively given by  $w_1(x)$  in Sec. 7.5 above.

Finally, it is important to note that these LOBE's [obtained from (9.1), (9.3)] are only practically AO and LOB when  $\theta^2 (= \langle a_o^2 \rangle)$  is sufficiently small, as in detection, i.e., there exists an  $\langle a_o^2 \rangle_{\text{max}}$  ( $\ll 1$ ), with  $\langle a_o^2 \rangle \leq \langle a_o^2 \rangle_{\text{max}}$ , such that for  $\overline{a_o^2} > \langle a_o^2 \rangle_{\text{max}}$  the threshold optimal character of  $g_j^*$  breaks down and becomes suboptimum. At larger input signals  $g_j^*$  ( $\rightarrow g_j$  now) and hence  $\gamma_m^* \rightarrow \gamma_m$ , etc., may or may not be monotonically better, in absolute terms, than  $g_j^*$ ,  $\overline{a_o^2} \leq \overline{a_o^2}_{\text{max}}$ . Usually, for sufficiently strong signals,  $g_j^*$  (now  $g_j$ ) is absolutely better, unless the information-bearing portion of the signal is destroyed by the algorithm itself, e.g., clipping

destroys waveform detection/estimation, but not phase parameter extraction, for example.

## 9.2 An Example: Amplitude Estimation with the SCF: Coherent Reception

The simplest useful example is that of estimating the scale (or amplitude)  $a_0$  of an otherwise fully known signal waveform received in (generally) nongaussian interference. This is also the problem of estimating signal intensity  $\hat{I}_S^* = \hat{a}_0^2$ .

Here we have  $\theta_m = \theta_1 = a_0$ , with  $\theta$  all other relevant signal parameters. With coherent reception, signal epoch  $\epsilon$  is precisely known, e.g.,  $\epsilon = \epsilon_0$ , and we select  $\langle s_j \rangle_\epsilon = s_{j-\max} = \sqrt{2}$ , with independent noise samples. Thus, we write  $\langle s_i \rangle_\theta = s_{\max} = \sqrt{2}$  here. Physically, our present example can represent slow fading, whose changes are negligible over the data acquisition period.

Accordingly, (9.5) reduces directly to

$$(g_{J-\text{coh}}^*)_{\text{SCF}} = -L^{(2)} a_{0J}^2 - a_0 \sqrt{2} \sum_{j=1}^J \ell(x_j). \quad (9.12)$$

Applying this to (9.3), with  $\theta_m = \theta_1 = a_0$ , gives

$$\left[ \frac{\sigma_1(a_0)'}{\sigma_1(a_0)} - L^{(2)} a_{0J}^2 - a_0 \sqrt{2} \sum_j \ell(x_j) \right]_{a_0 = \hat{a}_0^*} = 0, \quad (9.13)$$

whose solution yields the desired estimator  $\hat{a}_0^*(x)$ .

To proceed further, we need to know the a priori pdf of  $\theta_1 (= a_0)$ , e.g.,  $\sigma_1(a_0)$ . Let us assume, then, that  $\sigma_1(a_0) = 1/\Delta a_0$ , a uniform pdf on  $(0 < a_0 \leq a_0^+)$ , and zero elsewhere. Consequently,  $\sigma_1'(a_0) = 0$ ,  $0 < a_0 < \Delta a_0$  (the contribution of the  $\delta$ -functions at 0,  $\Delta a_0$  provide no meaningful solutions). Solving (9.13) gives

$$\boxed{\hat{a}_0^*(x) \Big|_{\substack{\text{coh} \\ \text{SCF} \\ \text{uniform}}} = - \sum_j \ell_j / J \sqrt{2} L^{(2)}} \quad , \quad \overline{a_0^2} \ll 1 \quad (9.14)$$

The optimum threshold estimate of signal intensity is accordingly

$$\hat{I}_s^* = (\hat{a}_0^*)^2 = \left( \sum_j \ell_j \right)^2 / 2J^2 L^{(2)^2} \quad (9.15)$$

Here  $\hat{a}_0^*$ , and  $\therefore \hat{a}_0^{*2}$  are UMLE for the assumed uniform pdf of  $a_0$ , and simultaneously CMLE for any (meaningful) pdf of  $a_0$ . Moreover,  $\langle \hat{a}_0^* \rangle_1 \doteq \bar{a}_0$ , because  $\langle \ell \rangle_{H_1} (= \langle \ell \rangle_1) = -\sqrt{2} \bar{a}_0 L^{(2)}$ , and we can show that

$$\text{var}_1 \hat{a}_0^* \doteq \bar{a}_0^2 (1 + O(\frac{1}{J})) - \bar{a}_0^2 \doteq \text{var } a_0 |_{J \gg 1}, \quad (\bar{a}_0^2 \ll 1) \quad (9.16)$$

from  $\langle \ell_i \ell_j \rangle_1 \doteq 2\bar{a}_0^2 L^{(2)^2} (i \neq j); \doteq \ell^2 + \bar{a}_0^2 L^{(2,2)} (i = j)$ . Thus,  $\hat{a}_0^*$  is unconditionally unbiased, e.g.,  $\langle \hat{a}_0^* \rangle_1 \doteq \bar{a}_0 (= \Delta a_0 / 2)$  and  $\lim_{J \rightarrow \infty} \hat{a}_0^* \rightarrow a_0$ , from (9.16).

The "smallness" condition on  $\bar{a}_0^2$  is (from Sec. 6.4, Eq. (6.71) of [15])

$$\bar{a}_0^2 \ll \frac{1}{2} \frac{\text{var}_0 \ell}{\text{var}_0 \ell^2} = L^{(2)} / [L^{(2,2)} - 2L^{(2)^2}] \equiv x_0; \quad L^{(2,2)} \equiv \langle (w_1'/w_1)^4 \rangle \quad (9.17)$$

Here, from  $\sigma_1(a_0) = 1/\Delta a_0$  we have  $\bar{a}_0^2 = (\Delta a_0)^2/3$  in (9.16) to establish an upper bound  $(\bar{a}_0^2)_{\max} (\ll 1)$  for which  $\bar{a}_0^2 \leq (\bar{a}_0^2)_{\max}$  and  $\hat{a}_0^*(x)$  is then LOBE and A0.

As a numerical example, consider a Class A noise for which  $\Gamma_A' = 10^{-4}$ ,  $A_A = 0.5$ , so that  $x_0 = 1.7 \cdot 10^{-4}$  (from Fig. 5.6 of [15]):  $\therefore x_0 \text{ dB} = -37.7 \text{ dB}$ , with the result that  $\bar{a}_0^2 \ll -38 \text{ dB}$  or  $(\Delta a_0)^2 \ll -37.7 + 4.8 = -32.9 \text{ dB}$ . Typically, we might choose  $(\bar{a}_0^2)_{\max} = -43$  or  $-48 \text{ dB}$  here. This means that sample size  $J$  should be large enough to ensure (9.16), i.e.,  $J = O(10^2$  or more) appears sufficient.

### 9.3 Discussion

First, let us note that our illustrative example is readily extended to the estimation of waveform itself  $S = \{S_j\}$ :  $\hat{\theta}_m \rightarrow \hat{S}_m$ , and we get a series of relations like (9.13), if  $\sigma(\theta) = \hat{\sigma}_{m=1}^{\Pi} \sigma_1(\hat{\theta}_m)$ ; otherwise one has  $M$ -coupled equations to be solved for  $\hat{\theta}_m = \hat{S}_m$ . Also, if the QCF is used, the structure

of the optimal estimator is generally much more complex, due to the non-linear functional relation between  $g_j^*$  and  $\gamma_j^*$ , cf. (9.2). If the parameters to be estimated appear functionally in the waveform  $S(t, \theta)$  then one obtains functional solutions for the estimators.

The important general result here (for all signal levels) is the explicit functional relation between the (optimum) detection algorithms and the resultant optimum estimators, cf. (9.1), (9.2): detector structure provides the initial analytic relation, from which the estimator is the appropriate functional relation, the form of which depends on the choice of cost function. Thus, to carry out the derivation of the desired estimator, we must start with the appropriate detector algorithm [16]. The evaluation of estimator performance is provided by using the estimator,  $\gamma_j^{(*)}$ , in the expressions for the average error (or risk), cf. (A.3-2).

Finally, one important extension of the analysis outlined above is to the frequently occurring situation (mentioned at the beginning of Sec. 9) necessitating joint detection and estimation, when it is not known precisely that the desired signal is present [59].

## 10. Concluding Remarks

In the preceding section we have outlined a comprehensive methodology for handling the general problems of acoustic signal transmission and reception in and through complex underwater media. Our approach has included the following important channel features: (1) inhomogeneous volumes and interfaces, both deterministic and random; (2) spatial as well as temporal effects; (3) the inherently nongaussian character of major components of the random fields arising both from ambient sources and produced by a variety of scattering mechanisms; (4) space-time processing by the distributed arrays which couple source and receiver to the medium; and (5) threshold detection and estimation of signals in these generally nongaussian environments.

In addition to the above topics we have touched upon a variety of specific methods and techniques for channel modeling, including operator formalisms and diagrammatic methods. A number of new results are also discussed: poisson field models and statistics, canonical threshold

estimators and estimates, for example, as well as measures of threshold detector performance which specifically incorporate the rôles of the receiving array, signal structure (with doppler smearing and fading), and mixed gaussian and nongaussian noise components in the interference. Spatial processing gains are seen to be achievable in the usually encountered nonuniform noise fields by suitable spatial sampling, for both detection and estimation, in addition to the capability of beam formation. Suboptimum, as well as optimum processing algorithms are noted.

The preceding sections are intended to be a general guide to the formulation and treatment of specific propagation and signal processing problems, wherein attention is called to the many physical features which may have to be taken into account in individual problems. The accompanying references should provide the in-depth analysis and/or specific results needed at each stage of the problem in question. As stated at the beginning, our general aim here has been to provide an overview, keyed to the realities of specific applications, and at the same time to exhibit a unifying and interdisciplinary approach, within which the many special modeling and processing tasks of underwater acoustic interests are embedded.



## Appendix A.1 Diagram Representations and Solutions [2]

Diagram representations and methods are very useful and compact forms for describing field interactions as is well known [23], [41]. For some of our subsequent results we shall include diagram equivalents, along with the corresponding analytic expressions, defining the symbol "vocabulary" in a consistent way. For our ensemble results [(3.4)-(3.9)], we write the equivalent ensemble diagrams:

$$\text{FOR: } -G_T \quad \begin{array}{c} \oplus \quad \hat{M} \\ \downarrow \quad \uparrow \\ \hat{Q} \end{array} \quad \left( \{\alpha\} \equiv \begin{array}{c} \hat{M} \\ \leftarrow \quad \rightarrow \\ \hat{Q} \end{array} \right) : \quad (\text{A.1a})$$

$$\text{FD: } \left\{ \begin{array}{c} \boxed{\phantom{\alpha}} \\ \{\alpha\} \end{array} \right. = \begin{array}{c} H \\ \boxed{\text{hatched}} \\ \alpha_H \end{array} + \begin{array}{c} \xrightarrow{\hat{M}_\infty} \\ \hat{Q} \end{array} \circ \boxed{\phantom{\alpha}}; \quad (\text{Eq. (3.4)}); \quad (\text{A.1b})$$

$$\text{FOS: } \left\{ \begin{array}{c} \boxed{\phantom{\alpha}} \\ \text{Eq. (3.8)} \end{array} \right. = \frac{\hat{1}}{\hat{1} - \xrightarrow{\hat{M}_\infty}} \begin{array}{c} \boxed{\text{hatched}} \\ H \end{array}; \quad \begin{array}{c} \boxed{\text{hatched}} \\ H \end{array} = \begin{array}{c} \circ \leftarrow \hat{M}_\infty \\ \hat{Q} \end{array} = -\hat{M}_\infty(G_T) \quad (\text{A.1c})$$

$$\begin{array}{c} \circ \leftarrow \hat{M}_\infty \\ \hat{Q} \end{array} = -G_T$$

$$\text{PTSS: } \boxed{\phantom{\alpha}} = \hat{1} + \begin{array}{c} \xrightarrow{\hat{M}_\infty} \\ \hat{Q} \end{array} \circ \boxed{\phantom{\alpha}} + \begin{array}{c} \xrightarrow{\hat{M}_\infty} \\ \hat{Q} \end{array} \circ \begin{array}{c} \xrightarrow{\hat{M}_\infty} \\ \hat{Q} \end{array} \circ \boxed{\phantom{\alpha}} + \dots \begin{array}{c} \boxed{\text{hatched}} \\ H \end{array}; \quad \text{Eq. (3.9)}, \quad (\text{A.1d})$$

where we define the symbols as we go along. Thus,  $\xrightarrow{\hat{M}_\infty}$  denotes the "feedforward" operator, while  $\leftarrow \hat{Q}$  denotes the (ensemble) "feedback" or scattering operator. The ensemble Feynman diagram (FD) equivalent of the FOR (A.1a) is just (A.1b), with (A.1c) giving the corresponding ensemble FOS, and (A.1c) the PTSS, obtained by iteration of (A.1b) or from (3.9) directly.

### A.1-1: Stochastic Solutions

As we have noted above [cf. Eq. (2.8) et seq.] the solutions to the Langevin equation (2.8) are the various statistics of the field  $\alpha$ , e.g., here the moments  $\langle \alpha \rangle$ ,  $\langle \alpha_1 \alpha_2 \rangle$ , etc.

Let us consider first the mean field  $\langle \alpha \rangle$ . Taking the average of (3.9), for example, gives directly

$$\langle \alpha \rangle = \alpha_H + \sum_{n=1}^{\infty} \langle \hat{\eta}^{(n)} \rangle_{\alpha_H}, \quad (\text{A.2})$$

which shows that all ( $n^{\text{th}}$ ) order moments of  $\hat{Q}$  are required. The diagram equivalent of (A.2) is, from (A.1d),

$$\left\{ \begin{aligned} \longleftrightarrow &= [\hat{1} + \text{diagram with } \hat{M} \langle \hat{Q} \rangle + \text{diagram with } \hat{M}_1 \langle \hat{Q}_1 \hat{M}_2 \hat{Q}_2 \rangle + \dots] \text{diagram with } \alpha_H; \text{ with} \\ \bullet &= \langle \hat{Q} \rangle; \text{ } \bullet \text{---} \bullet \text{---} \bullet \text{---} \bullet = \langle \hat{Q}_1 \dots \hat{Q}_n \rangle. \end{aligned} \right. \quad (\text{A.2a})$$

There is a second approach which leads to an equivalent deterministic formulation, which is usually more effective for approximations. Defining a deterministic operator  $\hat{Q}_1^{(d)}$  by

$$\hat{Q}_1^{(d)} \langle \alpha \rangle \equiv \langle \hat{Q} \alpha \rangle, \quad (\text{A.3})$$

we may again average (3.4) and use (A.3), to get

$$\langle \alpha \rangle = \alpha_H + \hat{M} \hat{Q}_1^{(d)} \langle \alpha \rangle = (\hat{1} - \hat{\eta}^{(d)})^{-1} \alpha_H = \alpha_H + \sum_{n=1}^{\infty} (\hat{\eta}^{(d)})^{(n)} \alpha_H, \quad (\text{A.4})$$

or, in diagram form,

$$\begin{aligned} \longleftrightarrow &= \text{diagram with } H + \text{diagram with } \hat{Q}_1^{(d)} \longleftrightarrow = \frac{\hat{1}}{\hat{1} - \text{diagram with } \bullet} \text{diagram with } H \\ &= \left[ \hat{1} + \sum_{n=1}^{\infty} (\text{diagram with } \bullet)^{(n)} \right] \text{diagram with } H \end{aligned} \quad (\text{A.4a})$$

respectively.

Equation (A.4) is a form of Dyson's equation (DE), where now the equivalent deterministic scattering operator,  $\hat{Q}^{(d)}$ , or (EDSO), is the analogue of the "mass-operator" ( $\hat{Q}$ ) in quantum electrodynamics (cf. 160,

[24]; [23]). The EDSO is always an integral, or global operator, over all pertinent space and time, and has the form

$$\hat{Q}_1^{(d)} = \sum_{m=0}^{\infty} \hat{A}_m(\underline{R}, t | \underline{R}', t') : \hat{A}_0 = \langle \hat{Q} \rangle ; \hat{A}_m = \langle \hat{Q} \hat{M} \hat{Q}^{(m)} \rangle - \sum_{j=1}^{m-1} \hat{A}_{m-j} \langle (\hat{M} \hat{Q})^{(j)} \rangle, \quad (A.5)$$

which at once permits a hierarchy of approximate forms, by stopping with term ( $m \geq 1$ ). The diagram equivalent of (A.5) is

$$\hat{Q}^{(d)} \equiv \leftarrow \bullet = [\bullet]_{m=0} + [\text{diagram}]_{m=1} + [\text{diagram}]_{m=2} + \dots \quad (A.5a)$$

Similar concepts may be applied to higher-order moments of the field. In fact, we may write the following FOS for the second-order, second moment of the field:

$$\langle \alpha_1 \alpha_2 \rangle = (\hat{1} - \hat{\eta}_{12}^{(d)})^{-1} (\hat{1} - \hat{\eta}_1^{(d)} \hat{\eta}_2^{(d)}) \langle \alpha_1 \rangle \langle \alpha_2 \rangle ; \hat{\eta}_{12}^{(d)} \equiv \hat{M}_1 \hat{M}_2 \hat{Q}_{12}^{(d)}, \quad (A.6)$$

where the EDSO,  $\hat{Q}_{12}^{(d)}$ , is defined by

$$\hat{Q}_{12}^{(d)} \langle \alpha_1 \alpha_2 \rangle \equiv \langle \hat{Q}_1 \hat{Q}_2 \alpha_1 \alpha_2 \rangle, \quad (A.6a)$$

cf.  $\hat{Q}_1^{(d)}$ , (A.3) above. Equation (A.6) is a second-order Dyson equation, analogous to a form of the Bethe-Salpeter equation in quantum electrodynamics ([21]; [60], [24]). Analogous to (A.4a), we have

$$\left\{ \begin{array}{l} \text{Diagram}_{12} = \text{Diagram}_{12} + \text{Diagram}_{12}^{(d)} \text{Diagram}_{12} ; \text{Eq. (A.6a);} \\ \langle \alpha_1 \alpha_2 \rangle \text{Diagram}_{12} \equiv (\hat{1} - \text{Diagram}_{12}^{(d)}) \text{Diagram}_{12} \text{Diagram}_{12} \end{array} \right. \quad (A.7a)$$

with obvious extensions of the second and third diagrams in (A.4a). The EDSO, (A.6a), is the extension of (A.5a):

$$\hat{Q}_{12}^{(d)} \equiv \leftarrow \overset{d}{\bullet}_{12} = \left[ \overset{\curvearrowright}{\bullet_1 \bullet_2} - \bullet_1 \bullet_2 + \overset{\curvearrowright}{\bullet_2 \bullet_1} - \bullet_2 \bullet_1 + \dots \right]_{m=0}^+ \dots \quad (\text{A.7b})$$

Higher order Dyson forms of the FOS, like (A.6), can be constructed for  $\langle \alpha_1 \dots \alpha_m \rangle$ . In addition, various approximations can be instituted, in  $\hat{Q}^{(d)}$  (series modification) where the series are infinite (for some form of strong scattering), or by truncation, for "weak" scattering (1st-Born approximation, for example [cf. (5.1)]), where one stops at the dotted line in (A.1d), (A.2a), with  $n=1$  in (A.4a), etc. Unfortunately, space does not permit us to pursue these topics further here.

#### A.1-2. Received Waveforms

The expression for the received waveforms, after sensing by the receiving array ( $\hat{R}$ ) may be similarly diagrammed. We start with (A.1), etc. applied to (4.1) and (4.2). Thus, we have

$$\hat{\ell} = \frac{\text{---} \leftarrow \bullet \text{---}}{\hat{1} - \text{---} \leftarrow \bullet \text{---}} \implies; \langle \hat{\ell} \rangle = \frac{\text{---} \leftarrow \overset{d}{\bullet} \text{---}}{\hat{1} - \text{---} \leftarrow \overset{d}{\bullet} \text{---}} \longrightarrow, \text{ etc. cf. (A.4),}$$

(A.8a) and, in PTSS form, cf. (A.1d),

Eq. (4.2):

$$\begin{aligned} \hat{K}_{\ell} = & \left[ \text{---} \overset{\curvearrowright}{\bullet_{11} \bullet_{22}} - \text{---} \bullet_{11} \bullet_{22} \right] \text{---} \overset{\curvearrowright}{\bullet_1 \bullet_2} \vdots + \left[ \text{---} \overset{\curvearrowright}{\bullet_{11} \bullet_{22}} \overset{\curvearrowright}{\bullet_{22} \bullet_{22}} + \text{---} \overset{\curvearrowright}{\bullet_{22} \bullet_{11}} \overset{\curvearrowright}{\bullet_{11} \bullet_{11}} \right. \\ & \left. - \text{---} \overset{\curvearrowright}{\bullet_{11} \bullet_{22}} \overset{\curvearrowright}{\bullet_{22} \bullet_{22}} - \text{---} \overset{\curvearrowright}{\bullet_{22} \bullet_{11}} \overset{\curvearrowright}{\bullet_{11} \bullet_{11}} \right] \text{---} + \dots \end{aligned} \quad (\text{A.8b})$$

The diagram of the mean field is given at once by (A.2a), or (A.4a), on multiplying the receiver operator  $\hat{R}$  since  $\langle X \rangle = \hat{R} \langle \cdot \rangle$ . The diagram for (4.5), in PTSS form for  $\langle X_1 X_2 \rangle$  is, similarly by direct expansion and averaging,

Eq. (4.5):

$$\begin{aligned}
 \langle X_1 X_2 \rangle = \hat{R}_1 \hat{R}_2 [ & \xrightarrow{1} \xrightarrow{2} + \{ \xrightarrow{1} (\xrightarrow{2} + \vdots \xrightarrow{2} \text{arc} \xrightarrow{2} + \dots) + \dots \}_2 + \xrightarrow{2} (\xrightarrow{1} + \vdots \xrightarrow{1} \text{arc} \xrightarrow{1} + \dots)_1 + \dots \\
 & + \{ \xrightarrow{11} \xrightarrow{22} + \vdots \xrightarrow{1} \xrightarrow{2} \xrightarrow{2} \text{arc} \xrightarrow{2} \xrightarrow{2} \text{arc} \xrightarrow{2} \xrightarrow{1} \xrightarrow{1} \text{arc} \xrightarrow{1} \xrightarrow{1} \text{arc} \xrightarrow{1} + \dots \} ] \text{H}_{12}
 \end{aligned}
 \tag{A.8c}$$

from which the various higher-order moments of  $\hat{Q}$  (at points 1,2) appear clearly.

## Appendix A.2 Canonical Scattering Operator Formalisms: Basic Decomposition Principle

For this it is necessary now to use a canonical formulation of the scattering operator,  $\hat{Q}$ , and in particular, the author's concept of a Basic Decomposition Principle (BDP), which permits both a statistical and physical quantification of this operator in terms of differential scattering elements (dse's) which, in turn, can be identified with specific physical mechanisms. Again, space limitations allow only the briefest summary of results below.

We write the following canonical expressions

$$\begin{aligned}
 \hat{Q} \rightarrow \hat{Q}_M(\underline{r}, t | \underline{r}', t') = \int_{-\infty}^{\infty} dt' \int_{\underline{Z}_R} dN(\underline{Z} | \underline{r}', t'; t) h_M(t-t', t | \underline{r}', \underline{r}, \dots) \\
 \cdot \hat{d}_{om}(\underline{r}, t | \underline{r}', t') ( )_{\underline{r}', t'} ,
 \end{aligned}
 \tag{A.2-1}$$

where

$$\left. \begin{aligned}
 dN_M &= \text{the number of available dse's in the domain } d\lambda_M; \int dN( ) \text{ is a "counting" functional.} \\
 h_M &= \text{weighting function, representing the reradiation response of a dse, now postulated to be a linear filter;} \\
 \hat{d}_{om} &= \text{the local interaction operator, determined by the Langevin equation (and boundaries), relating the dse and incident field.}
 \end{aligned} \right\}
 \tag{A.2-1a}$$

Here  $\underline{Z}_R$  is the space of all radiation "events," e.g., scattering, and  $\underline{Z} (= \underline{Z}_R \times \underline{Z}_{S \times \underline{\theta}})$  is the total random variable and parameter space ( $\underline{\theta}$ );  $(\underline{r}, \underline{r}')$  are vectors in the coordinate system of the scattering elements,  $\Lambda_M$ . In most cases we use the basic point-scatter model (BPSM) for  $h_M$ :

$$h_M(t', t | \underline{r}', \dots) = \gamma_0(\underline{r}', t - t')_M \delta(t - \Delta t_{dS}); \quad \Delta t_{dS} = f(t', t; \underline{r}', \underline{r}), \quad (\text{A.2-2})$$

where  $\Delta t_{dS} = t_{dS} - a$  is the displacement (in time units) due to doppler of the dse, away from some fixed position in  $\Lambda_M$  and  $\gamma_0 (> 0)$  is a "cross section" which depends on the nature of the medium (or boundaries).

The inhomogeneous character of the medium (and boundaries) is of two types, A, B. We have, with defining conditions:

$$\text{A. } \underline{\text{The Inhomogeneous}}: (0 \neq) \lambda_0 |\nabla \mu| + \frac{\lambda_0}{c_0} \left| \frac{\partial \mu}{\partial t} \right| \lesssim O(1), \quad c_0 = \lambda_0 f_0, \quad (\text{A.2-3a})$$

$$\text{B. } \underline{\text{The Discontinuum}}: \lambda_0 |\nabla \mu| + \frac{1}{f_0} \left| \frac{\partial \mu}{\partial t} \right| \gg O(1), \quad \mu(\underline{r}, t) = \varepsilon(\underline{r}, t), \text{ etc.} \quad (\text{A.2-3b})$$

where the latter represents a "hard" boundary and the former represents comparatively small changes in the continuous medium. The Discontinuum can be localized, e.g., particles, bubbles, etc., or distributed, like the air/water interface. It is then seen that

$$\text{A: } \hat{d}_{oM}|_{\text{Inhomog}} = \delta(\underline{r} - \underline{r}') \hat{Q}_{\text{coeff.}}(\underline{r}', t'); \quad \text{B: } \hat{d}_{oM}|_{\text{Discont.}} = \delta(\underline{r} - \underline{r}') \hat{1}, \quad (\text{A.2-4})$$

where  $\hat{Q}_{\text{coeff}}$  is the coefficient of  $\mu(\underline{r}, t)$  in the Langevin equation, e.g., of  $\varepsilon(\underline{r}, t)$  in (3.2), viz.,  $c_0^{-2} (\partial^2 / \partial t^2)$ , etc. In consequence of the assumed lack of motion of the fluid as a whole, there is no doppler associated with  $\mu(\underline{r}, t)$ , whereas there is always a (random) doppler associated with the Discontinuum elements, about some equilibrium position of the ocean wave surface, or particle displacement in the volume. (For a general treatment of these important doppler effects, see [36].)

Finally, to anatomize the various types of possible scattering interaction, we invoke the following Basic Decomposition Principle (BDP) for the number of available dse's,  $dN$ , [1], [2]. The BDP states that:

"From the viewpoint of radiative interactions among the dse's which constitute the medium, the argument ( $dN$ , cf. (A.2-1)), of the "counting" functional ( $\int_{\mathbb{R}} dN(\cdot) = N$ , (A.2-1a)), can be decomposed into  $k=1, 2, \dots, \infty$  distinct subsets of available dse's for radiation, each subset of which contains respectively distinct and independent  $k$ -couple radiating elements only." (A.2-5)

This may be expressed, after some manipulation, in terms of (radiative) mean values, e.g.,  $\langle \cdot \rangle_R$ , and fluctuations of the various densities,  $v^{(k)}$ , of different classes ( $k \geq 0$ ) of dse's, by

$$\begin{aligned} \text{BDP: } v(\underline{r}, t) &= \sum_{k=1}^{\infty} v^{(k)}(\underline{r}, t) = \langle v(\underline{r}, t) \rangle_R^{(0)} + \sum_{k=1}^{\infty} \Delta v^{(k)}(\underline{r}, t); \\ \langle v^{(0)} \rangle_R &\equiv \sum_{k=1}^{\infty} \langle v^{(k)} \rangle_R, \quad \Delta v^{(k)} = v^{(k)} - \langle v^{(k)} \rangle_R, \end{aligned} \quad (\text{A.2-6})$$

since  $\hat{N}\delta = v(\underline{r}, t)$ ,  $\underline{r} \in \Lambda_M$ , when  $M=S$  or  $V$  (or  $B$ ), of course. Here ( $k=0$ ) represents the average number of dse's (discrete or continuous) engaged in (re-radiation);  $k=1$  denotes the aggregate of independent, uncoupled dse's, while  $k \geq 2$  are the sets of pairs ( $k=2$ ), triples ( $k=3$ ), etc. of dse's available for (multiple) scattering. It follows directly from the BDP that all sets ( $k \geq 0$ ) are statistically independent. From this it can be shown, furthermore, cf. [21], that the fluctuations  $\Delta v^{(k)}$  obey (zero-mean),  $k^{\text{th}}$ -order poisson statistics, under very general conditions, reducing to gaussian statistics whenever the process densities are sufficiently great. Figure A.2-1 gives a schematic illustration of the decomposition principle presented here.

#### A.2-1. Operator Structure and Radiation Event Statistics

Further insight into the nature of the BDP, (A.2-5), and the canonical structure of the inhomogeneity operator  $\hat{Q}_M$ , (A.2-1), may be gained from the following. It can be shown for small regions  $d\Lambda_M$  in which  $dQ_M$  is accordingly the scattering operator, that the BDP can be anatomized as follows, cf. Fig. A.2-1:

$$\text{(BDP): } d\hat{Q}_M = \sum_{k=1}^{\infty} d\hat{Q}_M^{(k)} = \hat{\mathcal{L}}_{d\Lambda} \left\{ \sum_{k=1}^{\infty} a^{(k)} \gamma_{OM}^{(k)} v^{(k)} \right\}, \quad (\text{A.2-7a})$$

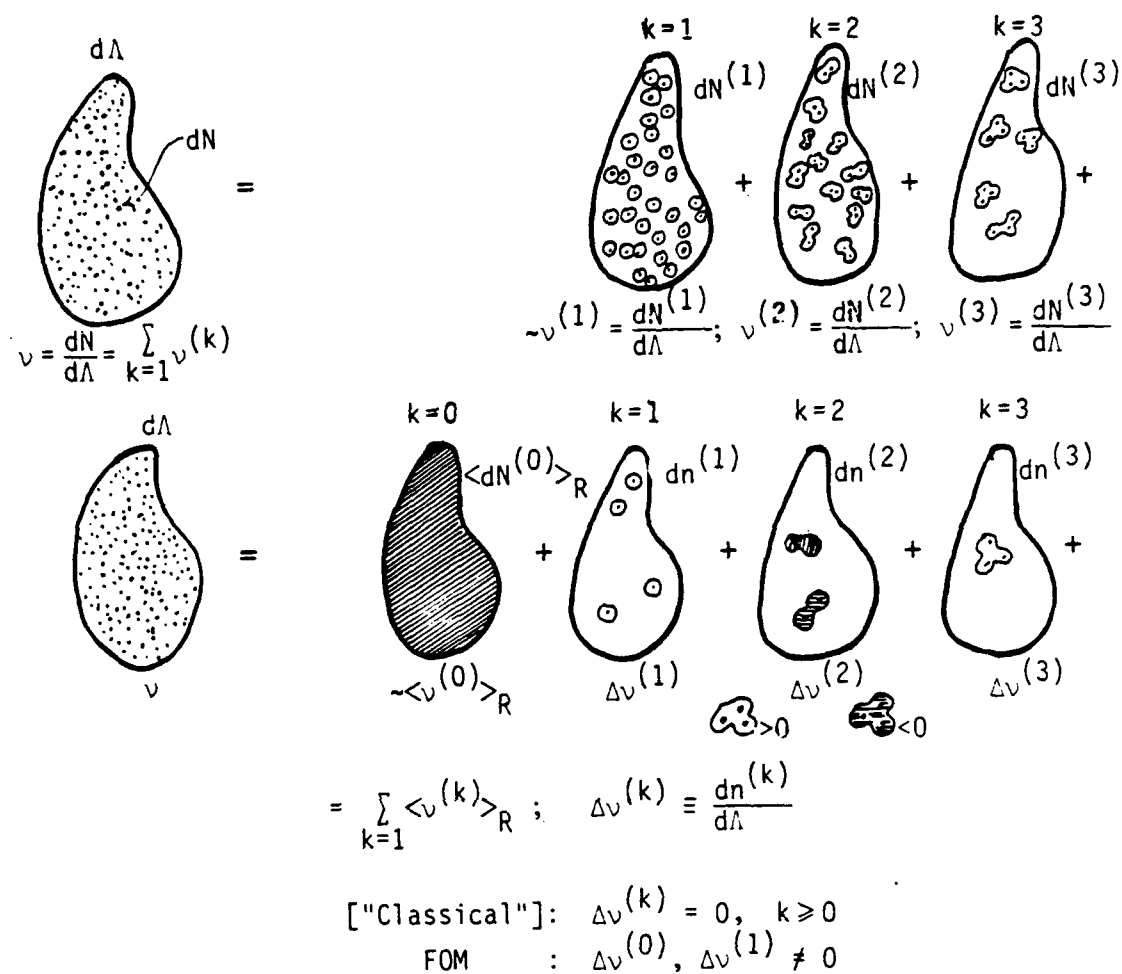


Figure A.2-1 Decomposition Principle:  $dv = \sum_{k=1} v^{(k)}$ ;  $dN = \sum_{k=1} dN^{(k)}$ : scattering domain resolved into hierarchy of independent,  $k$ -coupled scattering elements.

where  $\hat{\mathcal{L}}_{d\Lambda}$  is a linear (operator) functional, with

$$(BDP): \quad \hat{Q}_M = \hat{\mathcal{L}}_{\Lambda_M} \left\{ \sum_{k=1}^{\infty} a^{(k)}_{i_{OM}} v^{(k)} \right\} \quad (A.2-7b)$$

over the entire region ( $\Lambda_M$ ) of scatterers. Here  $v^{(k)} = v^{(k)}(\underline{r}, t)$  is the density of  $k$ -coupled scattering elements ("quasi-particles") in  $\Lambda_M$ . The quantities  $a^{(k)}_{i_{OM}}$ ,  $a^{(k)}$  are respectively the scattering "cross-section" of



the  $k^{\text{th}}$ -order "quasi-particles," and an appropriate weighting function, noted below. Thus, the BDP shows how a scattering region is decomposable into independent groups of interacting elements. [This decomposition has certain analogies with "Cluster Theory" in the statistical mechanics of a classical nonideal gas [42], but in any case we are not concerned here with the details of the k-tuple interactions.] Each k-tuple is entirely equivalent to a  $k^{\text{th}}$ -order (classical) "quasi-particle," in the language of particle physics ([41], Chapter 2). Thus, (A.2-6) can be interpreted as a sum of different densities of "quasi-particles," which interact with the incident field to produce corresponding orders of single- and multiple-scatter.

Comparing (A.2-7b) and (A.2-1) specifies  $\hat{\mathcal{L}}_{\Lambda_M}$ , namely,

$$\text{(BDP): } \hat{Q}_M = \int_{-\infty}^{\infty} dt' \int_{\Lambda_M} \sum_{k=1}^{\infty} v^{(k)}_{\gamma_0} h_F^{(k)}(t-t', t|\underline{r}', \underline{r}, \dots) \hat{d}_0(\underline{r}, t|\underline{r}', t') [ ]_{\underline{r}', t'} d\Lambda_M \quad (\text{A.2-8})$$

where  $a^{(k)} = h_F^{(k)}$  is a time-varying weighting function representing the reradiation process from the  $k^{\text{th}}$ -order "quasi-particles" (or scattering elements\*). Again,  $\hat{d}_0$  is a local interaction operator (A.2-1a), determined by the particular Langevin equation (3.2), for example (A.2-4) et seq. The key result of the BDP is that it removes our having to specify the details of the radiation interactions within the  $k^{\text{th}}$ -order "quasi-particle." Instead, we have a linear combination of quantities  $(\sim \gamma_0^{(k)} v^{(k)})$ , cf. (A.2-8), which are to be determined explicitly from the appropriate physics of the scattering situation in question.

At this point we consider further the concept of "radiation events" ( $Z_R$ ) (and their statistics), i.e., the interactions of the incident field with a quasi-particle, followed by emission, for given space-time

-----  
\*The vectors  $\underline{r}, \underline{r}'$  are defined in a coördinate system based in  $\Lambda_M$ , which is generally different from the coördinate system relating source (T), the "ideal" observer in the field (at  $P(\underline{r}, t)$ ), or the receiver (R), cf. Fig. A.2-5.

coördinates ( $S \equiv (r, t)$ ), i.e.,  $Z_{S \times \underline{\theta}}$  fixed. The classical description of scattering ( $Z_{\text{class}}$ ) is thus analyzed into a two-component process:

$Z_{\text{class}} = Z_{S \times \underline{\theta}} \times Z_R$ , and the classical statistical averages are  $\langle \rangle_{\text{class}} = \langle \rangle = \langle \rangle_R \rangle_{S \times \underline{\theta}}$ , where  $\langle \rangle_R$  = average over radiation events ( $Z_R$ ), and  $\langle \rangle_{S \times \underline{\theta}}$  = average over spatial and parameter values.

The importance of this decomposition is that it permits us to determine the overall statistics of the  $v^{(k)}$ . This is accomplished by our first noting that the fluctuation  $\Delta v^{(k)}$  in the number of  $k^{\text{th}}$ -order radiation interactions in  $\Lambda_M$  is given by (A.2-6).

Furthermore, we have the identity

$$\sum_{k=1}^{\infty} \gamma_0^{(k)} v^{(k)} h_F^{(k)} = \underbrace{\gamma_0^{(0)} h_F^{(0)} \langle v^{(0)} \rangle_R}_{k=0} + \sum_{k=1}^{\infty} \gamma_0^{(k)} h_F^{(k)} \Delta v^{(k)} = \Gamma^{(0)} + \sum_{k=1}^{\infty} \gamma_0^{(k)} h_F^{(k)} \Delta v^{(k)}, \quad (\text{A.2-9})$$

so that by (A.2-7b)

$$\hat{Q}_M = \hat{\mathcal{L}}_{\Lambda_M} (\Gamma^{(0)} + \sum_{k=1}^{\infty} \gamma_0^{(k)} h_F^{(k)} \Delta v^{(k)}). \quad (\text{A.2-9a})$$

It can be readily shown [11] that the radiation-event statistics (RES) of the  $\Delta v^{(k)}$  are zero-mean poisson, with the  $n^{\text{th}}$ -order characteristic function (c.f.)

$$F_n^{(k)}(i\underline{\xi}, it | Z_{S \times \underline{\theta}} | \Delta v^{(k)}) = \exp \left[ \int_{\Lambda_{1 \dots n}} R_n^{(k)} [\exp(i \sum_{\ell=1}^n \xi_{\ell}) - i \sum_{\ell=1}^n \xi_{\ell}] d\Lambda_{1 \dots n} \right],$$

(each  $k \geq 1$ , any  $n \geq 1$ );  $\Lambda_{1 \dots n} = \Lambda_1 \cdot \Lambda_2 \cdot \dots \cdot \Lambda_n$ , (A.2-10)

in which  $i\underline{\xi} = i\xi_1, \dots, i\xi_n$ ;  $it = it_1, \dots, it_n$  and  $R_n^{(k)} = R_n^{(k)}(\underline{\lambda}_1, t_1; \dots; \underline{\lambda}_n, t_n) \geq 0$ , ( $k, n \geq 1$ ) is the associated process density. Since the radiation events for different  $k$  are independent, the complete (conditional) c.f. of the  $\Delta v^{(k)}$ ,  $k \geq 1$  is

$$F_n^{(\infty)} = \prod_{k=1}^{\infty} F_n^{(k)}. \quad (\text{A.2-11})$$

The overall statistics of  $\gamma_0^{(k)} h_F^{(k)} \Delta v^{(k)}$  are found from the  $(n^{\text{th}})$ -order Fourier transform of  $\langle F_n^{(k)} \rangle_{Z_{S \times \underline{\theta}}}$ , and for  $\sum_{k=1}^{\infty} \gamma_0^{(k)} h_F^{(k)} \Delta v^{(k)}$  from the F.T.

$\{ \langle F_n^{(k)} \rangle_{Z_{S \times \theta}} \}$ . Thus, a central problem in applying our canonical development here is to determine the process densities  $R_n^{(k)}$  for the specific physical problem in question. We note some examples below in Sec. A.2-2.

## A.2-2 Examples: FOM and Classical Scatter Models

We begin by considering

### A. FOM Models:

As noted in Section 5, FOM models [28]-[30] are quasi-phenomenological in that:

- (i). they do not explicitly include boundary conditions, but rather subsume them in the  $\Gamma^{(0)}$  and  $\gamma_0^{(k)} h_F^{(k)}$  factors of the scattering operator,  $\hat{Q}_M$ , cf. (A.2-9);
- (ii). they permit only  $k=1$  (and hence  $k=0$ ) types of radiation interactions, namely, the so-called independent "point"-scattering. This latter constraint ensures only "weak-scattering" in volumes ( $M=V$ ), and correspondingly for surfaces ( $S,B$ ), e.g.,

$$\alpha \doteq \alpha_H + \hat{M}_\infty \hat{Q}_M \alpha_H$$

in (3.9), cf. (5.1) also, with the added condition that all  $k$ -order ( $k \geq 2$ ) interactions in  $\hat{Q}_M$  are omitted: no multiple scatter, cf. (5.8).

Thus, in the FOM cases we have the following relation for the governing process density  $R_n^{(1)}$ :

$$R_n^{(k)} \rightarrow R_n^{(1)} = \sigma_M^{(1)}(\underline{r}) \prod_{\ell=2}^n \delta(\underline{r}_\ell - \underline{r}_{\ell-1}), \quad (\text{A.2-12})$$

where now  $\sigma_M^{(1)}$  = average density of scatterers in the illuminated region  $A_M$ , ( $M=S,B,V$ ). From (5.9), (5.9a) we see that  $\langle v^{(1)} \rangle = v^{(1)}$ ,  $v^{(k)} = 0$ ,  $k \geq 2$ .

The original FOM models for surface scatter [28]-[31] postulated a flat surface ( $z=0$ ), but employed a dopplerized path delay,  $t_d$ , in  $h_F^{(k)}$  which implicitly contained the effects of the moving surface. FOM model extensions, FOM<sup>(1a)</sup>, explicitly include the surface elevation  $z$  in the doppler delay [36], viz.

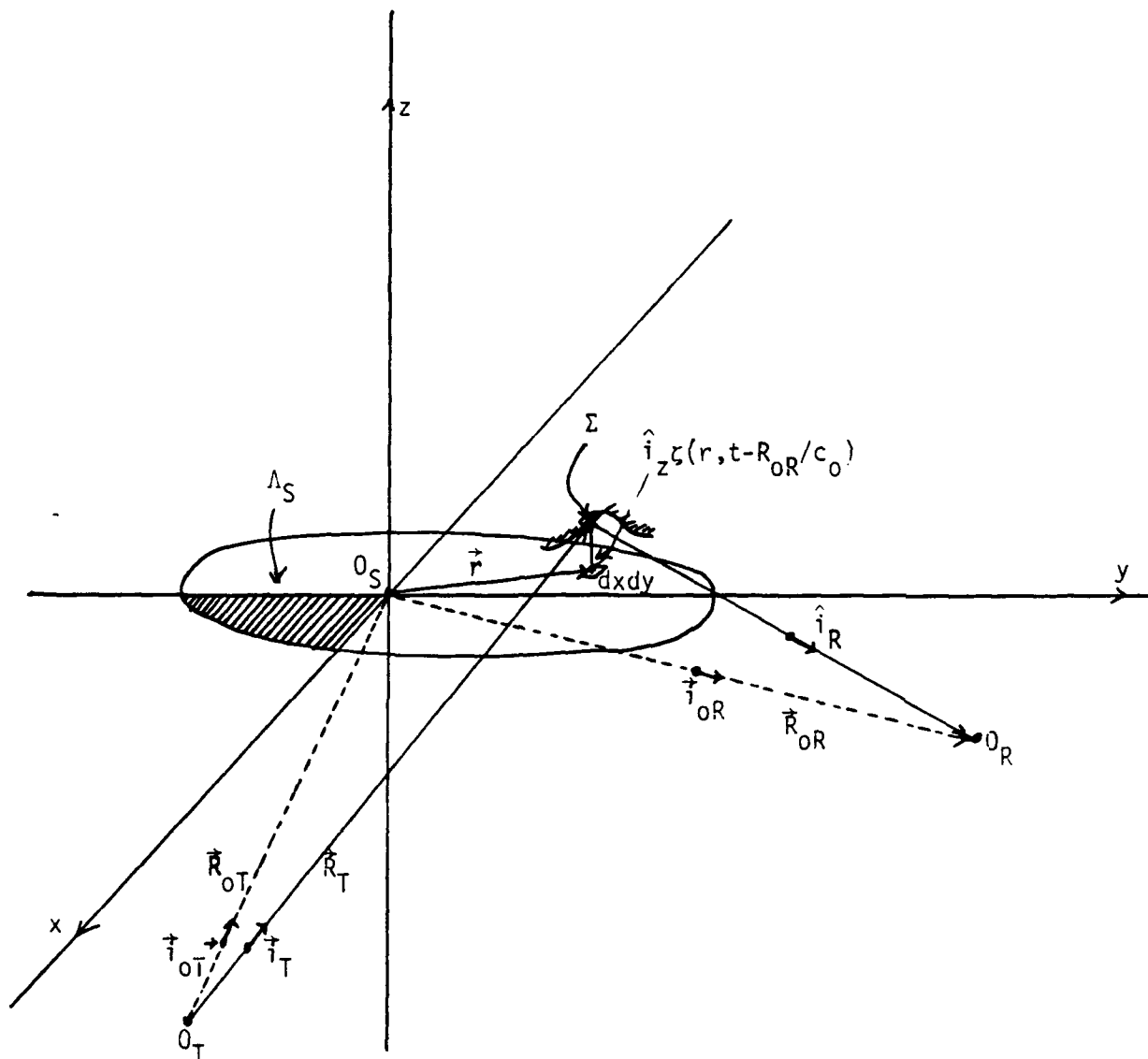


Figure A.2-2 Geometry of bistatic surface scatter.

$$t_d = T_0 + (\hat{i}_T - \hat{i}_R) \cdot [\underline{r} + \underline{\zeta}(r, t - R_{OR}/c_0)]/c_0, \quad T_0 = (R_{OR} + R_{OT})/c_0; \quad (A.2-13)$$

$$\underline{\zeta} = \hat{i}_z \zeta.$$

where  $\underline{r} = \hat{i}_x x + \hat{i}_y y$  on  $\Lambda_S$  ( $\zeta = 0$ ) and  $\hat{i}_T = \underline{R}_T/|\underline{R}_T|$ , etc., with  $c_0$  = mean speed of sound, as shown in Fig. A.2-2. A second extension (FOM<sup>(2)</sup>) of the original FOM model, in addition to the above dopplerized delay (A.2-13), explicitly includes the tilted surface  $\Sigma$  of surface wave heights in the "cross-section"  $\gamma_0^{(1)}$ , e.g.,

$$\hat{\gamma}_0^{(1)} = \gamma_0^{(1)} \hat{n}_g \cdot (\hat{i}_T - \hat{i}_R) \rightarrow \gamma_0^{(1)} \hat{n}_g \cdot (\hat{i}_{OT} - \hat{i}_{OR}), \quad (A.2-14)$$

where now  $\hat{n}_g$  is the normal to the (large-scale) component of the gravity-capillary wave surface

$$\hat{n}_g = \left\{ \frac{\hat{i}_x \zeta_x + \hat{i}_y \zeta_y - \hat{i}_z}{\sqrt{1 + \zeta_x^2 + \zeta_y^2}} \right\}_g = \{ (\hat{i}_x \zeta_x + \hat{i}_y \zeta_y - \hat{i}_z) n_z \}_g. \quad (A.2-15)$$

For both extensions  $\Gamma^{(0)} = \sigma^{(1)}(\underline{r}) \hat{\gamma}_0^{(1)}$ , where again  $\sigma^{(1)}$  is the mean density of (independent) scatterers on the surface. FOM<sup>(1a)</sup> and FOM<sup>(2)</sup> thus incorporate explicitly the physical geometry of the (wave) surface.

The practical utility of FOM models is that they replace the often very difficult problem of explicitly evaluating the boundary conditions at the scattering elements, by introducing a time-variable weighting function  $\gamma_0^{(1)} h_F^{(1)}$ , or  $\hat{\gamma}_0^{(1)} h_F^{(1)}$ , which also may include the extended doppler delay (A.2-13) [36]. Simple choices of  $\gamma_0^{(1)}$ ,  $h_F^{(1)}$  are then tested against experience [43]-[46]. The limitations of the FOM models are threefold:

- (1). They lack explicit physical structures. [This can be to a considerable extent overcome by using FOM<sup>(2)</sup> models, cf. above];
- (2). They are quasi-phenomenological, namely, they require a suitable choice of  $h_F^{(1)}$  and consequent calibration to the problem at hand; and
- (3). They (currently) omit multiple-scatter effects, or diffraction (e.g.,  $v^{(k)} = 0$ ,  $k \geq 2$ ). [This is also a limitation of most "classical" scatter models, as well [25]-[27], [37]-[39], [48], but see [51].]

#### B. Classical Scatter Models:

Classical scatter models cf. [25]-[27], [48], as noted in Sec. 5 earlier, in their practical formulations for the most part neglect multiple scatter effects ( $k \geq 2$ ), so that, in our formalism, cf. Appendix A.1,  $v^{(0)} = v^{(1)}$ ,  $v^{(k)} = 0$ ,  $k \geq 2$ . In the important cases of surface scatter, for example, it can be shown on comparing the classical approximations, namely Kirchhoff and perturbational boundary evaluations [48], that now

$$\gamma_{0v}^{(0)} \doteq \gamma_{0v}^{(1)} \doteq RS \frac{\omega}{c_0} \hat{n}_g \cdot (\hat{i}_T - \hat{i}_R), \quad (A.2-16)$$

cf. (5.10) above, with (A.2-15). Equations (5.6)-(5.7c) again apply here, so that

$$K_{\hat{Q}}|_{\text{surface}} = \mathcal{L}\{ \langle [\hat{n}_g \cdot (\hat{i}_T - \hat{i}_R)]_1 [\hat{n}_g \cdot \hat{i}_T - \hat{i}_R]_2 \rangle - \langle \hat{Q} \rangle_1 \langle \hat{Q} \rangle_2 \} \quad (A.2-17)$$

for the covariance of the incoherent scatter from a typical random (wave) surface. A detailed evaluation of (A.2-16) is described in [50], Part I, and extended to include explicit doppler measures in Part II. Higher-order moments are found similarly, viz.

$$\langle \hat{Q}_1 \hat{Q}_2 \hat{Q}_3 \rangle_{\text{surface}} = \mathcal{L}\{ \langle \gamma_{01v_1}^{(1)} \gamma_{02v_2}^{(1)} \gamma_{03v_3}^{(1)} \rangle \} , \text{ etc.}, \quad (A.2-18)$$

with the help of (A.2-16) explicitly, see [50].

### Appendix A.3 Bayesian Estimation: A Decision-Theoretic Formulation

Here we briefly summarize the needed main elements of the decision-theoretic formulation of signal estimation theory [15], [58], [20].

For an estimator we write

$$\underline{y} = \underline{y}_\sigma(\underline{\theta}|\underline{x}) = g_E(\underline{x}), \quad (\text{A.3-1})$$

where  $\underline{\theta} = (\theta_1, \dots, \theta_M)$  is a set of signal parameters (or waveform samples, etc.) to be estimated;  $\underline{x} = (x_1, \dots, x_J)$  is the set of received data samples in which the estimate is to be based; the "decisions," or estimates made are denoted by  $\underline{y} = (y_1, \dots, y_M)$ , and  $\sigma$  in  $y_\sigma$  indicates the a priori probability (density) governing the parameters  $\underline{\theta}$ , e.g.,  $\sigma = \sigma(\underline{\theta})$ , or  $\underline{s}$  in  $\sigma(\underline{s})$ . [We note that  $\underline{y}_\sigma$  is an estimator for all permitted  $\underline{x}$ , while for a particular set  $\underline{x} = \underline{x}'$ ,  $\underline{y}_\sigma$  becomes an estimate.] The decision rule  $\delta$  is here  $\delta(\underline{y}|\underline{x}) = \delta(\underline{y} - \underline{y}_\sigma(\underline{\theta}|\underline{x}))$ , which is an (M-dimensional) delta function. When  $\underline{y}_\sigma (=g_E)$  is given, i.e., the estimating receiver  $g_E(\underline{x})$  is specified, the average error (or risk) is determined from

$$R(\sigma, \delta)_{\underline{s} \text{ or } \underline{\theta}} = \int_{\Omega} \sigma(\underline{s} \text{ or } \underline{\theta}) d\underline{s} \text{ (or } d\underline{\theta}) \cdot \int_{\Gamma} F_n(\underline{x}|\underline{s}(\underline{\theta})) C(\underline{s} \text{ or } \underline{\theta}, \underline{y}_\sigma) d\underline{x} \quad (\text{A.3-2})$$

where  $C$  is an appropriately chosen cost function, naturally proportional to the measure of error selected. The estimator  $\underline{y}_\sigma$  is a point estimate, and  $F_n$  is the conditional pdf of  $\underline{x}$ , given  $\underline{s}(\underline{\theta})$ .

Another useful type of estimation procedure is interval estimation, defined by the probability  $P$  that a particular point estimate,  $\underline{y}_\sigma$  (for given  $\underline{x}$ ) falls within  $(1 \pm \lambda)$  100% of the true value of the quantity [ $\underline{s}$  = waveform, or  $\underline{\theta}$  = parameters in  $\underline{s}(\underline{\theta})$ ] being estimated, viz.:

$$P\{(1-\lambda)[\underline{s} \text{ or } \underline{\theta}] \leq \underline{y}_\sigma(\underline{s} \text{ or } \underline{\theta}|\underline{x}) \leq (1+\lambda)[\underline{s} \text{ or } \underline{\theta}]\}, \quad 0 < \lambda < 1 \quad (\text{A.3-3})$$

where  $\lambda$  is a measure of the prechosen confidence interval selected,  $-\lambda \underline{s}$  to  $+\lambda \underline{s}$  for example. In the case of a single parameter  $\theta$ , for instance, we can write

$$P\{(1-\lambda)\theta \leq \gamma_\sigma(\theta|\underline{X}) \leq (1+\lambda)\theta\} = \int_{(1-\lambda)\theta}^{(1+\lambda)\theta} W_1(\gamma_\sigma(\theta)) d\gamma_\sigma, \quad (\text{A.3-4})$$

where  $W_1(\gamma_\sigma|\theta) = p(\gamma|\theta)$  is the conditional pdf of the estimator  $\gamma$ , conditional on  $\theta$ , formed here from  $p(\gamma|\theta) = \int_{\Gamma} F_n(\underline{X}|\underline{S}(\theta)\delta(\gamma_\theta|\underline{X})) d\underline{X}$ , with obvious formal extensions to the multidimensional cases, cf. [16], [58], [20]. The unconditional pdfs of the estimators themselves are obtained from  $p(\underline{\gamma}) = \langle p(\underline{\gamma}|\underline{S} \text{ or } \underline{\theta}) \rangle_{\underline{S} \text{ or } \underline{\theta}}$ .

We emphasize that  $\underline{\gamma}_\sigma$  is a point estimator, embodying the specific structure,  $g_E$ , (A.3-1), of the receiver performing the estimation. On the other hand, interval estimators, as expressed by  $P$ , (A.3-3), (A.3-4), yield a probability which is a measure of the efficiency of the point estimator for any particular application (i.e., choice of  $\underline{X}$ ). The average error (or risk) (A.3-2) measures the expected cost or average error in using  $\underline{\gamma}_\sigma$ , considered over all possible  $\{\underline{X}\}$  received.

For optimum, or Bayes estimation we seek estimators  $\underline{\gamma}_\sigma^*$  which minimize the average error or risk  $R(\sigma, \delta)$ , (A.3-2). The general form of the resulting  $\underline{\gamma}_\sigma^*$  depends, of course, on the choice of "cost" or error function  $C(\underline{S} \text{ or } \underline{\theta}, \underline{\gamma}_\sigma)$ . For example, for the quadratic cost function (QCF)

$$C(\underline{\theta}, \underline{\gamma}_\sigma) = C_0 |\underline{\theta} - \underline{\gamma}_\sigma|^2 = C_0 \sum_{\hat{m}=1}^{\hat{M}} (\theta_{\hat{m}} - \gamma_{\sigma\hat{m}})^2, \quad (\text{A.3-5})$$

the associated optimum estimator is found to be (cf. Chapter 3, [58], Chapter 21, [20]) the set of equations

$$\underline{\gamma}_\sigma^*(\underline{\theta}|\underline{X})_{\text{QCF}} = \int_{\Omega_\theta} \underline{\theta} \sigma(\underline{\theta}) F_n(\underline{X}|\underline{S}(\underline{\theta})) d\underline{\theta} / \int_{\Omega_\theta} \sigma(\underline{\theta}) F_n(\underline{X}|\underline{S}(\underline{\theta})) d\underline{\theta}, \quad (\text{A.3-6})$$

with  $\underline{\theta} \rightarrow \underline{S}$ ,  $\sigma(\underline{\theta}) \rightarrow \sigma(\underline{S})$ ,  $d\underline{\theta} \rightarrow d\underline{S}$  in the case of estimating signal waveforms. Note that  $\underline{\gamma}_\sigma^*$  is generally a nonlinear operator on the received data,  $\underline{X}$ .

Another cost function of considerable interest is the simple (or rectangular) cost function (SCF) given by

$$C(\underline{\theta}, \underline{\gamma}_\sigma) = C_0 \sum_{\hat{m}=1}^{\hat{M}} [A_{\hat{m}} - \gamma(\gamma_{\hat{m}} - \theta_{\hat{m}})] \quad (\text{A.3-7})$$



with appropriate choices of  $C_0$ ,  $A_m$  to ensure meaningful results (e.g., positive errors, etc.). Minimization of average risk here leads directly to (cf. Sec. 21.2-1 of [20]) the following relations determining  $\gamma_\sigma^*$  SCF:

$$\left. \frac{\partial}{\partial \theta_m} \log \{ \sigma(\theta_m) W_J(X|\theta_m) \} \right|_{\theta_m = \theta_m^* = \gamma_m^*} = 0, \quad \text{all } m = 1, \dots, M, \quad (\text{A.3-8})$$

where  $W_J(X|\gamma_m = \theta_m) \equiv \langle F_n(X|S(\gamma_m, \theta')) \rangle_{\theta' = \theta - \gamma_m} / \sigma(\gamma_m = \theta_m)$ , and

$\sigma(\gamma_m = \theta_m) = \langle \sigma(\gamma_m, \theta') \rangle_{\theta'}$ , with  $\theta' =$  all  $\theta$  except  $\theta_m$ . The condition (A.3-8) determining  $\gamma_m^* = \{\gamma_m^*\}$  is precisely that determining the unconditional maximum likelihood estimates (UMLE's) of  $\theta = \{\theta_m\}$ , viz.  $\gamma_m^*$  here. [If  $\sigma(\theta_m)$  is omitted in (A.3-8) one has the corresponding conditional maximum likelihood estimates (CMLE's) of the  $\{\theta_m\}$ . The extension of (A.3-8) to waveform estimation is formally immediate: one replaces  $\theta_m$  by  $S_m$ ,  $\sigma(\theta_m)$  by  $\sigma(S_m)$ ,  $W_J(X|\theta_m)$  by  $W_J(X|S_m)$ , etc., with  $m = 1, \dots, J$  now.]

In summary, we remark that:

- I. The maximum (conditional) likelihood estimator (CMLE) maximizes the probability of a correct decision, without regard to incorrect decisions and their costs;
  - II. The maximum unconditional likelihood estimator (UMLE) maximizes the probability of a correct estimate, when all possible (signal or parameter) values are taken into account, again without specific regard for incorrect decisions and their errors;
  - III. The optimum quadratic estimator  $\gamma_{OCF}^*$ , (A.3-6), is an unconditional least mean-square error (LMSE) estimator, which accounts on the average for incorrect decisions and errors.
- (A.3-9)

## References

### A. References Devoted Primarily to Non-Gaussian Noise and Signal Processing

- [1]. D. Middleton, "Channel Characterization and Threshold Reception for Complex Underwater Acoustic Media," EASCON, Sept. 29-Oct. 1, 1980 [IEEE Pub. 0531-0863/80-0000-0171.], pp. 171-180.
- [2]. \_\_\_\_\_, "The Underwater Medium as a Generalized Communication Channel" (Invited paper), pp. 588-612 of Underwater Acoustics and Signal Processing (NATO Advanced Study), Ed. by L. Bjørnø, D. Reidel Publishing Co., Dordrecht, Holland, 1981.
- [3]. \_\_\_\_\_, "Multiple-Element Threshold Signal Detection of Underwater Acoustic Signals in Non-Gaussian Interference Environments," Contractor Report CR 231, May 18, 1984, Naval Ocean Systems Center (NOSC), San Diego, CA 92152.
- [4]. \_\_\_\_\_, "Space-Time Processing for Weak Signal Detection in Non-Gaussian and Nonuniform Electromagnetic Interference (EMI) Fields," Contractor Report 86-36, Feb., 1986, ITS/NTIA, U.S. Dept. of Commerce, 325 Broadway, Boulder, Colorado 80303.
- [5]. \_\_\_\_\_, "Non-Gaussian Underwater Acoustic Space-Time Signal Processing: The Threshold Régime," to be submitted to J. Acous. Soc. Amer., Fall, 1986.
- [6]. \_\_\_\_\_, "Statistical-Physical Models of Electromagnetic Interference," IEEE Trans. on Electromagnetic Compatibility, Vol. EMC-19, No. 3, pp. 106-127, Aug., 1977.
- [7]. \_\_\_\_\_, "Canonical Non-Gaussian Noise Models: Their Implications for Measurement and for Prediction of Receiver Performance," IEEE Trans. on Electromagnetic Compatibility, Vol. EMC-21, No. 3, pp. 209-220, Aug., 1979.
- [8]. "Canonical and Quasi-Canonical Probability Models of Class A Interference," IEEE Trans. on Electromagnetic Compatibility, Vol. EMC-25, No. 2, pp. 76-106, May, 1983.
- [9]. A. H. Nuttall, I. B. Cohen, and D. Middleton, "Performance Parameters for Quasi-Canonical Class A Non-Gaussian Noise: Source Distribution

Law  $\mu = 0$ , Propagation Law  $\gamma = 2$ ." Technical Report No. 7715, in publication, Fall, 1986, Naval Underwater Systems Center (NUSC), New London, Conn. 06320.

- [10]. D. Middleton, "Second-Order Non-Gaussian Probability Distributions and Their Applications to 'Classical' Nonlinear Processing Problems in Communication Theory," Proceedings, 20th Conference on Information Sciences and Systems, Princeton University, March 19-21, 1986, pub. Fall, 1986. [An extended version of this paper has been submitted to IEEE Trans. on Information Theory, Fall, 1986.]
- [11]. \_\_\_\_\_, "Non-Gaussian Random Field Models for Telecommunications, Scattering, and Remote Sensing," Proceedings 1986, IEEE International Symposium on Information Theory; also, submitted: Proceedings, IEEE Trans. on Information Theory, Dec., 1986.
- [12]. D. Middleton and A. D. Spaulding, "A Tutorial Review of Elements of Weak Signal Detection in Non-Gaussian EMI Environments," NTIA Report 86-194, May, 1986, Inst. of Telecommunication Sciences, National Telecommunication and Information Administration (ITS/NTIA), U.S. Dept. of Commerce, 325 Broadway, Boulder, Colorado 80303.
- [13]. D. Middleton, G. H. Hagn, and A. D. Spaulding, "Parametric Noise Models and Threshold Signal Processing in Telecommunications: A Tutorial Review," (Invited paper), Proc. IEEE, submitted early 1987.
- [14]. A. D. Spaulding and D. Middleton, "Optimum Reception in an Impulsive Interference Environment--Part I: Coherent Detection; \_\_\_\_\_, Part II: Incoherent Reception," IEEE Trans. on Communication, Vol. COM-25, No. 9, Sept., 1977, pp. 910-934.
- [15]. D. Middleton and A. D. Spaulding, "Optimum Reception in Non-Gaussian Electromagnetic Interference Environments: II. Optimum and Suboptimum Threshold Signal Detection in Class A and B Noise," NTIA Report 83-120, May, 1983, ITS/NTIA, U.S. Dept. of Commerce, 325 Broadway, Boulder, Colo. 80303.

- [16]. D. Middleton, "Threshold Detection in Non-Gaussian Interference Environments: Exposition and Interpretation of New Results for EMC Applications," IEEE Trans. Electromagnetic Compatability, Vol. EMC-26, No. 1, Feb., 1984, pp. 19-28.
- [17]. R. F. Dwyer, "A Technique for Improving Detection and Estimation of Signals Contaminated by Under Ice Noise," J. Acous. Soc. Amer. 74, (1), July, 1983, pp. 124-130.
- [18]. A. D. Spaulding, "Locally Optimum and Suboptimum Detector Performance in a Non-Gaussian Interference Environment," IEEE Trans. Communications, Vol. COM-33, No. 6, June, 1985, pp. 509-517.

B. References Primarily Devoted to Radiation and Scattering [cf. [1], [2], [11], also.]

- [19]. D. Middleton, "Multidimensional Detection and Extraction of Signals in Random Media," Proceedings of the IEEE, Vol. 58, No. 5, May, 1970, pp. 696-706.
- [20]. \_\_\_\_\_, An Introduction to Statistical Communication Theory, McGraw-Hill (New York), 1960, (Part IV).
- [21]. J. R. Breton and D. Middleton, "General Theory of Acoustic Propagation Through Arbitrary Fluid Media--I. Propagation Equations, Conditions of the Medium, and General Dynamical Solitons," J. Acous. Soc. Amer. 69 (5), pp. 1245-1260, May 1981. See also, Breton, J. R., A General Theory of Acoustic Propagation and Applications to Strong Acoustic Scattering in the Atmosphere and Ocean, Doctoral Dissertation, Elec. Eng. Dept., Univ. of Rhode Island, Dec., 1977; also as Technical Report TR-5871, Naval Underwater Systems Center (NUSC), New London, Conn., Jan., 1978.
- [22]. A. Ishimaru, Wave Propagation and Scattering in Random Media, Academic Press (New York, Vols. 1, 2), 1978.
- [23]. J. Frisch, "Wave Propagation in Random Media," in Probabilistic Methods in Applied Mathematics, Vol. 1, Ed. Bharucha-Reid, Academic Press (New York), 1968, pp. 75-198.

- [24]. V. I. Tatarskii, The Effects of the Turbulent Atmosphere on Wave Propagation, U.S. Dept. of Commerce, NTIA, Springfield, Virginia 22151, Vol. 66-68-50464, 1971.
- [25]. L. Fortuin, "Survey of Literature on Reflection and Scattering of Sound Waves at the Sea Surface," J. Acous. Soc. Amer. 47, 1209-1228 (1970).
- [26]. C. W. Horton, Sr., "A Review of Reverberation, Scattering, and Echo Structure," J. Acous. Soc. Amer. 51, 1049-1061 (1972).
- [27]. I. Tolstoy and C. S. Clay, Ocean Acoustics, McGraw-Hill (New York), 1966; esp. Chap. 6.
- [28]. P. Faure, "Theoretical Models of Reverberation Noise," J. Acous. Soc. Amer. 36, 259-268 (1964).
- [29]. V. V. Ol'shevskii, Characteristics of Ocean Reverberation (transl. of 1966 work, Moscow), Consultants Bureau (Plenum Press, N.Y., N.Y.), 1967.
- [30]. Statistical Methods in Sonar (Leningrad, 1973), and Plenum Pub. Co., New York, 1978 (D. Middleton, Scientific Editor); 2<sup>nd</sup> Edition, "Sudostroenie," Leningrad, 1983.
- [31]. D. Middleton, "A Statistical Theory of Reverberation and Similar First-Order Scattered Fields," Parts I, II, IEEE Trans. Information Theory, Vol. IT-13, 372-392; 393-414 (1967); Parts III, IV, *ibid.*, Vol. IT-18, 35-67; 68-90 (1972).
- [32]. \_\_\_\_\_, Invited lectures, at Acoustics Institute N.N. Andreev, Acad. Sci. USSR (Moscow), 1973, 1976, 1979, 1984, in Trudy "Acoustical Statistical Models of the Ocean"; also contributed and invited papers on the same subject by the author at meetings of the American Acoustical Society and others (1973-1979).
- [33]. P. M. Morse and K. U. Ingaard, Theoretical Acoustics, McGraw-Hill (New York), 1968; Chapter 6; esp. Sec. 6.1.
- [34]. R. B. Lindsay, Mechanical Radiation, McGraw-Hill (New York), 1960, Sec. 9.11, 12.4.
- [35]. P. M. Morse and J. Feshbach, Methods of Theoretical Physics, McGraw-Hill (New York), 1953, cf. Chapter 9.
- [36]. D. Middleton, "Doppler Effects for Randomly Moving Scatterers and Platforms," J. Acous. Soc. Amer. 61, 1231-1250, May, 1977.

- [37]. B. E. Parkins, "Scattering from the Time Varying Surface of the Ocean," J. Acous. Soc. Amer. 42, 1262-1267, No. 6, 1967.
- [38]. C. S. Clay and H. Medwin, Acoustical Oceanography, John Wiley (New York), 1977; Section A 10.2.
- [39]. C. Eckart, "The Scattering of Sound from the Sea Surface," J. Acous. Soc. Amer., 25, 566-570 (1953).
- [40]. D. Middleton, "A New Approach to Scattering Problems in Random Media," June, 1975, pp. 407-430 of Multivariate Analysis IV, Ed. P. R. Krishnaiah, North Holland Pub. Co. (New York), 1977.
- [41]. R. D. Mattuck, A Guide to Feynman Diagrams in the Many-Body Problem (2<sup>nd</sup> Ed.), McGraw-Hill (New York), 1976.
- [42]. J. E. and M. G. Mayer, Statistical Mechanics, John Wiley (New York), 1940, Chapter 13.
- [43]. T. D. Plemons, J. A. Shooter, and D. Middleton, "Underwater Acoustic Scattering from Lake Surfaces, I, II," JASA 52, 1487-1502; 1503-1515, 1972.
- [44]. G. R. Wilson, "Comparison of the Measured Covariance of Surface Reverberation for Horizontal and Vertical Arrays," JASA 73, 1905-1910, 1982.
- [45]. \_\_\_\_\_, "Statistical Analysis of Surface Reverberation," JASA 74, 1983.
- [46]. S. M. Flatté (Ed.), R. Dashen, W. H. Munk, K. M. Watson, F. Zachariasen, Sound Transmission Through a Fluctuating Ocean, Cambridge University Press (New York), 1979.
- [47]. B. F. Kur'yanov, "The Scattering of Sound at a Rough Surface with Two Types of Irregularity," Soviet J. of Physical Acoustics 8, No. 3, pp. 252-257, 1962; in English, 1963.
- [48]. F. G. Bass and I. M. Fuks, Wave Scattering from Statistically Rough Surfaces (trans. and ed. by C. B. and J. F. Vesecky), Pergamon Press (New York), 1979.
- [49]. S. T. McDaniel and A. D. Gorman, "Examination of the Composite Roughness Scattering Model," JASA 73, No. 5, pp. 1476-1480, May, 1983.

- [50]. D. Middleton, "Acoustic Scattering from Composite Wind-Wave Surfaces II. Backscatter Cross Sections and Doppler Effects at High Frequencies and Small Angles for 'Bubble-Free' Regimes," Tech. Report TR-7635, July 22, 1986, Naval Underwater Systems Center (NUSC), New London, Conn. 06320. See also Part I, NUSC Tech. Doc. TD-7205, 20 August 1984.
- [51]. J. S. DeSanto, "Coherent Multiple Scattering from Rough Surfaces," in Multiple Scattering and Waves in Random Media, Eds., P. L. Chaw, W. E. Kohler, and G. C. Papanicolaou, North Holland Publ. Co. (New York), 1981.
- [52]. D. Middleton, "Probability Models of Received Scattered and Ambient Fields," Intl. Conf. on Engineering in the Ocean Environment, Newport, R.I., Sept. 13-16, 1972, IEEE Pub. 72CH0-660-1-1-OCC, pp. 8-13.

#### C. Additional References for Non-Gaussian Noise and Signal Processing

- [53]. D. Middleton, "Procedures for Determining the Parameters of the First-Order Canonical Models of Class A and Class B Electromagnetic Interference," IEEE Trans. Electromag. Compat., Vol. EMC-21, No. 3, Aug., 1979, pp. 190-208.
- [54]. \_\_\_\_\_, "Canonically Optimum Threshold Detection," IEEE Trans. Information Theory, Vol. IT-12, No. 2, April, 1966, pp. 230-243.
- [55]. S. Ye. Fal'kovich, "Determination of an Optimum Space-Time Signal Processing System," Radioteknika y Elektronika, Vol. 11, No. 5, 1966 (Engl. trans., Scripta Pub., pp. 678-684.)
- [56]. V. S. Chernyak, "Space-Frequency Filtering of Signals in the Presence of Stochastic Interference in Multi-Element Receiving Systems," Radioteknika y Elektronika, Vol. 18, No. 5, 1973 (Engl. trans., Scripta Pub., pp. 696-705).
- [57]. J. Woods and A. J. Estes, "An Experimental Evaluation of the Neyman-Pearson Detector," J. Acoustic. Soc. Amer. 74, No. 2, Aug., 1983, pp. 518-526.
- [58]. D. Middleton, Topics in Communication Theory, McGraw-Hill (New York), 1965, Chapter 3.

- [59]. D. Middleton and R. Esposito, "Simultaneous Optimum Detection and Estimation of Signals in Noise," IEEE Trans. on Information Theory, Vol. IT-14, No. 3, May 1968, p. 434-444.
- [60]. L. LeCam, "On the Asymptotic Theory of Estimation and Testing Hypotheses," Proc. 3d Berkeley Symposium in Mathematical Statistics, Univ. of California Press, Berkeley, 1956, and "Locally Asymptotically Normal Families of Distributions," Univ. of California Press, 1960, Vol. 3, No. 1, p. 37-98, Publications in Statistics.
- [61]. B. R. Levin, Theoretical Principles of Statistical Radio Engineering, Vol. 3, "Soviet Radio," Moscow, cf. Chapter 3, (translation).



# INITIAL DISTRIBUTION LIST

Addressee	No. of Copies
NAVSEASYSOM (SEA-63D (CDR E. Graham))	1
NORDA (Code 530; 113 (B. Adams, Dr. R. Farwell T. Goldsberry, Dr. M.Y. Su); 240 (Dr. N. Kinney)	6
NOSC (Code 013 (Dr. E. Cooper) (3); 7133 (Dr. C. Persons); 5322 (Dr. J. Northrup); (B. Smith); Marine Physical Labs (Dr. F. Fisher, Dr. F. Spiess))	8
SACLANTCTR (Tech. Director (R. Goodman))	1
ONR (Code 1125 UA (Dr. R. M. Fitzgerald, Dr. R. Sternberg); 1125 AR (R. Obrochta); 1111 SP (Dr. N. Gerr); 111 (Dr. T. Berlincourt); 112 (G. Hamilton); 1122B (E. Hartwig); 1111 (Dr. E. Wagman, Dr. Ringison))	9
NRL (Code 5160 (E. Franchi); Code 5303 (Dr. L. Wetzel))	2
ITS/NTIA (U.S Dept. of Commerce (Dr. A. Spaulding, Dr. C. Rush))	2
ARL, UNIV OF TEXAS (G. Wilson, G. Ellis, Prof. C. Horton, Dr. H. Boheme, Dr. R. Culbertson)	5
DTIC	12
NAVPGSCOL (Prof. H. Medwin; Library)	2
SAIC (W. Chadsey, Dr. Tatrow, Dr. J. Brackett Hersey, Dr. R. Green)	4
YALE UNIVERSITY (Prof. P. H. Schultheiss)	1
Scripps Inst. of Oceanography, La Jolla, CA (Dr. W. Munk)	1
ARL/PENN STATE, STATE COLLEGE, PA (Dr. S. McDaniel, Dr. D. McCammon, Dr. F. Symon)	3
CYBERLINK, Boulder, CO (Dr. P. McManamon)	1
APL, Johns Hopkins (Dr. J. Apel)	1
WPL-NOAA (Wave Propagation Lab (Dr. S. Clifford, Dr. Derr))	2
NOAA (Dir. of NOAA Labs, (Dr. J. Apel))	1
Johns Hopkins Univ. (Dept. of Oceanography (Prof. O. M. Phillips))	1
UNIV OF WISCONSIN (Dept. of Geophysics (Prof. C. S. Clay))	1
UNIV OF NEW MEXICO (Dept. of Elec. Eng. (Prof. D. P. Petersen))	1
PSI, Inc. (Dr. R. H. Mellen, J. W. Fitzgerald)	2
UNIV OF MIAMI/RSMAS (Dr. F. D. Tappert)	1
Dr. David Middleton, New York, NY	15
APL/UW, (Dr. E. Thorsos, Dr. R. Jackson, S. McConnell)	3
ONT (T. Warfield, T. Kooij, B. Palmer)	3
NAOC (Code 3042 (T. Polaneczky))	1
UNIV OF ILLINOIS (V. P. Twersky)	1
FWG/Kiel, Germany (Dr. G. Ziehm, Dr. H. Herwig, Dipl. B. Nuetzel)	3
UNIV OF KANSAS (R. T. Lawner, Dr. R. K. Moore)	2
SONALYSTS, Inc. (W. Pugliese)	2
UNIV OF WASHINGTON (Dept. of Elec. Eng. and App. Math (Prof. A. Ishimaru))	2
UNIV OF NEBRASKA (Dept. of Elec. Eng. (Prof. E. Bahar))	1
DARPA (C. Stewart)	1
NCSC (Dr. L. J. Satkowiak)	1
RAYTHEON (S. Ehrlich)	1
SAI Space Systems Operations (Dr. R. Becherer)	1